Escola Tècnica Superior d'Enginyers
de Camins, Canals i Ports de Barcelona
UNIVERSITAT POLITÈCNICA DE CATALUNYA

PROJECTE O TESINA D'ESPECIALITAT

Títol

Site investigation for a new ski lift system in Sisimiut (Greenland)

Autor/a

Adrian Läufer Nicolás

Tutor/a

Nieves Lantada Zarzosa

Departament

Dpto.Ing.del Terreno, Cartográfica y Geofísica

Intensificació

Data

19 d'Octubre del 2011

Title: Site investigation for a new ski lift system in Sisimiut (Greenland)

Author: Adrian Läufer Nicolás

Supervisors: Nieves Lantada Zarzosa y Thomas Ingeman-Nielsen

Key words: ski lift, digital elevation model, rock mass rating, kinematic analysis, Sisimiut (Greenland)

Abstract

Greenlands second biggest city Sisimiut, which lies just above the Arctic Circle has increased in the recent years the number of incoming tourist. Aware of the touristic potential of the town and the interest of their inhabitants to have more numbers of ski slopes available, a local company is willing to build new ski lifts at Solbakken, where a lift is already built as well as create a new ski resort of international caliber North of Sisimiut.

Like any other civil engineering work, the construction of new ski lifts need previous site investigations for the drafting of the project to identify potential hazards that may appear during construction and commissioning work. This study is based on previous site investigations carried out North of Sisimiut to see the feasibility of such project ensuring compliance with European standards in construction of ski lifts DS/EN-12929-1.

Given the need to find the best location for the future ski lifts depending mainly on the compliance of the maximum height above ground, it was considered necessary to build a digital elevation model from which the best possible routes could be identified. In order to create such a DEM, GPS measurements were necessary in the areas where the ski lifts would be constructed, as the topographic information in this zone was not enough.

The geological field investigations are basic for the drafting of a schematic on paper and therefore it was considered appropriate to conduct geomechanical classifications as rock mass rating (RMR) and the rock tunneling quality index Q. Also the results obtained from the point load index tests were included to characterized efficiently the intact rocks resistance to uniaxial stress.

In the field investigations also measurements of the strike and dip direction of the main discontinuities were taken from the rock masses, so together with the results obtained from the DEM and the geomechanical rock classifications a stability analisis of the rock blocks with the kinematic method could be done. This type of analysis was realized in two different ways: first the classic method with stereographic projecciones and considering the average slopes of the lines and secondly with the use of GIS tools and the created DEM using all the different slope and orientation values of each individual rock block.

Título: Investigaciones de campo para la construcción de telesillas en Sisimiut (Groenlandia)

Autor: Adrian Läufer Nicolás

Supervisores: Nieves Lantada Zarzosa y Thomas Ingeman-Nielsen

Palabras clave: telesilla, modelo digital de elevaciones, rock mass rating, análisis cinemático, Sisimiut (Groenlandia)

Resumen

Sisimiut, la segunda ciudad más grande de Groenlandia situada justo encima del círculo polar ártico ha experimentado un aumento en el número de turistas en los últimos años. Consciente del potencial turístico del municipio y el interés de sus ciudadanos en incrementar el número de pistas de esquí disponibles, una empresa local ha ideado un proyecto para construir nuevos telesillas en Solbakken. De esta forma, las pistas de Solbakken situadas al norte de Sisimiut se deben de convertir en una estación de esquí de interés internacional.

Como cualquier otra obra de ingeniería civil, los telesillas necesitan de estudios previos a la redacción del proyecto para identificar posibles peligros que puedan producirse durante su construcción y puesta en obra. Esta tesina se basa en previas investigaciones llevadas a cabo sobre el terreno para ver la viabilidad de tal proyecto asegurándose el cumplimiento de la normativa europea en construcción de telesillas DS/EN-12929-1.

Vista la necesidad de encontrar la mejor localización de los futuros telesillas en función principalmente del cumplimiento de la altura máxima permitida, se consideró necesario la construcción de un modelo digital de elevaciones a partir del cual se pudiera identificar los mejores recorridos posibles. Con tal de crear dicho MDE fueron necesario tomar suficientes medidas GPS en puntos por donde aproximadamente iban a situarse los telesillas, ya que la información topográfica en la zona no era suficiente.

Las identificaciones de campo en el ámbito geológico son básicas en el anteproyecto y por ello se creyó oportuno realizar clasificaciones geomecánicas como el rock mass rating (RMR) y el índice Q de Burton a partir de observaciones sobre el terreno. Además se incluyó los resultados obtenidos a partir del ensayo del índice de carga puntual para caracterizar de forma más eficiente la resistencia a compresión simple de la roca intacta.

En las investigaciones de campo también se tomaron medidas de la orientación de las principales discontinuidades en el macizo rocoso, para junto con los resultados obtenidos del MDE y las clasificaciones geomecánicas analizar la estabilidad de los bloques de roca mediante el método cinemático. Este tipo de análisis se realizó de dos formas diferentes: primero la clásica mediante proyecciones estereográficas y a partir de las medias de las pendientes y posteriormente mediante la utilización de herramientas SIG y el MDE creado utilizando los valores de las pendientes y orientaciones locales de cada bloque individual.

Acknowledgements

Like most of written texts, which although individually written texts are collaborative works, this study has been possible thanks to the help of many people who I would like to thank.

First of all I would like to thank Lars Stenseng for his patience and whose instructive comments and teaching in the use of GPS devices help me to fulfill the fieldwork with a reasonable success and without his help probably none of this would have been possible. Also to Thomas Ingeman for being my supervisor and providing instructive comments and Darka Mioc for convincing me to venture the project in Greenland.

Next, I'll like to thank Nieves Lantada from my home university, who from the distance made everything possible to help me along the project whenever it was necessary. During the fieldwork Laarseraq Skifte and his son and friends, specially Steen, where a great help without whom it would have been impossible to bring all the necessary equipment to the needed place. I'll also like to mention Val Evans as her pictures and comments during the fieldwork were very helpful.

Among all the friends I made during my Erasmus year in Copenhaguen, which help me all of them to decide to extend my stay in Denmark, specially thanks to Guille and Javo, whose company made the stay in Sisimiut terribly shorter. Thanks also to the rest of the students and Artek members for making everything to enjoy the trip as much as possible.

Also thanks to my parents, Antonia and Bernd and my sister Amanda, for on-going support, economically and emotionally along all the studies, relieving me in the hardest days. Finally I would like to thank Pili, the most responsible person for having made me decide to realize this study abroad. Without her daily smile and love nothing woudn't have been so easy as it now seems.

Table of Contents

List of Figures

List of Tables

1. Introduction and Objectives

The idea of this study came from the need of site investigations for a coming ski slope and lift system East from Sisimiut, which will be part of a specific entrepreneurial project developed by Igloo Mountain.

Sisimiut lies just 75 km North of the Arctic Circle (66°56'N and 53°40'W) and is the second largest city in Greenland with 5.900 inhabitants considering the settlements of Kangerlussuaq, Sarfannguaq and Itilleq (figures 1 and 2). The town, whose first human traces are more than 4.500 years old, lives practically from the fishing industry as it has the biggest ice-free harbor during winter months above the Arctic Circle. A high-tech factory of Royal Greenland, where crabs and prawns are processed, gives evidence of that and is the biggest pride of "sisimiormiutts" as it's one of the most moderns in the world. Combining Inuit culture and Western society, Sisimiut has also become an important touristic highlight in Greenland as a lot of cruise ships are having a stop in the town. Although the town is considered a prime place for dog sledding, as "sisimiormiutts" have 1.300 sled dogs, skiing is also a very popular sport in Sisimiut. Alpine and cross-country skiing is practiced with enthusiasm as most of the citizens own a pair of skies. The Arctic Circle Race, a 160 km long cross-country race is the world's toughest and most beautiful race and takes place in the surroundings every year (Council, 2011).

Figure 1: Map of Greenland showing the location of Sisimiut (Lumholt, 2010)

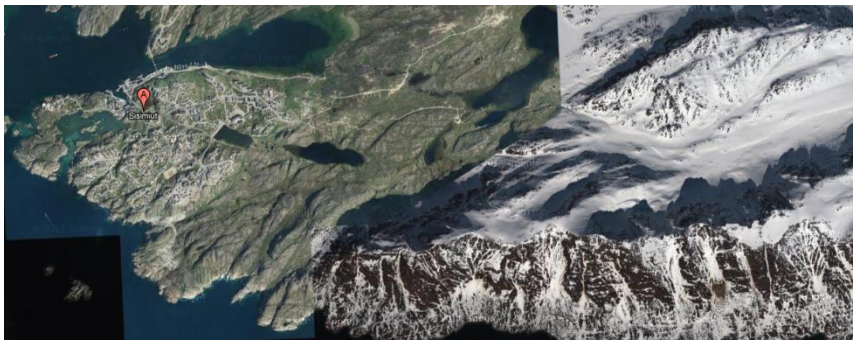

Figure 2: Map of Sisimiut (Maps, 2011)

Aware of the touristic potential of the town and the interest of their inhabitants to increase the number of ski slopes available, a local company is willing to build new ski lifts at Solbakken, where a lift is already built, as well as, create a new ski resort of international caliber North of Sisimiut. Besides the local authorities, Qeqqatta Commune and the Government of Greenland, some important international companies are also participating in the project. Among other things different periods have been established to develop all the stages in which the project is divided. The first of them, which is going to take place between midst 2012 and 2016 will convert the actual ski lift in a the big Solbakken Friluftcenter where the yearly amount of 9.000-10.000 cruise ship guest and the inhabitants of Sisimiut can enjoy, besides the new ski slopes, a Moskus-okse park, as well as different planned outdoor activities.

As a first step for the correct planning of the venture, site investigations have to be carried out to find the most suitable way where the ski lifts can be placed. During the construction of a ski lift, many problems can be found, as for example inconvenient design of the carriers, problems with the rope tension and guides, planning of the loading and unloading areas, unsuitable path for the ski lift, failure of the piles, etc.

The main focus of this work has been set in a study to find the most suitable way where to place the ski lift considering the fulfillment of European standard and the evaluation of the failure of the terrain during the construction of the piles. Safety regulations have establish different safe distances as, for example, a maximum height between the carrier and the terrain that should be carried out. Owing to the fact that a digital terrain model gives the opportunity to check the accomplishment of all the possible safe distances, GPS measurements have been captured among previous defined lanes for all the three ski lifts that are planned to be constructed. On the other hand the analysis of the failure of the piles has been performed with stereographic analysis after the estimation of the predominant dip directions and the superficial geological survey.

Due to the fact that the study will go through two complete different themes – geodesy and geology – in some points of the report – Theoretical Background, State of The Art, Fieldwork and Results – it has been distinguished between each theme, while in the last ones the main purpose was to have a general overlook at the fulfillment of the standards and the most correct placement of the ski lift system.

Although digital terrain models have become in the present an interesting tool for the organization of ski resorts with detailed analysis of ski slope (Collinse and Loubier, 2003) this option has not been taken into account due to the lack of time as more GPS measurements had to be taken in the mountains.

2.Background

2.1. Skiing in Greenland

Alpine, cross-country and heli-skiing can be practiced in Greenland. Nevertheless, the opportunities for it are scant and spread over the huge island, except for the cross-country discipline, which can be practiced almost everywhere. Anyway, Greenland's status as relatively unspoilt ski destination, makes it more attractive specially to heli-skiers. In the following paragraphs a brief description is given about where and when the different ski disciplines can be practiced:

Classic ski disciplines:

The high season for skiing in Greenland is from February until April when it is possible for skiers to enjoy Greenland's extensive nature in the classic cross-country disciplines, as well as the alpine disciplines in some of the larger towns. At certain places in Greenland it is also possible to go skiing during the summer, as for example at Apussuit Adventure Camp, situated on the top of a glacier and just 25 km from Maniitsoq (see figure 3).

The Arctic Circle Race considered the world's toughest cross-country race, is held in Sisimiut every year, where more than 100 competitors from more than 10 different countries complete a 160 km distance in three days (Council, 2011). On the other hand, the alpine discipline can only be practiced close to large towns as Sisimiut and Nuuk. Solbakken in Sisimiut and Sisorarfiit in Nuuk are the only two places where ski lifts are available for skiers. The ski resort

Sisorarfiit (figure 4) is funded by the municipality of Nuuk and has two different ski lifts, which walk up the Lille Malene's west side, starting from the airport. Their lengths are around 400 and 500 m and from the top of the mountain you have between 5 to 11 km of ski slopes available depending on the snow conditions. The season usually starts at the end of December or January, when there is enough snow on the ski slopes and goes till the end of April or middle of May. Sometimes the ski resort has to close in some of the winter months, especially in February, when the temperatures are extremely cold. A ticket for a day costs around 170 Dkk (22 €) and a season ticket 1.500 Dkk (200 €) (Sisorarfiit, 2011).

Figure 3: Map showing the skiing options in Greenland. The red underlined places have ski "resorts" while the other places offer heli skiing options. (Maps, 2011)

Figure 4: Sisorarfiit Skiliften (Sisorarfiit, 2011)

Heli-skiing:

For intrepid souls looking for a more extreme form of the sport, the areas around Maniitsoq and Uummannaq are perfect for heli-skiing. The practice of heli-skiing is specially advantageous in Greenland as the areas for heli-ski are located at lower altitudes than those in Europe or the USA, where this discipline is realized at heights of 2.000 to 4.000 m. In Maniitsoq the heights of the tops of the fells range from 700 to 1.500 m, whilst in the Fjord Eternity a few of the mountains rise more than 2.000 m into the sky. This means that there is more oxygen in the air in Greenland and thus more energy for those wishing to enjoy the chance of skiing in virgin snow and unspoilt scenery. For this type of ski modality the season runs from the middle of March until the beginning of June with powder snow conditions at the start of the season and 'corn' snow as the season draws to a close. It's remarkable that the midnight sun from the end of April enables skiing at all hours of the day and that the areas

have a stable coverage of snow with minimal chances of avalanches. The most common places for this type of sky are Maniitsoq, Uummannaq and Kisaq (Council, 2011).

2.2. Solbakkens Actual Situation

The ski lift in Solbakken is situated East from Sisimiut in an approximated distance of 5 km, which can easily been covered in winter by snowmobile. On the other hand in summer, it's inaccessible by car as the closest road just finishes 2,5 km before it reaches the cabin on the ski station. The lift constructed in the 1970s goes up along the South side of the Oqummiannguaq mountain reaching the height of 294 m and giving the opportunity of skiing 5 different slopes. Snowmobiles drive the users also to the top of the mountain around 400 m enhancing the number of total slopes available. A small cafeteria gives skiers the opportunity to take a break and warm up from the cold temperatures characteristic of arctic climates.

The actual ski lift with T-form carriers (figure 5) finishes in a very inappropriate place as a big fall just at the end of the track makes it almost impossible for skiers to get down easily (figure 6). Experience has shown employees at Igloo Mountain that a lot of snow has to be moved around the surroundings of the end of the lift before it can be started into run, taking them around 2 to 3 weeks of work to prepare the ski slopes.

Figure 5: Actual ski lift in Solbakken (Mountain, 2011)

Figure 6: The picture shows the problem that the actual ski lift has, as a lot of snow is required to fill the gap between both hills (Evans, 2011).

2.3. Igloo Mountain Project

Due to the adverse placement of the actual ski lift and it's old system that makes it extremely expensive to renovate, Igloo Mountain has decided to renovate their ski lift system by constructing two chair lifts and a ski tow for children. One of the two chairlift should be placed

close to the actual situation of the ski lift, although reaching the highest peak of the mountain, while the other has to be constructed in a small area very suitable for snowboarders and young skiers, that have recently started with this sport class. Besides, the ski tow perfect for beginners will cover a small and almost flat area very close to the location of the cabin, which is used as cafeteria nowadays.

Furthermore, the project of Igloo Mountain won't finish here. In order to develop the tourism in and around Sisimiut, the Solbakken Friluftscenter (Solbakken Outdoor Centre) sets its target in attracting the almost 10.000 cruise ship guests that Sisimiut would welcome each year. A muskox park with space for 50-80 muskox or reindeers, 25 Family Igloos for lodging 4 persons in each, a Snow Ice Hotel and a Visitors Center for the Snow Village and the Igloo Village has to be constructed as well as different activities, like Snowmobile Safaris and Mountain bike trails will be planned.

Finally, as a last stage in the project, a part of the road between Sisimiut and Kangerlussuaq should be constructed as well as the development of the Igloo Mountain Glacier Park, placed North-East from Sisimiut and which is going to be the world biggest summer ski station.

3.Safety Requirements

In order to identify the most suitable line for the installations of the chairlift and the ski-tow, the safety requirements of the Danish standard DS/EN 12929-1 (2004) have been followed. This national standard is actually a European standard and the regulations regarding the ski-tow part have been guided by the works of the International Organization for Transportation by Rope (OITAF), an international association whose goals are the promotion of studies and experiments for the improvement of ropeway business and the elaboration of standardized international guidelines for projection and construction of ropeways among other objectives (O.I.T.A.F, 2011).

The requirements exposed in other standards, as for example EN 13107 (Safety requirements for cableway installations designed to carry persons – Civil engineering works), have not been considered as the different actions, loads and states had to be defined previously. In the same way, demands regarding the running speed and interval and drive systems should be taken into consideration by the manufacturer and are not mentioned in this work either.

As the offering process in the project is still a budget price, no specific technical data for the lifts is available, although it´s known that lifts from the German company Loipolder Seilbahn technick have been offered. Therefore, the products of these company have been used to consider the fulfillment of the requirements mentioned in the DS/EN-12929-1 (2004).

In the following paragraphs, the main requirements for both planned installations have been summarized. Nevertheless, to ensure that there is no risk to safety of passengers, the

characteristics of the terrain for the evacuation of passengers, geological and hydrological conditions of the subsoil and natural hazards such as avalanches, rock falls, landslides or exposure to adverse weather conditions have to be taken into account as well.

3.1. Chairlifts (Monocable Aerial Ropeways)

For a chairlift in a monocable aerial ropeway other requirements have to be fulfilled in order to make the travel safe and comfortable for the passengers. First requirement that has to be considered is that the line of the aerial ropeway has to be a straight line between the stations with a constant gauge (separation between cables of the chairlift). The length of spans and their relationship to each other shall be selected so that they do not have an adverse affect on the dynamic behavior of the moving ropes.

The space envelope of aerial ropeways is defined by the lateral (wind pressure) and vertical (ice load, working load of the carriers and dynamic effects when breaking) deviations of the ropes, the transverse and longitudinal swaying of the carriers and the hand, foot and ski areas. Considering that the lateral and vertical deviation of the ropes shall be taken into account by the manufacturer as the dynamic effects had to be defined these have been excluded. A minimum transverse sway of 0,34 radians shall be considered in the worst case, when an empty open carrier is being transported. While the transverse sway is considered when the ropeway shall pass through tight passages the longitudinal sway is more a measure to avoid collision between different carriers and has therefore also been neglected.

The hand and foot area, a very important space to consider for the safety of the passengers is defined in the form of a four sided pyramid, whose base is formed by the surface of the seat and whose height is 1 m. A half meter in all directions of the external surface of this pyramid, the hand and foot area is established. The ski area is located in a plane 0,5 m below the seat surface and it extends parallel to this surface 1 m in front and behind measured from the vertical plane passing through the front edge of the seat.

After this, the clearance envelope of the carriers is determined by adding the required safety distances to the space envelope. This safety distances are: 2,0 m in all directions (in relation to the ground on all sides and to fixed objects and structures, if these areas are not accessible to persons not forming part of the personnel), 3,0 m (if these areas are accessible by persons not forming part of the personnel), 4,5 m (if piste grooming machines may operate below the chairlift) and 1,5 m in relation to the clearance envelope of areas used by traffic.

The maximum permissible running height above ground (distance between the seat surface of open carriers and the surface of the ground without taking into account any covering snow) is

chosen taking into account the possibility of evacuation. For these kind of aerial ropeways with open carriers, the rope profile shall be designed with a maximum running height above ground not greater than 15 m. Some exceptions are presented in the Standardization (2004) described in point 8.3.2.

Chairlift loading and unloading areas:

The distance between the surface of the loading or unloading areas and the seat surface under static load shall be (46 ± 5cm), considering any layer of snow required for operation. The loading areas of chairlifts should be rectilinear, where the horizontal length of the loading area of transportation of skier should be between 2,5 and 3,5 m. A stabilization area is defined between the loading point up to 3,5 seconds travelling time and it is characterized by the area where the skis should slide. In this area the height above the ground should not be greater than 1,5 m. If the gradient of the terrain is greater than 60% after the stabilization area a catch net should be provided.

After the stabilization area, a safety area is defined as the area which is 7 seconds travelling time from the loading point, and where the height above ground can't be greater than 3 m. (Annex A of Standardization, 2004)

For the unloading area, the horizontal surface should be the distance travelled by a chair in 1,5 seconds with a tolerance of 0,5 m. The stabilization area is defined as the distance from the unloading point separated by 5 seconds travel distance. Before the unloading area a ramp shall be provided in order to prevent skiers from getting their skis caught in the structure. Also a catch net should be installed if the ground changes suddenly in less than 1 meter or the height above ground exceeds 3,0 m. After the unloading area a ramp with 15% up to 25% slope has to give skiers the opportunity to stabilize themselves after getting of the chairlift. The distance between the seat surface and the ground after the ramp should not exceed 2,5 m. Another requirement is that the unloading area has a lateral safety distance of 1,25 m in both directions of the chairlift. (Annex B of Standardization, 2004).

Regulating devices like barriers should be placed at least 0,6 meters from the space envelope of the carriers.

3.2. Ski-Tow

First of all in a ski-tow the line should be designed so that all passengers could leave the tow-track without danger at any moment. Considering that the design of the ski-tow at Solbakken should be for low level skiers, this tow-track can't be over 300 m long and can't exceed a

longitudinal gradient of 40%. On the tow-track, downhill slopes are permissible but only with a maximal longitudinal gradient of 5%. Regarding the transverse gradient along the track, tolerances up to 10% are permissible although it's recommended to have a horizontal surface in order to prevent skiers from sliding away from the track.

For single tow-hangers the minimal width of the tow-track should be 2 m. The clearance envelope is defined as the area 1,25 m from the centerline of the tow-track and up to 2 m height above the surface of the snow. In this area no line support structures and other fixed elements can be installed. Crossings with ski runs at the same level are to be avoided whenever possible and are completely forbidden within 15 m of loading and unloading areas and on low-level ski-tows.

Loading and unloading area:

The loading area should be more or less horizontal, while the unloading area can have a maximum gradient of 20% for a minimal length of 8 m. In this area, the clearance envelope can be reduced by a 20%. The distance between the T-bars or platters and the surface of the snow in the loading area should be between 0,6 and 0,8 m.

4. Theoretical Background

4.1. Digital Elevation Model

4.1.1. Introduction

By definition GIS is a system of hardware, software, data and organizational structure that captures, stores, analyzes, manages and presents geographically referenced data. GISs are nowadays one of the most powerful technologies because it integrates the knowledge from different sources (as layers inside a map) and creates transversal relationships to collaborate easily between them (Foote and Lynch, 1995). The use of this application is wildly spread as its used by business (banking, insurance, logistics, media, etc.), governments (military defense, homeland security, etc.), educators and scientists (research, libraries and museums, etc.), environmental and conservation organizations (water, oceans, land, etc.), natural resource groups (agriculture, forestry, mining, oil and gas, etc.), and utilities (power management, electricity, gas, telecommunications, water and wastewater management) (ESRI, 2010).

Although the first time the term GIS appeared was in the 1960s for developing Canada's Geographic Information System (CGIS) used for determining the land capability of rural Canada, this technology was used more than 150 years ago. One of the first examples of the map overlay concept (one of the tools in GIS) was given by John Snow in 1854, who tried to overlay wells locations and cholera deaths in a map to analyze possible infection points (Wolf and Ghilani, 2008). Nevertheless, CGIS has been considered the "father of GIS" and most of its features were considered by ESRI (Environmental Systems Research Institute) to create and

commercialize a GIS software. The growth of industry at the end of the 20th century has required new data formats and transfer standards as more GIS packages have been developed and more users are acquiring data through the internet and other sources.

A GIS system can mainly be explained with the concept of the different layers. Different thematic layers with spatially related information between them can be stored independently in completely different formats, allowing users to work with each of them separately. Nevertheless, when a common coordinate system is used the information can be presented in the same map, where all the layers overlap.

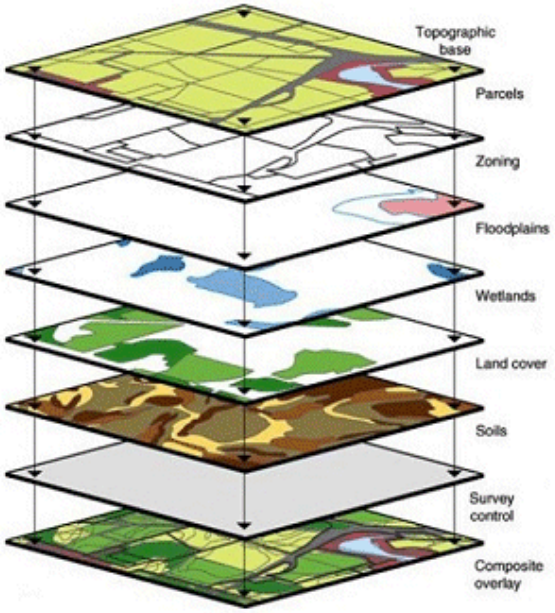

Figure 7: Concept of map overlay (Hippolyte, 2011)

One of the most important types of information used in GIS are digital terrain models (DTM), which are numerical data structures that represent the spatial distribution of a qualitative and continuous variable, like temperature, contamination, elevation, rainfall, etc. While in the conventional cartography, the description of the elevations is given by a topographic map and constitutes the basic infrastructures for the rest of the maps, in DTM this function is developed by the digital elevation models (DEM). DEM is defined as a statistical representation of a continuous surface of the terrain, with an elevated number of points selected with known coordinates (x,y,z) in an arbitrary coordinate system (Felicísimo, 1995).

4.1.2. Structure of The Data for a DEM

In a general way, the basic unity of information in a DEM is an enclosed point defined with an altitude z, with its corresponding values x and y. The different variants appear when the elemental units of the points with their altitude are organized in structures that represent the

spatial and topological relationships. While in conventional maps the representation of the terrain was exclusively done with contour lines in a DEM the data structure has been divided in two clearly distinguishable groups: vector and raster format. Vectors represent the world as objects with well-defined boundaries in an empty space. Points are used to define specific locations of objects (intersection of streets, buildings, etc.), lines and strings represent rivers or streets for example and areas define regions with common attributes. Vector representation of the data can be achieved with tables that list all the different objects and related them spatially with coordinates of points and topological relationships. On the other hand, raster format uses a fields or grid cells to represent the world (Wolf and Ghilani, 2008).

Each of the data models can be expressed with different structure of data. From the two basic models, the experience has reduced the potential variety of the structuring in a few described in the following lines:

1. Vector Model

1.1. **Contour lines:** Contour lines connect points of equal value (such as elevation, temperature, precipitation, pollution, or atmospheric pressure) which show how the variable they describe vary along the surface. In the simplest case the DEM is constituted by a number of contour lines that pass the zone to be represented and are separated by a constant interval of altitude.

1.2. **TIN:** A triangulated irregular network is a surface made of triangles that are created by adjusting a plane into three close points, which are not in the same line. The realization of such a network will be explained in further parts.

2. Raster model

2.1. **Regular matrix:** This type of structure is the result of overlaying a grid over a terrain and extract the exact altitude in each of the different cells. Usually the grid adopts the form of a regular and quadratic grid.

2.2. **Others:** Tree data structure matrices have been occasionally used in raster models to solve the problem of a constant resolution in regular matrixes. These types of matrixes were known as quadtrees and characterized by the peculiarity that the cells of a regular grid could be divided in four smaller cells.

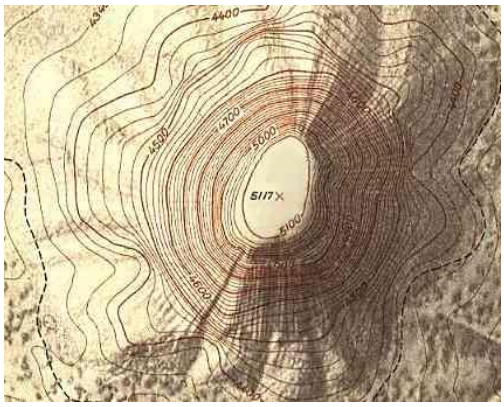

Figure 8: Contour lines (Dude, 2011)

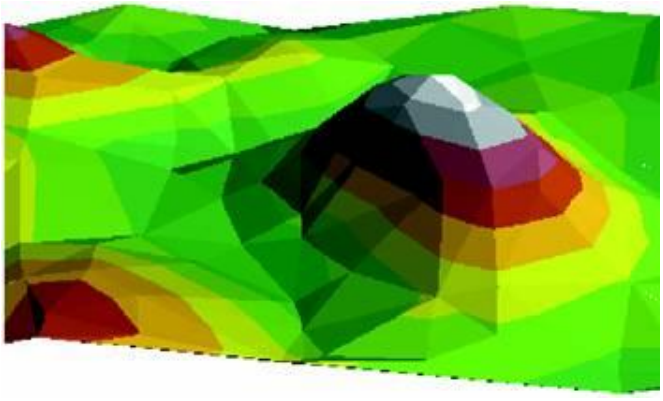

Figure 9: Triangulate Irregular Network (Analysis, 2011)

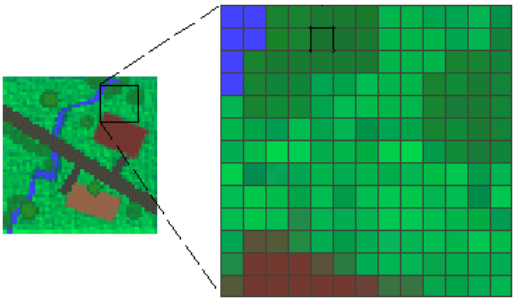

Figure 10: Raster model (ESRI, 2010)

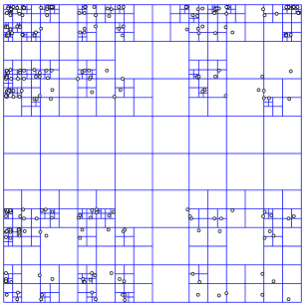

Figure 11: Quadtree (Eppstein et al., 2005)

4.1.3. Data Capture

The capture of altimetry information constitutes the initial step in the process of construction of a DEM and is the phase, were the geographical reality is transformed in a digital data structure. It's one of the most important steps as the quality of the data that is obtained, is the first limitation factor in data treatment. The basic methods to obtain altimetry data can be divided in two groups: direct methods, which produce primary data and are realized directly on the real terrain and indirect methods, which on the other hand utilize analog or digital documents that have been previously elaborated and produce secondary data. The most common methods are explained in the following graph:

1. **Direct Methods:**
    a. **Radar altimeters:** Some satellites have incorporated altimeters between their equipment so that it's possible to directly record altitude data in digital format. Radars transmit a sign that is reflected on the earth surface and recording the emission time, the distance between satellite and terrain can be estimated. These instruments have the inconvenient that need a relative homogenous

wide area of terrain to be recorded so they are especially interesting for the ocean-surface topography, while they are less useful for the Earth surface.

b. **LIDAR:** Light Detection and Ranging is an optical remote sensing technology able to measure distances or other properties just by illuminating the target with a laser.

c. **GPS survey:** Global Positioning System is a system that uses a constellation of satellites to establish by triangulations, the position of a receiver in the field. Although it has the inconvenient that a survey needs to be realized, this has been the used method and a more enhanced description is given in the next pages.

d. **Total station survey:** With a total station a complete survey of the terrain can be realized and transformed to digital format like it's done in a GPS survey.

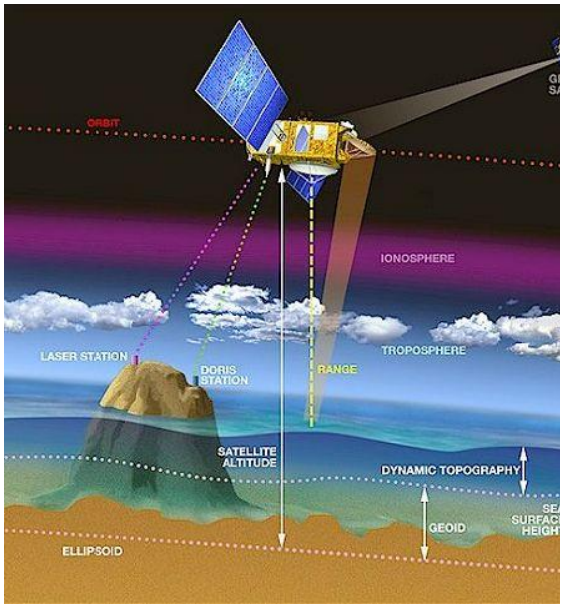

Figure 12: The principle of altimetry (Satellites, 2011)

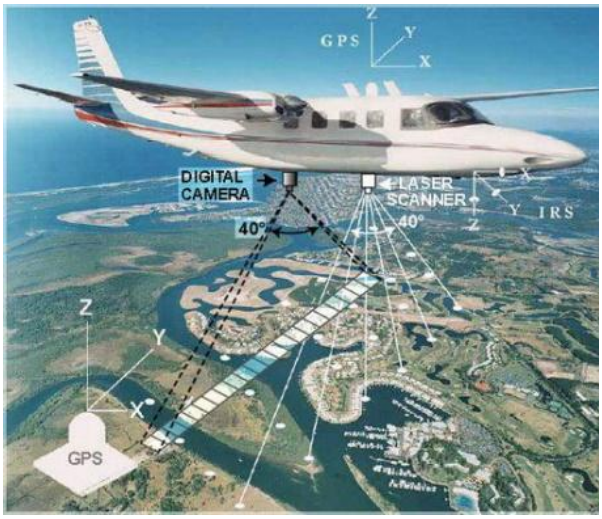

Figure 13: LIDAR system used in a plane (Ciencia 101, 2011)

Figure 14: GPS Survey (Ltd, 2011)

Figure 15: Total station surveying (Landsurveyors.com, 2011)

2. **Indirect Methods:**

   a. **Digitalization of topographic maps:** Conventional topographic maps are manually (with a digital table) or automatically (with a scanner) digitalized. In this process the original document is analyzed with a scanner (or with the users eyes in case of doing it manually) and the optical sensor translates the information (contour lines, numbers, etc.)in a certain color.

   b. **Stereophotogrammetry:** In this method, different aerial images of a concrete zone are overlapped creating stereographic pairs. When analyzing homologous points in the different pairs it's possible to calculate the exact altitude of this point.

   c. **Interferometric synthetic aperture radar:** The idea consist in comparing two different pictures of the same place taken from the same point but in different moments. The phase difference in wave returning of both images is used to generate digital elevation models.

Figure 16: Map digitalization (SIG, 2011)

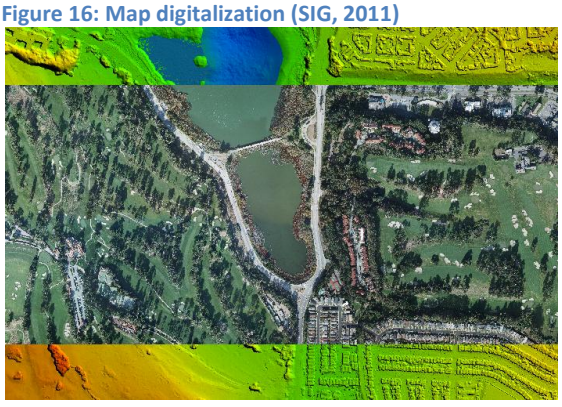

Figure 18: Stereo photogrammetry (Imaging, 2011)

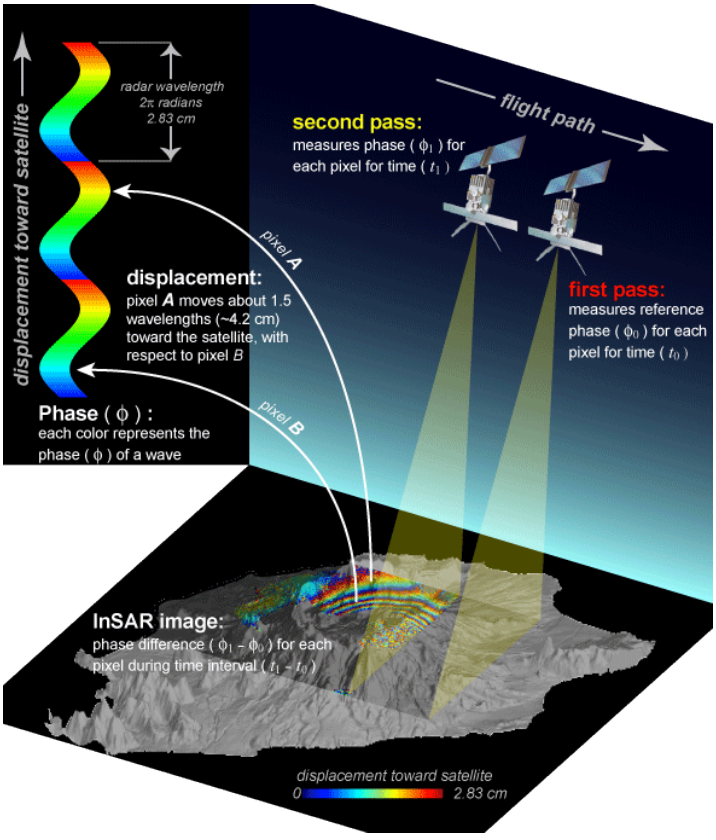

Figure 17: Description of Interferometric Synthetic Aperture Radar (InSAR) (Trussty-Jasmine.blogspot.com, 2011)

Among the presented methods the most used methods are the indirect ones, as they don't need a physical presence in the study area and they are therefore easier realized. Nevertheless,

these methods are more expensive as they require special equipment for analyzing the data (scanners, radars, etc.) and could also not been employed as the information for the required zone was not enough. Between the direct methods, the disadvantages of radar altimeters has already been presented and the LIDAR technology requires also the use of a plane where the laser is being transported. In this case, the only available methodology to acquire altimetry data in the required zone was a survey with a GPS or a total station and due to the easier way of operating with GPS controllers, this last method was used.

GPS

Introduction and History

The Global Positioning System (GPS) emerged in the 1970s from the Navigation Satellite Timing and Ranging (NAVSTAR) Global Positioning System (GPS) program, developed by the U.S. Department of Defense to produce a global coverage and continuous operational system to obtain precise timing and positioning information anywhere on the Earth. Based on the signal transmitted from satellites, whose position is precisely known, today GPS is a universal approach to surveying. GPS is a dual-use system as it provides separate services for military users (PPS, Precise Positioning Service) and civil users (SPS, Standard Positioning Service). The constellation of GPS consists of 24 satellites arranged in 6 different orbital planes with 4 satellites in each (mean altitude of 2.200 km above the Earth and an orbital period of 12 sidereal hours). After the success of the American global positioning system other satellite navigation systems have been implemented or planned as the GLONASS Constellation (by the Russians), Galileo System (European Union) or Compass (China) but without the same success. Nevertheless none of them are completely operational and all receivers using this systems mostly also support GPS (Hegarty and Kaplan, 2005)

Principles of GPS

The global positioning systems consists of three different parts: the space segment (24 satellites), the control segment (monitoring stations where the signals from the satellites and their orbits are monitored) and the user segment (all the receivers that are used, which can be distinguished between the services they offer: PPS or SPS) (Wolf and Ghilani, 2008).

While the PPS is broadcast on the L1 and L2 microwave radio frequency, the SPS is just provided on the L1. The orbiting satellites continually transmit a unique signal on these two carrier frequencies, which are modulated with different codes: the L1 frequency is modulated by both the C/A (coarse/acquisition) code and the P (precise) code and the L2 frequency is modulated only in the P code. The signal that is transmitted from the satellites in these two

bands is a pseudorandom noise code (PRN) which is a sequence of binary values generated according to a complex mathematical algorithm.

In order to determine the position of a user with a receiver, the satellite sends the PRN code in a certain instant of time, which is the same code that is producing the receiver signal. Matching the incoming satellite signal with the identical one produced by the receiver derives to the time that needed the signal to reach the receiver from the satellite. Multiplying the time with the speed of the signal, the distance from the satellite where the user is placed can be determined.

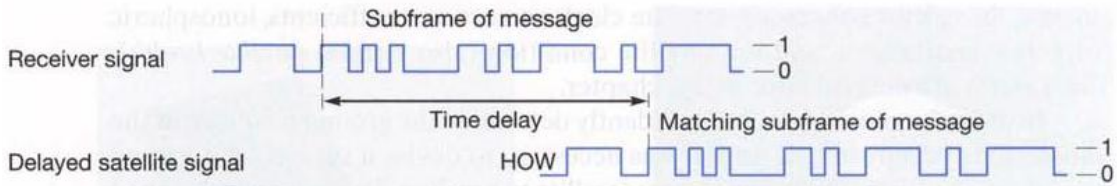

Figure 19: Determination of signal travel time by code matching (Wolf and Ghilani, 2008)

Once the distance r_1 between the user and the satellite is known, the position of the first one can easily be determinate, as all points situated a distance r_1 from a satellite can be represented in a sphere with the mentioned radios. If we receive the signal from 3 different satellites, the user will be situated in the point where the 3 spheres match. Anyway, to reach a better accuracy and release the error of the different measurements, at least 4 satellites have to be used.

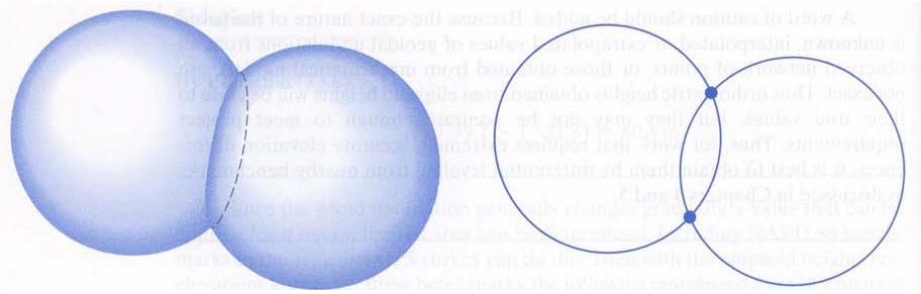

Figure 20: Basic principle of calculating the position with a GPS: a) Intersection of two spheres b) Intersection of the two circles (Wolf and Ghilani, 2008)

Differential GPS

The measurements of the GPS observations are affected by several error sources. Some of these errors provide from the clock bias (from satellite and receiver), refraction of the signal, multipathing, satellite ephemeris, errors in measuring antenna height,etc. (Wolf and Ghilani, 2008). Therefore Differential GPS was introduced to improve the accuracy of the surveying. In DGPS measurements are taken from two or more receivers, one of who has to placed in a base station, that means a point whose coordinates have been fixed before and are known. As base

station and receiver are staying very closed, the error, which is going to be very similar in both, can be calculated from the measurements of the base station.

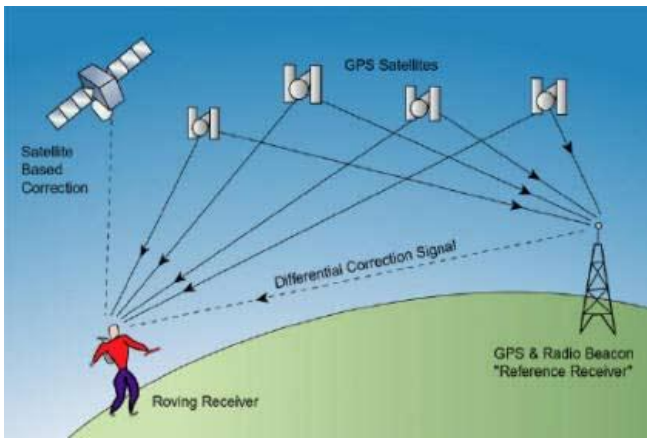

Figure 21: Real-time differential GPS (Ltd., 2011)

4.1.4. Construction of the DEM

After the altitude data has been captured the construction of the DEM as a regular matrix based on vector data (points) is basically an interpolation problem: the unknown altitude of points in the grid are estimated with the data from the surrounding points in the vector model. From a general point of view the problem could be presented as: given a number of points with coordinates (x,y,z) irregularly distributed, generate a new collection of points placed on nodes of a regular grid so that the interpolated surface is a representation of the original with the lowest lost of information (Felicísimo, 1995). In order to minimize the lost of information, different interpolation techniques are used to create the regular surface: inverse distance weighting, natural neighbor, spline and ordinary kriging. On the other hand, when creating a TIN structure, instead of interpolating first a selection of the more convenient points is done and after the triangulation is realized.

IDW: Inverse Distance Weighting

The easiest way to assign to a point an altitude is by giving this point the value of its closest point with a known altitude. Although this method is very easy to employ, it's not recommendable to be used as it's physically illogical considering that the altitude of one point is only determinate by the closest point to it. A more common distance-weighted interpolation is the inverse distance weighting. In this case the value of the altitude at a certain point is determinate using linear-weighted combination as it can be seen in the following formula and picture:

$$z_j = \frac{\sum_i^n \frac{1}{d_{ij}^p} z_i}{\sum_i^n \frac{1}{d_{ij}^p}} \quad (4.1.)$$

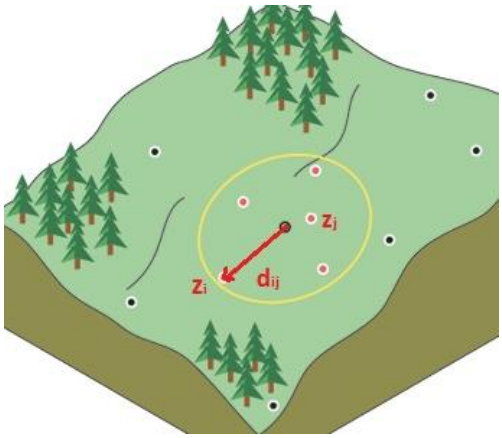

Figure 22: Concept of Inverse Distance Weighting (ESRI, 2010)

The weight assigned is a function of the distance of an input point from the output cell location d_{ij}^{-1}. Clearly, the greater the distance to the input point, the less influence the cell has on the output value. The parameter p, called power of the IDW is normally equal to 2 and a brief description of its influence will be seen later.

Spline

Spline estimates the values of the altitude using a mathematical function that minimizes overall surface curvature. The basic two conditions are impose on the interpolant: 1) The surface must pass exactly through data points, 2) The surface must have minimum curvature- the cumulative sum of the squares of the second derivative terms of the surface taken over each point on the surface must be a minimum (ESRI, 2010).

There are two variations of spline –regularized and tension. In the regularized spline, the first, second and third derivative are included in the minimization calculations while in the tension spline only the first two derivatives are used but more points are included in the calculations. The following formula for the spline is used for the surface interpolation:

$$S(x,y) = T(x,y) + \sum_{j=1}^{N} \lambda_j R(r_j) \quad (4.2.)$$

where the definition of T(x,y) and R(r) depend on the selected option, r is the distance from the point (x,y) to j and λ_j are coefficients found by the solution of the system of linear equations (ESRI, 2010).

Kriging

The IDW and Spline interpolation tools are referred to as deterministic interpolation methods because they are directly based on the surrounding measured values or on specified

mathematical formulas that determine the smoothness of the resulting surface. On the other hand, kriging is a geostatistical method as it's based on statistical models that include autocorrelation. In this way, kriging has the capability of producing a prediction surface and also measure the certainty or accuracy of the predictions. Kriging assumes that the distance or direction between sample points reflects a spatial correlation that can be used to explain varation in the surface (Childs, 2004). Like IDW, Kriging weights the surrounding measured values to derive a prediction for an unmeasured location:

$$Z_j^* = \sum_{i=1}^{N} \lambda_i Z_i \quad (4.3.)$$

In this case, the weights λ are estimated so that they minimize the variance of the estimator:

$$\sigma_E(u) = Var\{Z^*(u) - Z(u)\} \quad (4.4.)$$

Under the constraint $\omega^T 1=1$.

Different types of kriging are available, from which the most common are simple, ordinary and universal kriging. In simple and ordinary kriging it's assumed that a mean value exists and while it's known in simple kriging it's unknown in ordinary kriging. On the other hand, universal kriging assumes that there is an overriding trend in the data-for example, a prevailing wind- and it can be modeled by a deterministic function, a polynomial. This polynomial is subtracted from the original measured points, and the autocorrelation is modeled from the random errors (Nielsen, 2009).

Natural Neighbor

Natural neighbor is another weighted-average method based on proportionate areas and defined by Sibson in 1981. It's basic equation is identical to the one used in IDW interpolation. Nevertheless, the natural neighbors of any point are those associated with neighboring Voronoi (Thiessen) polygons. After a Voronoi diagram is constructed with all the given points, like the green ones in the picture, a new Voronoi polygon is created (beige colored) around the interpolation point (red star). The proportion of overlap between this new polygon and the initial polygons are then used as the weights.

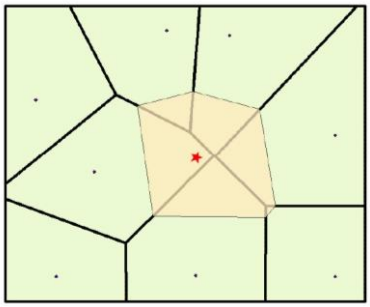

Figure 23: Concept of Natural Neighbor (ESRI, 2010)

By comparisons, a distance-based interpolator would assign similar values to the two points more to the right, while a natural neighbor interpolation assigns a much higher value to the upper point than to the lower one, as seen from the picture (ESRI, 2010).

TIN: Triangulate Irregular Network

The previously described methods produce a DEM in raster form. Some of them allow the incorporation of auxiliary structures like breaklines although these methods based on weights better respond on smooth variable distributions. The apparently more convenient solution is the treatment of the topography with a vectorial structure: a network of irregular triangles. The most common method of triangulation in GIS is the Delaunay triangulation, which considers that for a set of points in a plane, no point will be inside the circumcircle of any triangle in the triangulation. In this way, Delaunay triangulation maximizes the minimum angle of all the angles in the triangles in the triangulation, producing a unique solution (except in some special cases) with the most equilateral triangles possible.

Different algorithms are available for the construction of a TIN surface, although the most common one is the incremental construction in which continuously a new vertex is added to the triangulation and a better TIN is calculated (De Berg et al., 2008).

4.2. Geological Part

4.2.1. Introduction

To realize an analysis in the failure of the slopes before piles are going to be constructed a specific characterization of the material has to be realized in the zone in order to determinate the expected mechanical behavior of the soil. The characterization of rock mass and the study of its mechanical behavior as well as it's deformation is a very complex task due to the big variability of characteristics and properties that rock masses present and due to the big amount of parameters that affect those. The physical properties, like mineral composition, density, structure, porosity, permeability, hardness, etc. control the resistant characteristics of the rock and are the result of geological and tectonic processes suffered by the stones along their history. On the other side, the mechanical behavior of rock mass is characterized by geological properties, like the lithology, stratigraphy, geological structure, discontinuities, in situ strength states, etc. In both cases, physical and mechanical properties will also depend on hydrological, meteorological and environmental conditions which have modified the initial properties of the rock. Like the piles that are going to be constructed for the ski lift, engineering works modify the tensional state in which rock masses are submitted to in short periods compared to the geological processes which they are suffering instantaneously.

Therefore, it's very important to know the previous tensional state of the terrain, in order to magnify the possible response that it could have when engineering works are developed on it (Vallejo, 2002).

In order to make the most complete analysis of the material presented in the area different evaluations will be done to classify it after a description of the lithology of the rocks has been given. Nevertheless, an brief overview of the geology of Sisimiut is presented in the following paragraphs in order to acquire sufficient knowledge of the expected material in the zone.

4.2.2. Geology of Greenland

Greenland is the largest island on Earth with a surface of 2.186.000 km^2 which about 80 % is covered by Inland Ice. To have an idea of the rank of grandee of the ice-free strip of land surrounding the Inland Ice, this has an area of 410.000 km^2 around 30% bigger than the British Isles (Escher and Watt, 1976). The geological development of Greenland spans a period from Eoarchean to the Quaternary, almost 4 Ga. It´s dominated by crystalline rocks of the Precambrian shield formed during a succession of Archaen and Palaeoproterozoic orogenic events. The shield area of Greenland can be divided into three different types of basement:

-Archaean rocks that were almost unaffected by Proterozoic or later orogenic activity (3.200-2.600 Ma)
-Archaen terrains reworked during the Palaeoproterozoic (1.900-1.750 Ma)
-Terrains mainly composed of juvenile Palaeoproterozoic rocks (200-1.750 Ma)

In North and East Greenland sedimentation continued into the Palaeozoic. In mid-Palaeozoic tectonic and metamorphic events of some of these deposits and the underlying basement produced the continental break-up and the formation of rift basins.

In the Precambrian shield four major structural provinces are recognized (figure 24): Archaen gneiss complex (Southern-West and Southern-East Greenland), Naqssugtoqidian mobile belt (active till the Proterozoic and situated northern from the Archaen complex), Ketildian mobile belt (also till the mid-Proterozoic active and placed in the South of the island) and the Rinkian mobile belt (Proterozoic and situated in Center-West of Greenland) (Henriksen et al., 2009). The first of them is characterized by quartzo-feldspathic gneisses derived from igneous rocks, and some metavolcanic amphibolites as minor amounts of metasedimentary gneisses are also intercalated. The Nagssugtoqidian mobile belt, which I'll talk about later consist mainly of Archaen gneisses and thin layers of supracrustal rocks which are interlayered and formed

within the first type of material. Rinkian mobile belt consist of isoclinals folds and nappes as well as large open gneiss domes surrounded by rim synclines of metamorphosed supracrustal rocks. Finally the Ketilidian is typified by large late intrusive granite plutons and in the northern margin sediments and volcanic rocks overlie the Archaein gneisses (Henriksen et al., 2009).

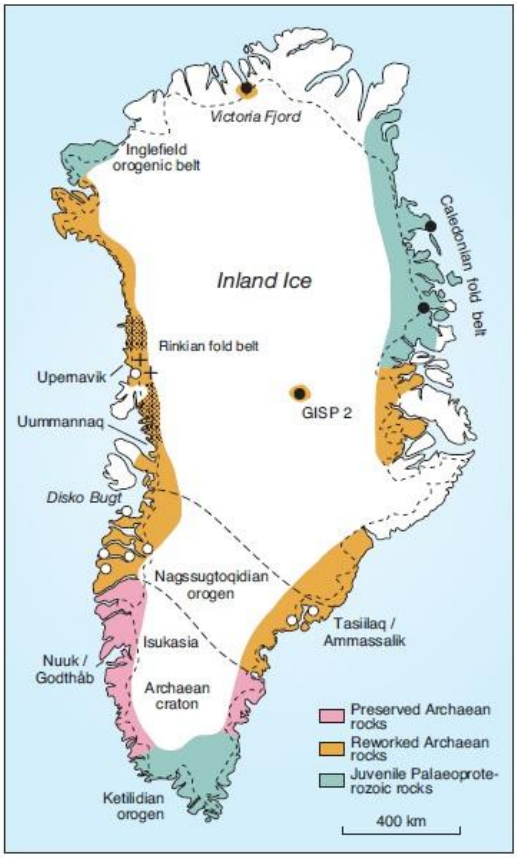

Figure 24: Simplified map showing the distribution of Archaen and Palaeoproterozoic basement provinces in Grenland (Henriksen et al., 2009)

On the other hand there are two Paleozoic fold belts: the Caledonian fold belt (in the North-East Greenland) and the North Greenland fold belt. The first fold belt contains extensive areas of Archaen and Proterozoic gneisses and the North Greenland fold belt, which is a continuation of the Innuitian orogenic system of Arctic Canada, is characterized by geosynclinals conditions and the accumulation of a thick clastic sequence.

4.2.3. Geology of Sisimiut

Sisimiut is placed in the Naqssugtoqidian mobile belt, which had its main phase of deformation and metamorphism around 2700 Ma ago although it was active till the Early-mid Proterozoic. Palaeoproterozoic supracrustal rocks (metasediments and metavolcanics) form thin layers together with the Archaen gneisses, which is the main component of this fold beld (figure 25). The basement gneisses are mostly granodioritic to quartz dioritic and in this zone they are light

grey amphibolite facies gneisses consisting of plagioclase, microcline, quartz, biotite and green hornblende with minor amounts of garnet. Although there is not an extreme difference between the Archaen rocks in the South of Sisimiut and the hypersthene gneisses that cover the intrusive complex it´s worth to mention that these gneisses were made in the Palaeoproterozoic (1910-1870 Ma). (Jensen et al. , 2001; Jensen and Secher, 2004 and Hollis et al, 2006). No large granite areas occur within the Nagssugtoqidian mobile belt in West Greenland. Nevertheless, between Sisimiut and Itivdleq (approximately 50 km South from Sisimiut) the basement gneisses appear to have been derived from granites due to less intense deformations. Thus, can be seen East from the Ulkebugten fjord, which lies next to Sisimiut.

Although nowadays the Sisimiut/Itilleq area lies approximately 200 km to the west of the present ice margin between Sondre Stromfjord and Nordre Isotoq (figure 25) this region has been dissected over multiple glacial cycles by SW-flowing outlet glaciers from the main ice sheet (Roberts et al., 2009). In the Quaternary, Greenland was almost completely covered by ice. Climatic oscillations led to shrinkage of the ice sheet and formation of interglacial deposits around the coasts (Escher and Watt, 1976). The earliest glacial deposits in West Greenland belong to the Fiskebanke glaciations (MIS 6; 130 ka), but these are only partially preserved on coastal mountains (Roberts et al., 2009). Thus, evidence of glacial erosion and deposition are still present in the mountains surrounding Sisimiut.

Although it's known that most main structures in West Greenland trend ENE-WSW, no specific faulting directions have been found for the surroundings of Sisimiut.

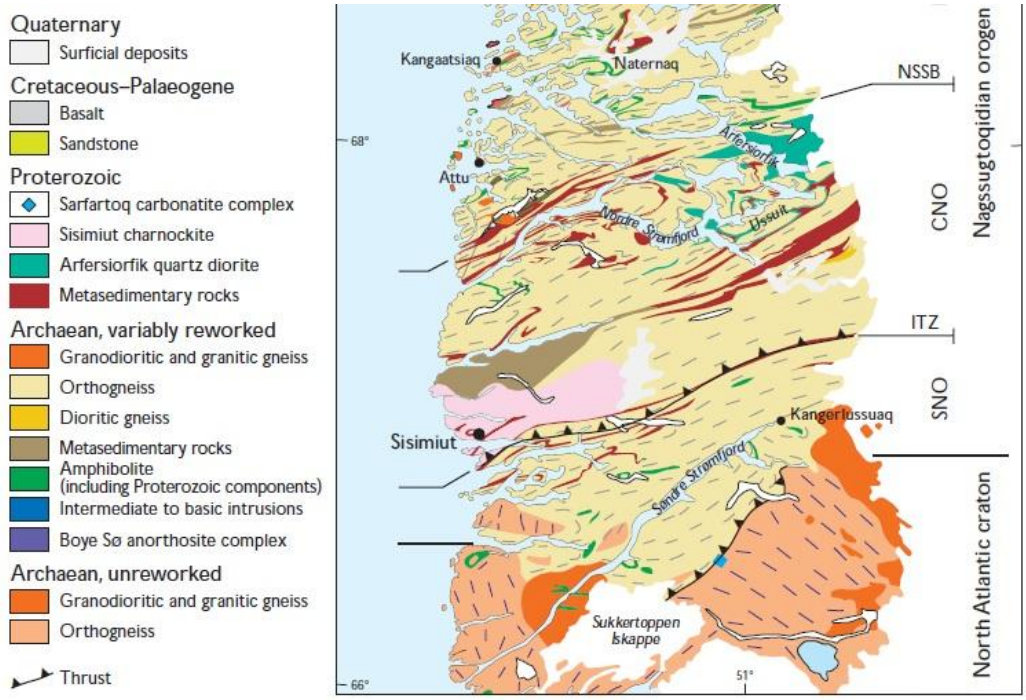

Figure 25: Geological map of the Nagssugtoqidian orogen, West Greenland (Hollis et al., 2006)

4.2.4. Rock Mass Classifications

Rock mass, as a discontinuous middle has a complex geomechanical behavior, which can be studied and categorized in a simplified way as a function of its probable use. In this way, rock mass geomechanical classifications appeared and with in situ observations and some easy to realize tests, quality index related to geomechanical parameters could be calculated (Vallejo, 2002).

Although rock mass classification schemes have been developed for over 100 years since Ritter in 1879 attempted to define an empirical approach to tunnel design, it has not been till 1946 when Terzaghi presented the first reference to the use of rock mass classificacion. Terzaghi estimated the rock loads carried by steel sets on the basis of a descriptive classification and classified the rock mass depending on the use for the design in tunnel supports. Afterwards, different rock classification methods have been presented and mostly all of them were developed from the civil engineering case in order to classify the material depending on its further use (Hoek, 2006).

During the viability and preliminary design stages of a project, when the amount of available information about rock mass and its stress and hydrologic characteristics is insufficient, the use of a rock mass classification scheme can be of considerable sake.

The characteristics of the rock mass which are considered in the different classification methods are the following:

- Intact rock strength
- Rock Quality Designation (RQD) Index
- Condition, spacing and orientation of discontinuities
- Geological structure and faults
- Groundwater outflows
- Strength state

Other factors as the method of excavation, the slope height and dip, the grade of weathering of the rock mass, etc. are only relevant in some rock mass classification methods. In the actuality the most used geomechanical classifications are the Rock Mass Rating (RMR) and the Rock Tunneling Quality Index (Q Index) but there are also others like the Geological Strength Index (GSI), Slope Stability Probability Classification (SSPC), Rock Mass Strength (RMS), etc. (Pantelidis, 2009).

Rock Quality Designation Index (RQD)

Deere developed in 1967 the rock quality designation index to provide a quantitative estimation of rock mass quality from drill core logs. The RQD is a parameter which estimates

the grade of fracture as its defined as the percentage of intact core pieces longer than 10 cm in the total length core.

$$RQD = \frac{\sum(length\ of\ core\ pieces\ \geq 10\ cm)}{Total\ length\ of\ core\ run} \cdot 100 \quad (4.5.)$$

When no test drilling is available but discontinuity traces are visible in surface exposures, the RQD can be estimated by the following formula which was suggested by Palmström (1982):

$$RQD = \begin{cases} 115 - 3{,}3\,J_v & for\ J_v > 4{,}5 \\ 100 & for\ J_v \leq 4{,}5 \end{cases} \quad (4.6.)$$

where J_v is the sum of the number of joints per unit length for all joint sets known as the volumetric joint count. As it can be seen from the formula, the RQD goes from 0 till 100 and while lower values than 25 % describe a poor quality rock an RQD over 90 % is for an excellent rock, with almost no discontinuities.

Although it's utility, this index doesn't consider some transcendental aspects like the orientation, separation, filling and other conditions of discontinuities and in this way it's not a sufficient value to describe rock mass (Vallejo, 2002). It's also a directionally dependent parameter and its value may change significantly depending upon the borehole orientation.

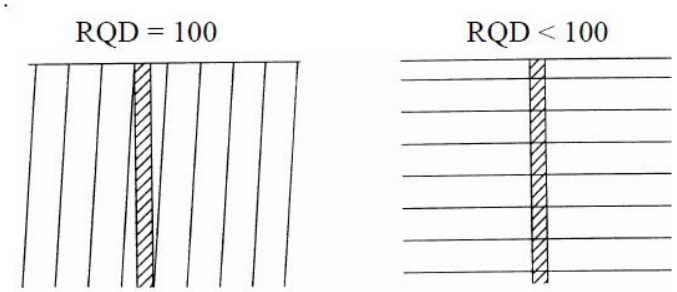

Figure 26: Evaluation of Rock Quality Designation Index (Deere et al., 1967)

Rock Mass Rating Classification (RMR)

Published by Bieniawski in 1973, with some actualization in 1979 and 1989, the Rock Mass Rating constitutes a system of rock mass classification which at the same time relates quality indexes with geotechnical, drilling and reinforcement parameters. The classification considers the following geomechanical parameters and gives each the following importance:

Parameter	Value
Resistance of intact rock – Uniaxial compressive strength -	0-15
RQD	0-20
Spacing of discontinuities	0-20
Condition of discontinuities (Longitud, aperture, roughness, infilling, weathering)	0-30

Table 1: Parameters participating in the evaluation of Rock Mass Rating

An exact evaluation of each parameter can be found in Annex A. When evaluating each of this parameters, 5 options are given, and each of this gives a different value to the characteristics,

which have to be summed altogether providing the total RMR. For its application its necessary to make some observations and field measurements, as they are the fundamentals of this method. This index can also vary between 0, which represents a very bad rock and 100, that describes a complete healthy rock. In applying this classification method, the rock mass is divided in zones that present more or less uniform geological characteristics. According to Bieniawski (1989), the following classification is given depending on the value of RMR:

Rock mass class	RMR
Very good rock	81-100
Good rock	61-80
Fair rock	41-60
Poor rock	21-40
Very poor rock	<20

Table 2: Classification of rock mass according to RMR

The calculation of the RMR index allows the estimation of strength parameter and deformability of the rock mass and establish its most probable behavior in diggings. Therefore its use has been centered in tunnel constructions, although Romana (1993) designed an adjustment of this classification for the use in slopes giving the Slope Mass Rating index. This index differs from the original one in the fact that it considers 4 additional parameters which evaluate the stability of the slope (Romana, 1993).

$$SMR = RMR + (F_1 \cdot F_2 \cdot F_3) + F_4 \quad (4.7.)$$

While the first three parameters are factors for the adjustment of the orientation of the discontinuities, the last one takes into account the digging technique that is going to be used.

Another modifications of the RMR is the Modified RMR, which takes the basic of the RMR and adjusts it to account for in situ and induced stresses, stress changes and the effects of blasting and weathering. The MRMR was developed to take into consideration different factors that affect mining applications (Pantelidis, 2009).

Rock Tunnelling Quality Index, Q

Developed by Barton, Lien and Lunde in 1974 after the study of a big number of tunnels, constitutes a classification system of rock mass which allows the estimation of geotechnical parameters and the design of reinforcements for tunnels and subterranean caves. The Q Index is based on a numerical evaluation of 6 parameters and varies on a logarithmic scale from 0,001 to a maximum of 1000. The definition of the Q Index is:

$$Q = \frac{RQD}{J_n} x \frac{J_r}{J_a} x \frac{J_w}{SRF} \quad (4.8.)$$

RQD is the Rock Quality Designation

Where:
- J_n is the joint set number
- J_r is the joint roughness number
- J_a is the joint alteration number
- J_w is the joint water reduction factor
- SRF is the stress reduction factor

Each of the 3 quotients has a different meaning: RQD/J_n represent the structure of the rock mass and is a measure of the block or particle size, J_r/J_a represents the roughness and frictional characteristics of the joint walls or filling materials and the last one consists of two stress parameters, the SRF which takes into account the total stress state and J_w, which is a measure of the water pressure that has an adverse effect on the shear strength reducing the effective normal stress (Vallejo, 2002). The following classification is used with the Q Index:

Value	Rock Quality
0.001-0.1	Extremely bad rock
0.1-1	Very bad quality rock
1-4	Bad quality rock
4-10	Medium quality rock
10-40	Good quality rock
40-100	Very good rock
100-1000	Extremely good rock

Table 3: Classification of rock mass according to Q Index

4.2.5. Uniaxial Compressive Strength (UCS)

As it has been seen in the different rock mass classification, the strength of intact rock is one of the most determinant parameters in civil engineering purposes. Among all the different physical (density, porosity, water absorption, durability, weakening, etc.) and mechanical (uniaxial compressive strength and deformability) properties, it has been considered that the most appropriate and necessary to the determinate is the UCS. The resistance to simple compression is the maximum strength that withstands a rock subjected to UCS, determinate through a test in a laboratory and is given by:

$$\sigma_c = \frac{F_c}{A} = \frac{Applied\ compressive\ strength}{Area\ of\ application} \quad (4.9.)$$

To determinate the UCS the following tests are used.

Uniaxial Compression Test

The most common laboratory test for UCS is the Uniaxial Compression test, in which also the Young Modulus E and the Poisson coefficient ϑ are determinate. The resistance and deformability test is done with cylindrical cores which are subjected to an axial force gradually increased till the fracture of the rock is reached (Rodríguez, 2007).

While this test method appears to be relatively simple, it is time-consuming, comparably expensive and requires carefully prepared rock samples, which are mostly very difficult to

extract. Considering this difficulties, this method hasn't been used in the current study, as others were simpler, quicker, and less costly rock test.

Schmidt Rebound Hammer Test

The Schmidt rebound hammer (SRH), originally developed to measure the surface hardness of concrete, is a common way to estimate the resistance of rock with an easy correlation. The SRH consist of a compact, lightweight and cost-effective device with a cylindrical geometry that has a dumper inside and a retractable end, which after being pressed against the rock makes the dumper jump. When realizing the test, a clear surface without discontinuities has to be identified and after the SRH should be pressed against the rock. Depending on the hardness of the rock, the dumper will suffer different rebound, which will be recorded on the device. At least 10 measurements should be taken excluding the 5 lowest values. The recorded rebounds are related with abacus to the uniaxial compressive strength. Nevertheless, the measurements of the SRH should be calibrated with data obtained from at least one laboratory test (Vallejo, 2002).

Figure 27: Schmidt rebound hammer test (Survey, 2011)

Point Load Test

The point load test is a strength index test for the classification of rock materials. Although it doesn't report the rock strength directly the point load test measures the rock strength with an index test. The samples will contain all the constituents of the in-situ rock mass in their original proportions and these will retain their strength and deformation properties, water content, density and porosity. Nevertheless, the structure of the rock mass may be disturbed and so the mentioned properties of the rock mass. As the evaluation of rock characterization and predictions of other strength parameters are based on statistical approaches the test data should consist of at least 10 single test, from which the two highest and two lowest values shall be deleted (ISRM, 1984). Considering that the rock qualities may be similar in the zone and that the number of test for a rock sample is at least 10, it has been pondered over that it

would be sufficiently to take a total amount of 30 rock samples, 10 in the lower zone of the chairlift, 10 in the middle altitude and 10 in the peak of the mountain.

The test is done by breaking a rock specimen fitted between two platen contact points separated a distance D. The system measures the load P to break the specimen. As it's not expected to find rock specimens in the form of either core or cut blocks, the irregular lump test is going to be done. These rock blocks should have the size of 50 ± 35 mm and the shape shown in the figures:

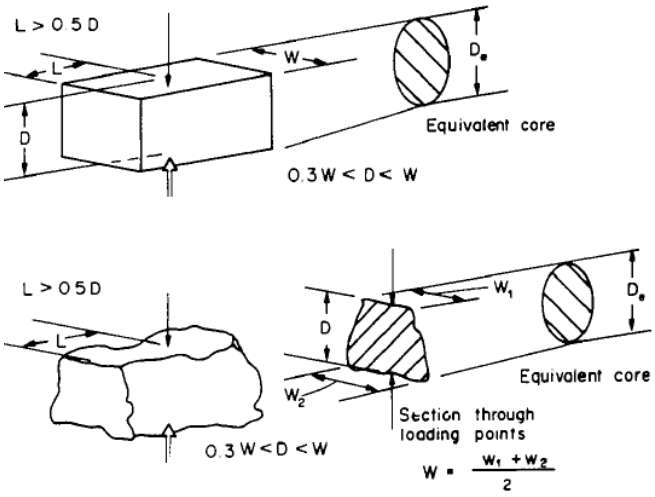

Figure 28: Specimens shape requirements for the block test and the irregular lump test (ISRM, 1984).

Figure 29: Point load index machine used in the Artek School

In order to get lumps of the established dimensions, the ratio D/W should be between 0,3 and 1,0 and the length L should be at least 0,5 W. If the width W is not parallel in both sides, this should be calculated by the average of both widths W_1 and W_2.

Once the rock specimens have been chosen with the explained limitations, and the breaking load P has been measured, the uncorrected point load strength I_s is determinate by:

$$I_S = \frac{P}{D_e^2} \qquad (4.10)$$

where $D_e = 4\frac{A}{\pi} = 4\frac{WD}{\pi}$ is the "equivalent core diameter" and A is the minimum cross sectional area of a plane through the platen contact point. Finally, as the value of I_s is defined as the diametral test for a rock specimen with D=50 mm, a correction for rock specimens with different size has to be done. The recommendation for the correction factor F is:

$$F = \left(\frac{D_e}{50}\right)^{0.45} \qquad (4.11)$$

After that, the point load strength index can be calculated by:

$$I_{s(50)} = F \cdot I_S \qquad (4.12)$$

The compressive strength is related with the point load index with the following empirical relationship (Bieniawski, 1989):

$$\sigma_c = 24 \cdot I_{s(50)} \qquad (4.13)$$

Geological Hammer

In addition to the testing techniques explained above, the intact rock strength can be estimated with simple test as the one involving the use of a geological hammer. The rock is then crumbled by manually done hammer blows. Hack and Huisman (2002) provided a list of such simple means and asserted that the estimation of rock strength using “simple means” is more representative for establishing the intact rock strength of a rock mass than establishing the intact rock strength through more elaborate testing.

5.State of The Art

As different themes are mentioned in this project, a brief introduction of the state of art in all the different aspects will be given in the continuation, considering the same order that has been used in the Theoretical Background analysis.

5.1. GPS Surveys and Topographic Maps in Greenland

Prior to the use of GPS satellites and the development of REFGR (Greenlandic Reference network), a triangulated survey network with more than 6000 points was used to determine Greenland's geodesy. This reference points were mainly surveyed with theodolites and a few of them were corrected with astronomical observations to locate the reference system in relation to the centre of the earth.

With the advent of Doppler satellite technology in the 1970s, Greenland's triangulated reference network was supplemented with 350 readings from the satellite based navigation system Navy Navigation Satellite System (NNSS)

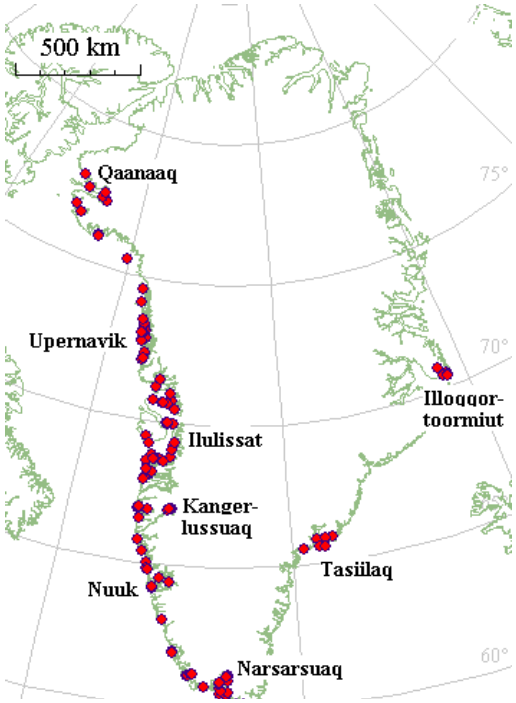

Figure 30: Reference points of GR96 reference system (Environment, 2011)

also known as NAVSAT or TRANSIT. After some decades, the need for a more accurate reference system in Greenland became evident with the use of GPS. Therefore, the National Survey and Cadastre established between 1996 and 2001 the Greenland reference system REFGR. The network consist of 258 GPS-surveyed points which are located in the most populated zones of Greenland (figure 30). In winter 2006 all Doppler observations included in the first aerotriangulation were recalculated and assigned coordinates within the new datum GR96 (Environment, 2011).

In the homepage of KMS all the GPS coordinates can be downloaded in 3 different projections: geographic and UTM 22N and 24N and 2 different Datums: GR96 and NAD83g (the adaption of WGS84 in Greenland called after the North American Datum of 1983). By downloading this data in the UTM 22N GR96 and projecting it in ArcGIS 10 it could be seen that the closest points laid at least 700 m away from the zone of interest, so that none of these point coordinates could be useful for the project.

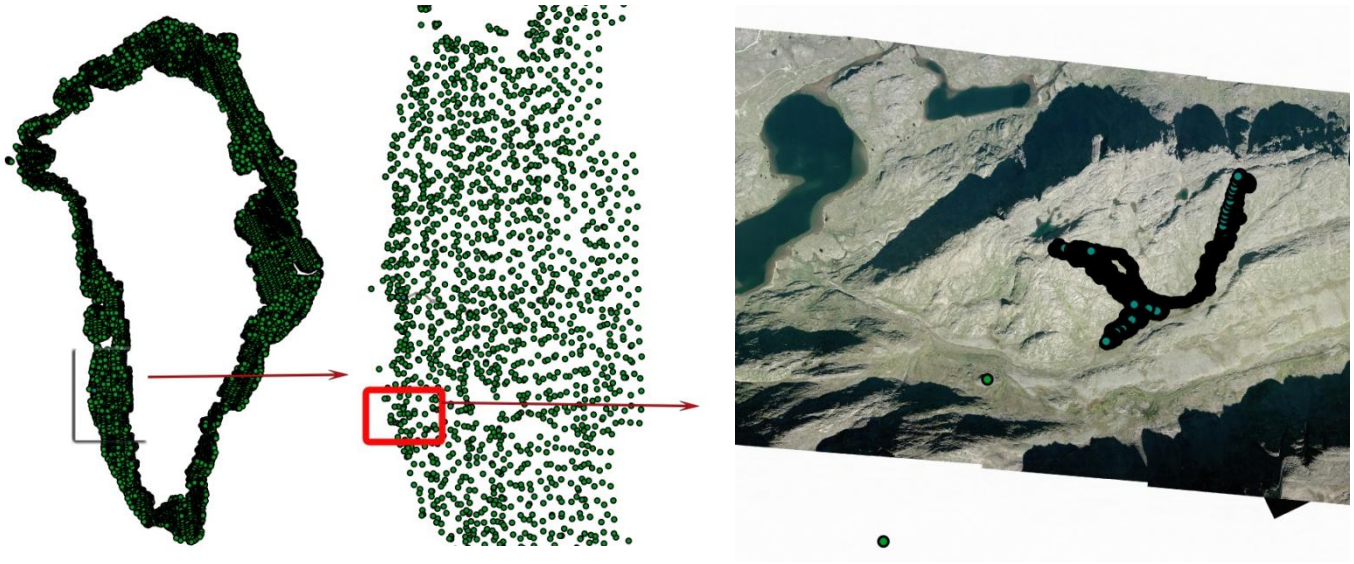

Table 4: GPS Measurements from KMS and the own GPS Measurements

NunaGIS is a governmental projected operated through a steering committee and by Asiaq. It's the official webGIS for all the administrations in Greenland. NunaGIS displays maps over all Greenland through the internet.

There are three different scales for the maps:

-1:250.000 for all of Greenland (+landsat photos) (analogue and old)

-1:100.000 for North-East Greenland (digital and new)

-1:5.000 for towns and settlements (+ortho photos) (also digital and new)

On top of these maps, different geographical information themes can be displayed from hunting districts to territorial boundaries and historical buildings (Department of Housing, 2011).

The second of the maps also displays contour lines with an equidistance of 100 meters around all the North-East of Greenland. Although it has the option of downloading the maps as an ESRI shapefile, MapInfo Tab, GML, GPX fil, Microstation DGN or csv, none of them displays the contour lines of the interested zone, as they just show the different thematic layers in different projections.

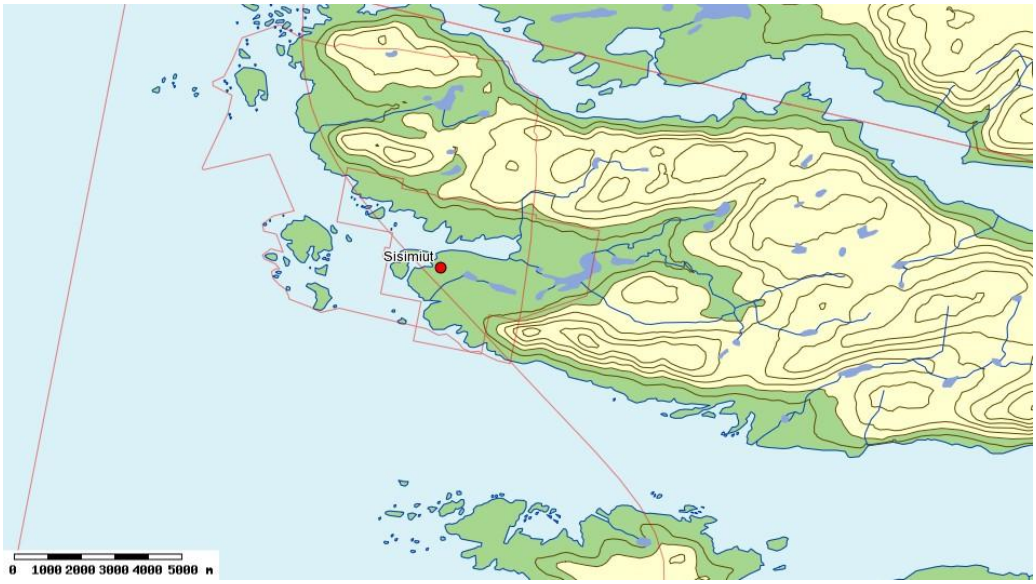

Figure 31: Map of Greenland 1:250.000 with contour lines of 100 meters of equidistance (Department of Housing, 2011)

Figure 32: Topographic map 1:100.000 with contour lines of 50 meters (Department of Housing, 2011)

On the other hand previous surveys realized by Artek in the surroundings of Sisimiut and Kangerlussuaq have obtained contour lines with equidistance of 2,0, 1,0 and 0,5 meters.

Although these maps have been done very close to Sisimiut, none of them represent the zone that was needed for the developing of this project.

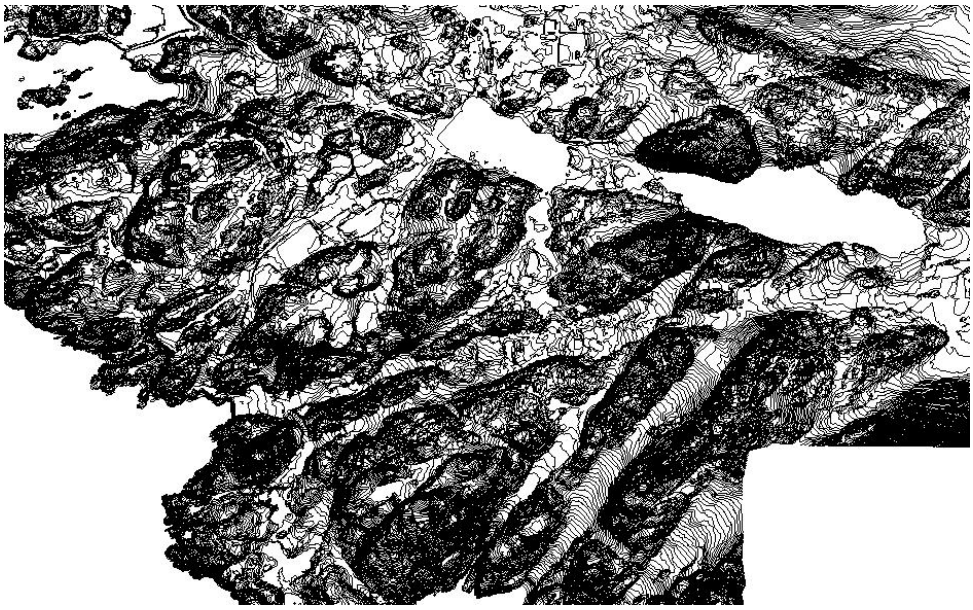

Figure 33: Topographic map from Sisimiut with contour lines of 1 meter of equidistance (done with MapInfo Professional)

5.2. Ortophoto and Other Elevation Data

In 2006 a lot of ortophotos along the 130 kilometers that separate Sisimiut and Kangerlussuaq were taken from a plane. The purpose of such project was to start prior investigations for the construction of a future road between both cities. With those ortophotos stereo photogrammetric methods were applied to acquire 85.300 points in a zone of approximately 35 km^2 with altitudes between -27 and 643 m. Although this points had just a spacing of 20 m additional measurements where considered necessary in order to obtain a better accuracy in the future traces of the ski lifts.

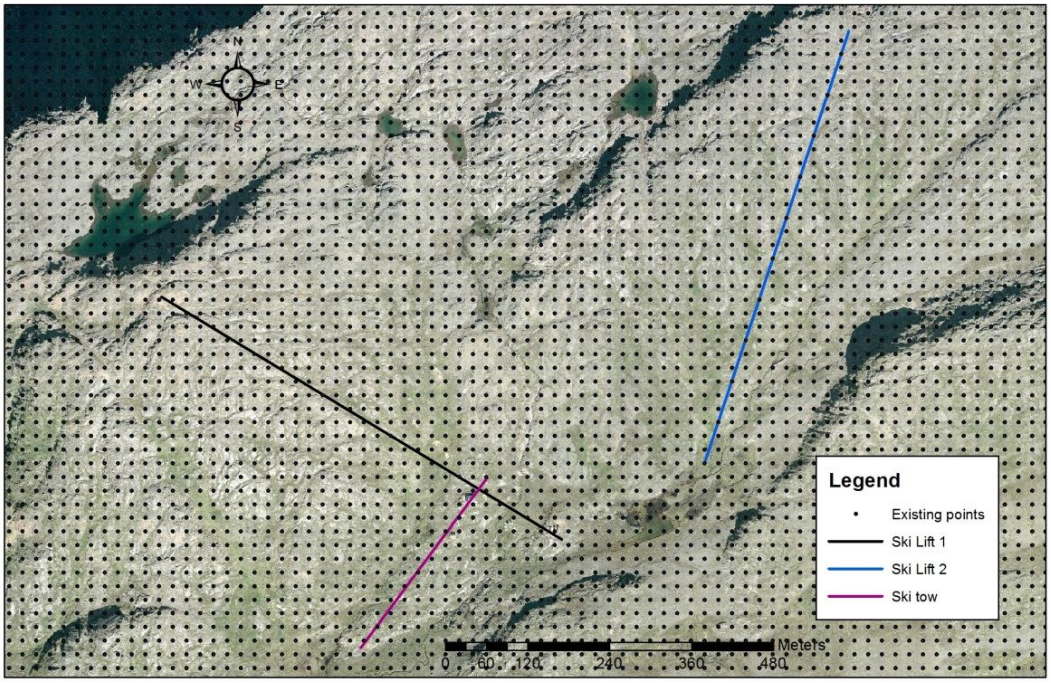

Figure 34: Existing Points and Planned Ski Lift Lines

5.3. Digital Elevation Models

In recent years, digital elevation models and altitude data has been available for the whole world. One of the first DEM available for the public has been GTOPO30, a global DEM with a horizontal grid spacing of 30 arc seconds (approximately 1 km) which was derived from several raster and vector sources of topographic information (USGS, 1998). Although, an elevation model of Greenland could be downloaded, none of this information was relevant to the project as the grid spacing was extremely large and no detail information could be downloaded. The Advanced Spaceborne Thermal Emission and Reflection Radiometer (ASTER) instrument has also a freely available DEM of the globe with much higher quality. Some information, like a digital elevation model of Nuuk is available but information about the specific area in this project could not been found (NASA, 2004).

The Shuttle Radar Topography Mission (SRTM) provides with another high accuracy DEM, where the United States of America are covered in a 1 arc-second grid (30 m) and the rest of the world is covered with 3 arc-second grid (90 m). Nevertheless, the information could not be downloaded as it's not able for public domain.

5.4. Rock Classification Methods in Sisimiut

According to the needs in different Artek projects previous geology investigations have been carried out in the surrounding of Sisimiut. Dahl (2009) made some investigations for the construction of a tunnel that should connect the first fjord with the second fjord North of

Sisimiut, in order to have a connection between the city and the hydropower plant. During his fieldwork which was developed in the surroundings of the hydropowerplant placed in the second fjord, Dahl measured the quality of the rock and classified it with the Q-Index method. His studies were based on field tests instead of optical descriptions, considering the following empirical relationship between the velocity of p-waves and the Q-Index:

$$Q = \frac{100 \cdot 10^{(vp-3.5)}}{\sigma_c} \qquad (5.1.)$$

Dahl estimated the Q-Index after having measured the uniaxial compressive strength of the rock, σ_c and the velocity of p-waves in a seismic survey. The obtained results can be seen in the following table:

Station	RQD	Q-værdi	Rock type	Kohæsion [Mpa]	Friktion [^{0}]	V_p [km/s]	E_{mass}[Gpa]
10	75	5	Gnejs-granit	5	30	3,5	14
20	75	5	Gnejs-granit	5	30	3,5	14
30	80	13	Gnejs-granit	10	45	4,5	23
40	80	9	Gnejs-granit	9	44	4,4	21
50	80	9	Gnejs-granit	9	44	4,4	21
60	80	9	Gnejs-granit	9	44	4,4	21
70	85	10	Gnejs-granit	9	44	4,4	21
80	85	17	Gnejs-granit	12	48	4,7	23
90	80	9	Gnejs-granit	9	44	4,4	21

Table 5: RQD and Q Index results from Mathias Dahl (Dahl, 2009)

During the evaluation of the Q-Index with the above mentioned formula, the UCS was already determinated with the point load index test and Schmidt hammer. On the other hand the friction angle and the cohesion have been estimated with empirical relationships with the Q-Index. As it can be seen the material North from Sisimiut is a granitic gneiss with medium quality rock up to good quality rock in some special locations.

5.5. Point Load Index Test

One of the first projects were point load index tests have been realized was also carried out by Mathias Dahl in summer 2009. In his technical studies for the construction in rocks in Greenland he also presented some measurements of point load indexes, which were done with samples taken from the lake Nalunnguarfik that supplies the city with water. The results for the compressive strength vary between 114,63 and 151,57 Mpa.

Holm (2011) realized the point load test to optimize the construction of the training site for mine and construction students at Sisimiut in August 2010. His specimens came from 1,5 km South of the city, and the results he obtained were slightly less than the normal measurements

for granodiorite. While it is expected that granodiorite has a compressive strength between 160 and 240 Mpa, Anders Holm obtained σ_c=114 Mpa. Nevertheless, his tests were done with samples that were taken from the zone were the garage of the mine had to be placed and not from the zone were the mine was going to be constructed.

On the other hand, Larsen (2008) realized a feasibility study for the construction of a swimming pool in the North of Sisimiut. The used samples had a strength of 94 Mpa, which were also slightly below the reported pressure forces for gneiss (160-280 Mpa), granite (160-240 Mpa) and amfobolit (154-280 Mpa), the rocks that predominated this area (Larsen, 2011).

Figure 35: Map of Sisimiut showing where the previous investigations were done. (Maps, 2011)

6.Fieldwork

6.1. GPS Measurements and Processing The Data

The GPS survey was realized along the already planned paths that should follow the different ski lifts. These tracks are the ones shown in the following picture.

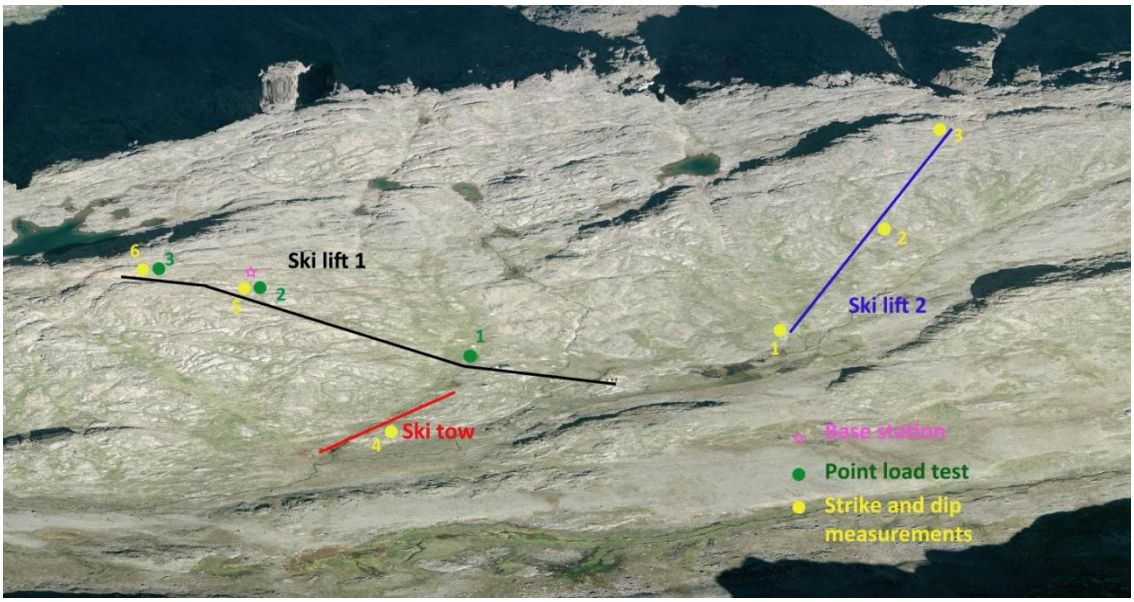

Figure 36: Aerial photography showing the location were the GPS measurements, Point load test samples and strike and dip measurements have been taken.

Considering that one of the most important parts of the ski lifts are the loading and unloading areas, special emphasis was taken in the base and the highest part of the mountain in order to have a special coverage of this parts.

6.1.1. Post-Processing Kinematic Survey

The most common types of GPS surveys are static and kinematic surveys. The first is done with a base receiver placed over an existing control station and other receivers, called rovers occupying stations with unknown coordinates. For the first session measurements are taken from all the receivers simultaneously along at least one hour and after all the rovers except one can be moved and measure other stations with unknown locations. The remaining rover will, in this second case, act like the base station in the first session (Wolf and Ghilani, 2008). On the other hand, in the kinematic survey the rover can be in continuous motion, allowing the user to take a lot of locations in a short period of time. Like these second type of survey is much productive than the first and it's able to obtain reasonable accuracy, a kinematic survey was realized.

In order to realize a kinematic survey, firstly a real time kinematic was tried as it provides immediate results. A repeater, which should be placed between the base station on the highest point of Sisimiut and the rover taking measurements in the valley where the ski lifts would be going to be constructed, should be transmitting the base receiver coordinates and its raw GPS observations to the rover. Nevertheless, from the repeater a clear sight of view is a requirement for the correct procedure of RTK during the entire survey to both: base station and rover. As this could not be fulfilled, considering that even at the highest point of the mountain the rover could not be seen during the measurements in most of the points, a post-processing kinematic survey was considered. In PPK surveys, the requirement is that the base receiver is collecting data at the same epoch rate as the rover. Normally, the base receiver is set over a reference station whose coordinates have been established from a prior static survey, but such points are almost impossible to find for specific surveys in Greenland.

In this way a TSC2 Controller with a Trimble R8 Antenna was placed almost in the top of the mountain realizing a static survey during the entire PPK survey. On the other hand a Trimble R8 VRS Rover was used to take all the measurements in the different points. The survey was done during the 10th, 11th and 13th of August.

6.1.2. Post-Processing The Data

Once the data was taken to get the coordinates of the points, this had to be processed as the observations of the rover were not corrected with the measurements of the base station. First the receiver files from both, the base station and the rover had to be converted from t01 extension (receiver file) to Rinex. Receiver Independent Exchange Format (Rinex) is data interchange format for raw GPS data and it consists of 3 ASCII file types: Observation data file

(.11o), Navigation data file (.11n) and Metereological data file (.11m). This task was done with the commandline tool teqc (Translate Edit Quality Check) and the program Convert to RINEX. The files from the base station in Kellyville was downloaded from the IGS Tracking Network homepage[1] as a compressed Rinex file (.11d) and had to be uncompressed with the program CRX2RNX to navigation and observation rinex files.

After all the conversion process, the files split in observation hours were merged in files that consisted in the observations of a whole day. At the same time, with the teqc commandline tool a quality check was undertaken and the bad observations were erased. Once this process was done, the post-processing of the data could be started with the Leica Geo Office 8.1. As an accurate positioning of the base station can be achieved by post-processing the base receiver's data with an established reference network station (Kellyville station) prior to the processing of the roving receiver positions, firstly a post-processing of the data of the base station and Kellyville station was done. In this case, the first station was considered as a Rover and the second as a Reference station. Once the post-processing of this data was done, the exact coordinates could be extracted of the base station, and afterwards establish in the post-processing of the rover data. In this second case, the rover data was post-processed with the Kellyvillle data (Reference station) and the base station (defined as Rover and whose coordinates have already been defined).

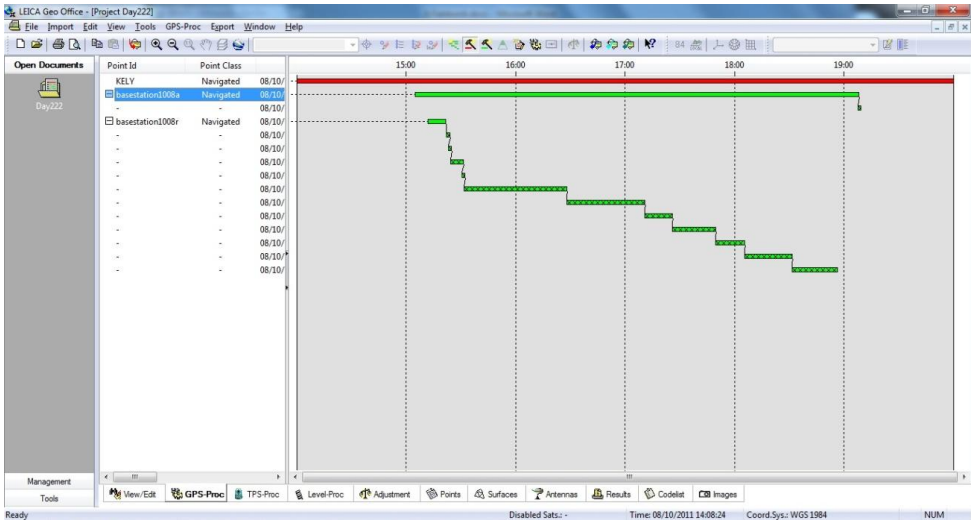

Figure 37: Leica Geo Office window when post-processing the data (Leica Geo Office, 2011)

After the post-processing the positions could be stored as a text-file either in the Geodetic or Cartesian coordinate system. The data was saved in the geodetic coordinate system and the positions were defined in degrees minutes and seconds, which had to be converted to decimal degrees for the correct importation in ArcGIS 10.

[1] http://igscb.jpl.nasa.gov/network/netindex.html

6.1.3. Coordinate Transformation

The GPS observations were defined in the reference ellipsoid World Geodetic System 84 (WGS84) and as it has been said their coordinates could be stored in the Cartesian coordinates (X,Y,Z) or in the Geodetic coordinates (longitude, latitude and height) (figures 38 and 29).

Figure 38: Cartesian coordinate system (Research, 2011)

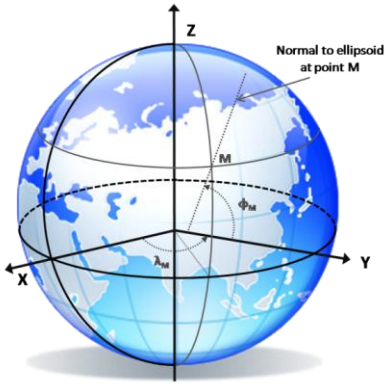

Figure 39: Geodetic coordinate system (Research, 2011)

Nevertheless, the height observations of the points needed to be corrected as they were defined over the WGS 84 reference ellipsoid, which is a simplified mathematical representation of the Earth. Despite, the Earth is a irregular surface and the heights are usually given according to the mean sea level, which doesn't coincide with the reference ellipsoid. In this way, the geoid surface is introduced as a equipotential surface which could coincide exactly with the mean ocean surface of the Earth in case the ocean were in equilibrium (figure 40). The orthometric height is the height above the geoid and differs from the ellipsoidal height by the geoid height, a value which differs from each position as the geoid is an imaginary surface which approximates the real shape of the Earth. As most of the GIS programs are not equipped with the Danish/Grenlandic reference system, the transformation of the coordinates has been done with the program developed by the Danish National Survey and Cadastre, KMSTrans.

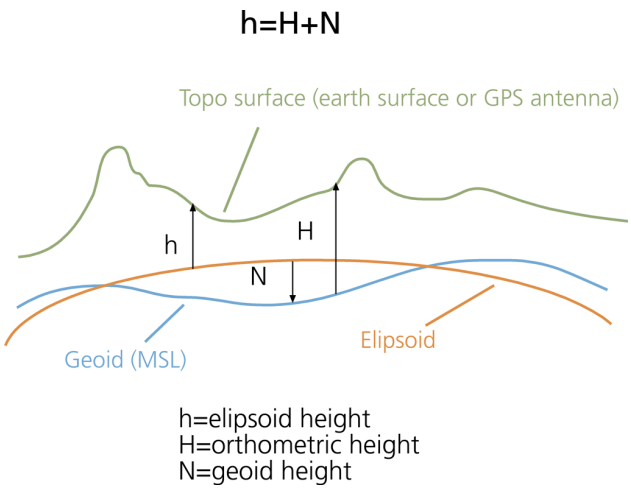

Figure 40: Representation of the difference between ellipsoidal height and geoid height (ESRI, 2010)

As an orthophoto taken from Sisimiut to Kangerlussuaq has been used to create the digital terrain model, and this had been defined in the UTM coordinate system, a transformation between the geographic coordinate system WGS84 and the projected UTM22N had to be done, before importing the points to ArcGIS 10. This could be done with the application of ArcGIS 10: Data Management Tools→ Projections and Transformations→Feature→Project. The Universal Transverse Mercator projections is a cylindrical projection of the Earth capable of reproducing a large extension North-South with a low amount of distorsion, that separates the Earth in 60 different zones of 6° of longitude in width. The zone in which this survey has been realized and Sisimiut lays is the UTM 22 North.

6.2. Geological Survey

A general description of rock mass needs to include the identification, conditions and general characteristics of the rock mass and all of its components: rock, soil, zones with water, single discontinuities, etc. A gradually procedure is going to be used, starting with a general description of the aspects and characteristics observables at a glance, that will set different zones more or less homogeneous in base to lithology, tectonic structure, etc. Afterwards, a detailed description and characterization is given of the different components that form the rock mass, and finally a geomechanical classification will be delivered.

6.2.1. General Description and Division in Similar Regions

As it has been mentioned before, the area was formed during the Palaeoproterozoic, although some reworked material from the Archaen is also present. Kimberlite, Archaen rocks and Supracrustal rocks are the most common materials.

Looking at the geological map of Sisimiut, the ski lift is going to be constructed in a mountain which is dipping 60° and almost facing North. At a first sight this can be confirmed and almost no extreme change can be observed along the mountain range. Nevertheless, a change in the facing direction can be observed between the region where the two chairlifts have to be placed, which is probably due to the presence of a small fault. Two small streams along the mountain give evidence of a more than probable fracture or discontinuity of the rock, but still the material remain unchanged.

Figure 41: The picture shows the two streams, one on the right side of the actual ski lift and the other left from the cabin.

The fieldwork was done in August, period when the most ice is defrosting and the most vegetation grows in Greenland. Dwarf scrubs and a lot of grass made it sometimes difficult to find a clear rock mass. Anyway it could be seen that the basic problem in the zone was some weathering processes, due to ice, wind, water, etc. that had suffered the rock, and that are the origin of a poor quality rock in the top, while on the ground of the hill a more good rock could be observed.

In this way, it has been though convenient to establish three different zones where to evaluate the rock mass depending on the height: one survey close to the actual placement of the cabin, another at a middle height and the last one on the top of the mountain. Anyway, due to the little observation change in strike direction, measurements of dip and strike have been taken for different placements like the one where the family chairlift and the basic chairlift are going to be constructed, although they will almost cover the same heights.

6.2.2. Characterization of The Intact Rock

Lithology: Identification and Description

Figure 42: Archaen Gneiss - Diorite

Figure 43: Charnockite

Figure 44: Archaen Gneiss

Figure 45: Charnokite

The four pictures that can be seen represent the most common rocks that have been found in the area. Their mineral composition is characterized by mica, feldspar, quartz, although some of the rocks also have some granate, magnesian ilmenite, pyroxene and even some have a little content in olivine.

The color of the rocks depends on the minerals that its compose of. Some minerals have characteristic colors, although the presence of other substances or impurities may let them change their color. Most of the rocks have an orange to reddish color, which may be due to the presence of magnesian ilmenite, granate and/or iron. Anyway the second mostly group of rocks just have white and black tones due to the main presence of mica, quartz and feldspar. Finally, some rocks tend to present a greenish color due to the presence of olivine.

The grain size of the rock makes reference to the dimensions of the minerals and the fragments of rock that compose the intact rock. In all of the rocks, the grain could be differentiated with an eye overlook and it was not considered very big, so that the best classification is a medium grain size, which is between 0.06 – 2 mm. Nevertheless, the size of

the minerals that compose the rock is more or less homogeneous as all of them have the same size. Regarding the foliation, none of them present a clear foliation in the rock, although some like the rock in figure 44, has an identifiable stratification of the minerals.

Porosity is not a characteristics of the rock founded in this area. None of the rock types have empty holes, so that it can be said that it is a massive rock.

Once that a brief description of the intact rock is given, a lithological classification can be realized. Probably the most common rock type that can be found in the area is the Sisimiut charnockite, which can be seen in figure 43 and 45. This magmatic rock with faces of granite and of gneiss has a granoblastic structure and is mainly composed of quartz, feldspar and hypersthenes. Other very common rock has been the Archaen gneiss, like the one in figure 42 and 44, which is a very typical rock formed by regional methamosphism, in which a sedimentary or igneous rock (like in this case) has been deeply buried and subjected to high pressures and temperatures. Gneiss is therefore characterized by foliation which is only clearly observable in figure 44. Another observed rock type is kimberlite, a volcanic rock, best known for sometimes containing diamonds and periodiotite.

Meteorization

The grade of meteorization in rock is an important observation as it conditions in a significant way its mechanical properties. While the process of weathering increases, porosity, permeability and deformability of the rock material increase, as well as, resistance decreases. In this case, the weathering is mainly only observed in the highest part of the mountain. The rock in this part is in some places almost disintegrated to a gravel and bleached to more brownish colors, due to the presence of other minerals. As it will be seen in the next section, the intact rock strength in this region of the mountain is considerably decreased due to weathering processes, which in this case are probably because of external factors, as temperature, humidity, wind, rain, snow and ice. Nevertheless, the meteorization of the rock could also be given due to changes in mineralogy, like the changes in color evidence or other processes.

Figure 46: Picture from the top of the mountain where the weathering process can clearly be seen (Evans, 2011)

Physical and Mechanical Properties (Point Load Index Test)

Different physical properties characterize an intact rock. Density, porosity, water absorption, swelling, resistance to abrasion, resistance to fragmentation, etc. are considered physical properties and resistance to uniaxial stress, traction and deformability are considered mechanical properties. As almost all of these properties have to be determinate by laboratory tests, only the most crucial constants have been calculated. In this way, the resistance to uniaxial stress has been determinate in two ways: the geological hammer and the point load index test. While doing these measurements also the density of the rock has been estimated. As it has been said before, three different altitudes where taken to see the influence of the weathering processes in this parameter.

-Low altitude: around the cabin

The base of both chairlifts should be placed around the actual cabin position. When realizing the geological survey with a geological hammer, it was noticed that at least 5 hammer blows were needed to break a normal rock. According to the ISRM this value stands for a σ_c between 50 and 100 MPa and represents a hard rock. On the other hand, rocks from the surroundings of the cabin were taken to determinate their resistance to uniaxial strength with the Point Load Index Test as mentioned before. As the first measurements of point load index were done with this rocks, a bigger amount of samples were taken in order to have a more accurate average in case mistakes were done. As most of the samples were lumps or blocks, the width of each sample was calculated with the average of the two widths measured in the plane of fracture. While A is the approximate area of the plane of fracture -D times W- the approximate

volume has been calculated by considering the rock block a regular block of length L and with a base equal to the area.

Just to have an approximation of the density, this has been calculated with the volume explained above. Finally, the average point load index and resistance to compression has been calculated without considering the two highest and lowest values, as it is explained in the ISRM (1984). As it can be seen in the table 6 (whereas the whole measurements can be found in the Annex C) the average $I_{s(50)}$=2,88 MPa and the resistance to uniaxial strength has been found equal to 69,1 MPa, which is the same result found with the geological hammer and represents a hard rock.

-Middle altitude

The middle altitude was considered to be around the position of the GPS base station, although the base station was placed a little bit more to the top of the mountain. The results with the geological hammer let to 3 to 5 hammer blows, the same result like in the surroundings of the cabin. Nevertheless, the stones taken from this placement and used for the point load index, let to a much higher value than expected. In this case the resistance to compressive strength obtained with the point load test was 131,4 MPa, a value representative for a very hard rock.

Although this second measurements were taken with less rocks than the first, it has to be said that the value of the compressive strength in this second test is probably more accurate than the one obtained in the first region. The first test was done with some stones taken from a place where some blasting were realized and the rock had suffered changes, which probably led to a decrease in compressive strength. Thus could be a reason for why the value of the point load index in lower altitudes is considerable lower than the one obtained in middle altitudes, although it could also be possible that some geological structures or processes around the valley in which the cabin is placed could let to a decrease of rock strength as well.

-Top of the mountain

On top of the mountain some rocks were broken with 1 or 2 blows, while others needed more than 8 blows to be broken. Nevertheless, the biggest amount of the rocks could be broken easily, as also shows the point load index test results. As it can be seen from the table 3 in Annex C, the strength used to brake the rocks in this case has been much lower than in the other two tests. It's clearly seen in the value of $I_{s(50)}$ that the resistance decreases as in this region the rock has been subjected to more weathering processes. The weathering was only clearly seen at the top of the mountain.

	$I_{s(50)}$ (Mpa)		σ_c (Mpa)	
Altitude	μ	s	μ	s
Bottom	2,88	0,94	69,1	22,5
Middle	5,48	1,16	113,4	27,9
Top	1,35	0,57	32,3	13,6

Table 6: Mean value (μ) and standard deviation (s) of the Point Load Index and the resistance to uniaxial stress

As it can be seen in the table 6, the standard deviation in each of the point load index tests for the different altitudes has been a little bit too high as it shows an excessive spreading of the values, specially in the first case. As said before, the first measurements were not taken with total equal material as some of them might have suffered from the blasting realized in the area and others not. Nevertheless, in the middle altitude -where no meteorization and weathering of the material has been observed- the compressive strength has been between the values that Holm (2010) and Larsen (2011) obtained, which were also lower than the ones expected for the respective materials: gneiss and granodiorite.

6.2.3. Description of Discontinuities

The discontinuities determine in a definitive way, the properties and the resistant, deformational and hydraulic behavior of the rock mass. The resistance of the discontinuities is the most important aspect in strong rock masses that present a lot of fractures and its estimation is necessary to define the characteristics and properties of the planes of discontinuity. The description and measurement of the following parameters in each family of discontinuities has to be done in the fieldwork in order to determinate the mechanical behavior and resistance of the discontinuities.

-Orientation

The systematic discontinuities are presented in families with almost homogeneous orientations and characteristics. The relative orientation and the spacing of the different families in a rock mass define the form of the blocks that determinate the rock mass. The orientation of the discontinuities is defined by its strike or dip and dip direction and both angles have been measured with a compass with clinometer (figure 48). As it has been seen that some faults between the placement of both chairlifts may produce a dipping direction change, it has been considered necessary to take measurements of these values in different places at the same altitudes.

It's important to mention, that the values of the strike and dip needed to be corrected with the magnetic declination, as the value given by the compass points to the magnetic North Pole and it's of real interest to have the angle with the geographic North Pole.

-Spacing

The spacing between two planes of discontinuity determine the size of the blocks in the rock mass and has therefore also a crucial job in the mechanical behavior of it. In rock mass with big spacing in the order of meters, the intact rock will be conditioning the processes of deformation and fracture, while in rock mass with shorter spaces, in the order of decimeter, the mechanical behavior will be subjected to the weak planes of discontinuities. The spacing is defined as the distance between two planes of the same family of discontinuities, measured at a perpendicular direction of these planes.

In most of the rock mass analyzed these parameter has been considered to be between 0,6 and 2 m, especially in the rock mass analyzed around the cabin and in middle altitudes, although in the rock mass in top of the mountain, discontinuities had smaller spacing between 0,2 and 0,6 m (figure 47). While the first type describes very separated discontinuities, the second represents some closer discontinuities. Nevertheless, the value is still far away to consider these kind of discontinuities as extremly close, as those are represented by spacing values of less than 20 mm.

Figure 47: Picture showing the spacing, cloase to the top of the mountain.

Figure 48: Taking strike and dip measurements during the fieldwork.

-Discontinuity Length (Persistence)

The continuity or persistence of a plane of discontinuity refers to its superficial extension, which is measured as the longitude along the direction of the plane and its dipping direction. It's a very important parameter although it's very difficult to quantify considering that most of

the rock masses can't be observed in three dimensions. In this case the big amount of vegetations presented in the area made it almost impossible to have a view in 3D of the blocks, so the estimated persistence is a very objective measurement. While in the lower and middle altitudes, when it was possible to see the three dimensions of the discontinuities, they seemed to have 1 to 3 m length, in the peak of the mountain, where it was much clearer to see, as less vegetation was presented and the discontinuities had less than 1 meter length. In both cases this values represent short persistent discontinuities, as in other cases with very long discontinuities they can go up to 20 m.

-Roughness

The roughness of a discontinuity may be an important factor influencing the shear strength of the discontinuity, as an increase in it lets to increase in shear strength, which at the same time decreases with bigger spacing and with the size of its infilling. Different techniques as linear profiling, have been applied along the years to estimate and give an order of magnitude of the roughness of the surface, but most of them needed a lot of effort. Nevertheless, a visual comparison with standard profiles of roughness has been applied in this case, a sufficient measurement to estimate it according to RMR classification. While the first rock masses analyzed had almost smooth or slightly rough plane surfaces along the discontinuities, the rock masses on the top of the mountain had rough and more undulated surfaces.

-Aperture and Infilling

As it has been said before, the aperture is another crucial parameter which influences the shear strength resistance of the discontinuity. This parameter changes a lot in different zones of the same rock mass, while the aperture can be considerably high in the surface, it can considerably decrease with the depth even to complete close the opening. In the rock masses that were analyzed most of the discontinuities had extended apertures, around values between 5 mm and some centimeters. These where mostly filled with soft material like sand and some vegetation, which can probably suffer important variations and let to changes in resistant properties.

-Groundwater Conditions

There are two different types of permeability in rock mass: primary permeability coming from filtration from the intact rock and secondary permeability which origins from water flow around the discontinuities (Vallejo, 2002). Mostly the water flow inside the rock mass comes from this second type of permeability. While the rock mass in top of the mountain were

completely dry, the ones observed in the lower altitudes were considered slightly humid, although in none of them the presence of water has been observed and it has only been determinate by the tact of the material inside the discontinuities.

6.2.4. Rock Mass Classifications

Rock Mass 1: Low Altitude

According to the descriptions given before, the following values for each coefficient of the Rock Mass Rating and Tunnel Quality Index were considered. As it can be seen, in the lower part of the mountain a good rock qualification with RMR=62 and with Q=12,5 has been obtained and in both cases the values are pretty close to a fair or medium quality rock.

	Parameter		Observed value	Assigned value	Max value
1	Strength of intact rock material (PLT Index and Geological hammer)		2,88 Mpa	7	15
2	Drill core Quality, RQD		100%	20	20
3	Spacing of discontinuity		0,6 - 2 m	15	20
4	Condition of discontinuities	Discontinuity length (persistance)	1-3 meters	4	6
		Separation (aperture)	> 5 mm	0	6
		Roughness	Slightly rough	3	6
		Infilling (gouge)	Soft filling > 5 mm	0	6
		Weathering	Moderately weathered	3	6
5	Groundwater inflow and general conditions		Damp	10	15
	Value of RMR			**62**	100

Table 7: RMR Evaluation of the first rock mass.

The RQD, which has been used in both classifications has been calculated with the formula suggested by Palmström, after measuring a J_v=2 (in 1 m^3 only 2 number of joints could be found).

	Parameter	Observation	Assgined value
1	RQD, Rock Quality Designation	100%	100
2	Jn, Joint set number	One joint set plus random	3
3	Jr, Joint Roughness number	Rock wall contact before 10 cm shear - Rough or irregular, undulating	3
4	Ja, Joint alteration number	Medium or low over-consolidation, softening clay mineral fillings	8
5	Jw, Joint water reduction	Dry excavation or minor inflow i.e. < 5l/m locally	1
6	Stress Reduction Factor, SRF	Competent rock, medium stress problems	1
	Tunnel Quality Index Q		**12,5**

Table 8: Evaluation of the Q Index in the first rock mass

Rock Mass 2: Middle Altitude

In this case, the values for RMR and Q Quality Index are 67 and 5,95, respectively. While the RMR gives us information about a good rock quality, the Q Index describes a more medium quality rock. From personal experience the RMR value could be more trustful, although it gives a slight higher value than the one obtained in the lower part of the mountain, which is the opposite that has been observed in the field as weathering problems increase with the altitude. Despite, the difference between both rock masses is not that high and the obtained value can be accepted without problems.

As in the first rock mass, the RQD was calculated after measuring the J_v, which in this case has been equal to 6.

	Parameter		Observed value	Assigned value	Max value
1	Strength of intact rock material (PLT Index and Geological hammer)		5.48 Mpa	12	15
2	Drill core Quality, RQD		95.2 %	20	20
3	Spacing of discontinuity		0,6 - 2 m	15	20
4	Condition of discontinuities	Discontinuity length (persistance)	1-3 meters	4	6
		Separation (aperture)	> 5 mm	0	6
		Roughness	Slightly rough	3	6
		Infilling (gouge)	Soft filling > 5 mm	0	6
		Weathering	Moderately weathered	3	6
5	Groundwater inflow and general conditions		Damp	10	15
	Value of RMR			**67**	100

Table 9: Evaluation of the RMR in the second rock mass

	Parameter	Observation	Assgined value
1	RQD, Rock Quality Designation	95.2 %	95,2
2	Jn, Joint set number	Two joint sets plus random	6
3	Jr, Joint Roughness number	Rock wall contact before 10 cm shear - Rough or irregular, undulating	3
4	Ja, Joint alteration number	Medium or low over-consolidation, softening clay mineral fillings	8
5	Jw, Joint water reduction	Dry excavation or minor inflow i.e. < 5l/m locally	1
6	Stress Reduction Factor, SRF	Competent rock, medium stress problems	1
	Tunnel Quality Index Q		**5,95**

Table 10: Evaluation of the Q Index in the second rock mass

Rock Mass 3: Highest Point

As it has been explained earlier, a lot of weathering of the rock material has been observed on top of the mountain. This problem was spread all around the top of the hill, although the grade of erosion process was quite different depending on the placement of the measurements. A more or less average point was used to obtain a real value of the rock quality. Although RMR

gives us information about a more fair rock, the Q Index suggests a very bad rock quality, as its value is between the bounders 0,1 and 1.

	Parameter		Observed value	Assigned value	Max value
1	Strength of intact rock material (PLT Index and Geological hammer)		1.35 Mpa	4	15
2	Drill core Quality, RQD		95.2%	20	20
3	Spacing of discontinuity		6-20 cm	8	20
4	Condition of discontinuities	Discontinuity length (persistance)	1-3 meters	4	6
		Separation (aperture)	> 5 mm	0	6
		Roughness	Slightly rough	3	6
		Infilling (gouge)	Soft filling > 5 mm	0	6
		Weathering	Moderately weathered	3	6
5	Groundwater inflow and general conditions		Damp	10	15
	Value of RMR			**52**	100

Table 11: Evaluation of the RMR in the third rock mass

	Parameter	Observation	Assgined value
1	RQD, Rock Quality Designation	95%	95,2
2	Jn, Joint set number	Three joint sets plus random	12
3	Jr, Joint Roughness number	Zones containing clay minerals thick enough to prevent rock wall contact	1
4	Ja, Joint alteration number	Zones or bands of disintegrated or crushed rock and clay	6
5	Jw, Joint water reduction	Dry excavation or minor inflow i.e. < 5l/m locally	1
6	Stress Reduction Factor, SRF	Competent rock,low stress near surface	2,5
	Tunnel Quality Index Q		**0,53**

Table 12: Evaluation of the Q Index in the third rock mass

Different authors as Bieniawski (1989) and Barton (1995) have suggested empirical correlations between both parameters – the RMR and the Q-Index-:

$$RMR = 9 \cdot \ln(Q) + 44 \qquad \text{(6.1.) Bieniawskis correlation}$$

$$RMR = 15 \cdot \log(Q) + 50 \qquad \text{(6.1.) Bartons correlation}$$

Other authors like Abad et. al. (1987) and Rutledge and Preston (1978) have also obtained similar correlations just differing in the result of parameters A and B. Comparing the obtained results in difference altitudes with the above formulas, it could be said that these approached considerably to both correlations, especially to Bartons. The worst correlation was obtained in the top altitude where RMR described a much better rock than the Q-Index, as already mentioned.

7.Analysis and Results

7.1. Digital Elevation Model Creation and Analysis

The Digital Elevation Model has been created with the GIS software ESRI ArcGIS 10 and all the different options that have been presented in the theoretical part have been tried in order to obtain the most suitable DEM. After adding all the GPS points and the ortophoto of Sisimiut taken in 2006 in the same coordinate system, an overview over the different points were done and some, which were laying in wrong positions were eliminated. Nevertheless, just 2 points around the cabin were considered laying in the wrong position and erased. Also other points were added close to specific places were the altitudes were the same, as for example the cabin and the lake, which were thought to lay in the same altitude. In this way, breaklines could be added to the TIN model and more information was available to create the raster model as well. When taking the GPS measurements, more points were taken around the water streams as the altitude was changing less abruptly around the stream. These higher density of points was clearly seen when representing the data in the map and also coincided with the placement of the water streams in the ortophoto. Therefore the points around those streams have been defined as other feature classes and afterwards converted to lines. The coordinates of the points mentioned in 5.2. have been also considered to create the DEM.

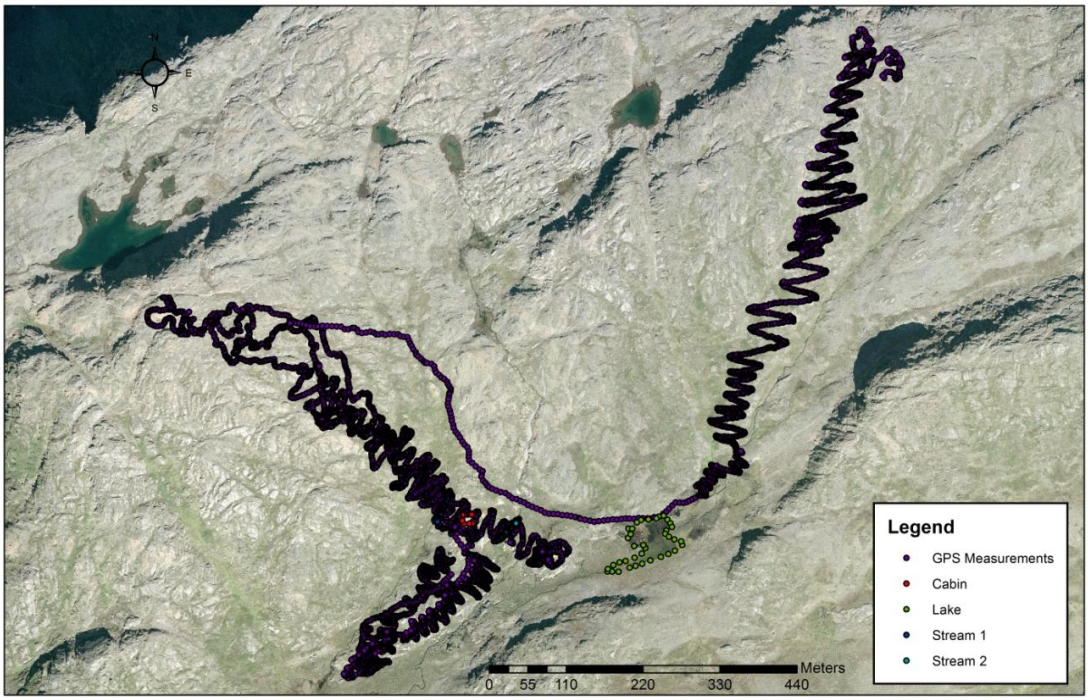

Figure 49: GPS Measurements following the expected ski tracks

7.1.1. TIN Model Considering the Existing Points

First of all a TIN model with the existing points and the GPS measurements was done with ArcGIS to see how the own taken GPS measurements fitted in the existing measurements. Although including both points a realistic 3D model of the whole area could be created, not all of them where included in the further analysis and just a brief selection in the surroundings of the interested zone were chosen after dismissing the ones that didn't match with the own measurements.

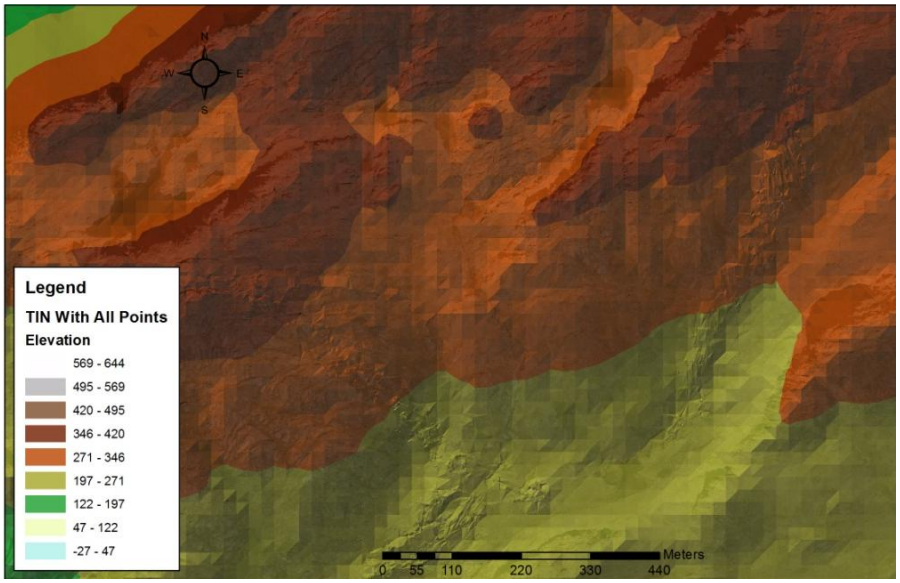

Figure 50: TIN with all the points in the ski resort area. While very equally distributed triangles have been created all around the terrain, small and thin triangles are present in the zone where the GPS measurements have been taken (distances in m).

Figure 51: 3D-Model created with the TIN Surface where the ski resort area can be found in the mountain placed at the right side of the figure (elaboration with ArcScene)

7.1.2. TIN Model

As the zone of interest is the one where the ski lift lines will be placed, and this zone has been extremely high covered with the GPS measurements the further analysis will only take into consideration this points and not the ones mentioned earlier. The application of the 3D Analysis extension in ArcGIS, TIN Management, easily creates a TIN when entering the GPS points as mass points in the input features (figure 52). Despite, polygons and lines can also be added to the input features as it has been done in the second option, when the water streams and the lakes have been considered as hard breaklines. In this way, breaklines define interruptions in surface smoothness, although the only observable difference between both results is that the output TIN considering the breaklines is done so that the line defining the stream or lake supports all the collidating triangles (figure 53). Finally, another available option in ArcGIS is to follow Delaunay triangulation everywhere also along breaklines (figure 54). Using traditional Dalaunay triangulation, breaklines are densified by the software to ensure that the resulting TIN remains Delaunay conforming. In the constrained Delaunay TINs are produced with fewer, long and skinny triangles, which are undesirable for surface analysis.

For further analysis the TIN surface obtained with all the breaklines (figure 53) was converted to raster surface as otherwise ArcGIS doesn't allow to make other types of analysis.

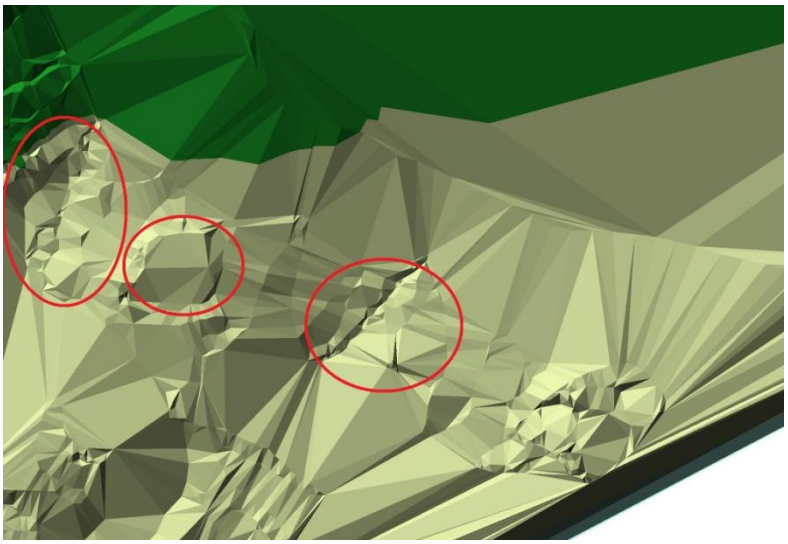

Figure 52: Option 1) TIN considering only the GPS Measurements

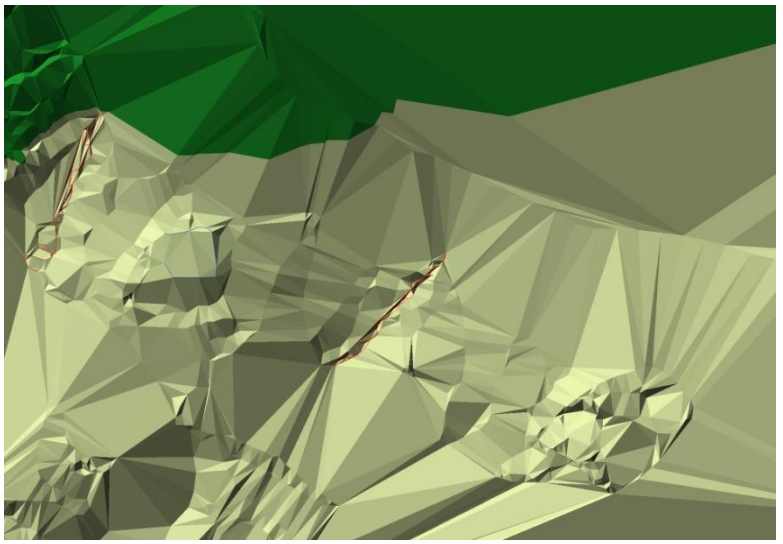

Figure 53: Option 2) TIN considering the lake, cabin and both water streams as hard breaklines

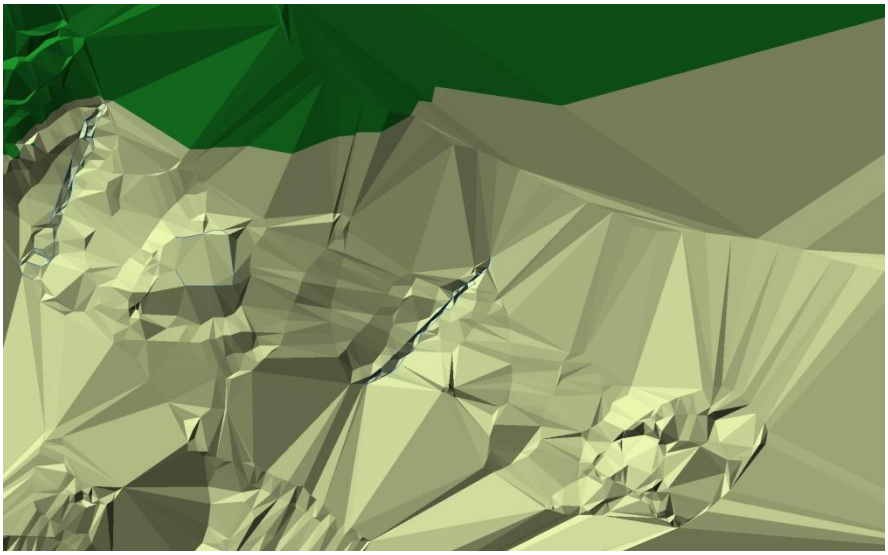

Figure 54: Option 3) Constrained Delaunay TIN with breaklines

7.1.3. Raster Interpolations

A raster surface could be created just considering the points were the GPS measurements have been taken and dismissing the pre existing points. In order to create a continuous raster surface all the different interpolation methods that have been presented earlier have been applied with the application Interpolation of the Spatial Analyst extension.

IDW

When applying IDW interpolation four different options will determine the feature of the output raster: cell size, power of the weight, search radius and input barrier each of whom changes the outcoming surface in a different way. In this way, an “equilibrium” has to be found between cell size, power and search radius as they affect the outcoming raster surface

in similar ways. To obtain a smooth surface a cell size of 0,371 m (1/10th of the cell size the program recommended) was used. The search radius had to be considered as a fixed search radius, due to when considering a variable search radius, points further away from the measurements were considered and their values were calculated taking into account points that were very far away. In this case, the outcoming raster surface had points whose values were calculated but without sense as they were estimated with other points that laid very far away to them. With this results a fixed search radius was established, so that the number of points that were considered in each interpolation were those laying inside a circle of a radius of a determinant distance: 18,55 m. The most important parameter was the power of the interpolation. Although a default value of 2 was the initially used parameter, after trying higher values it could be seen that by defining higher power values more emphasis could be put on the nearest points. Thus, nearby data would have the most influence, and the surface will have more detail. An optimal power value can be determined by minimizing the root mean square prediction error (RMSPE), which is a statistic that is calculated during cross-validation (ESRI, 2010). This procedure is characterized by predicting a known value of a point with the other measurements and in this way estimate the error.

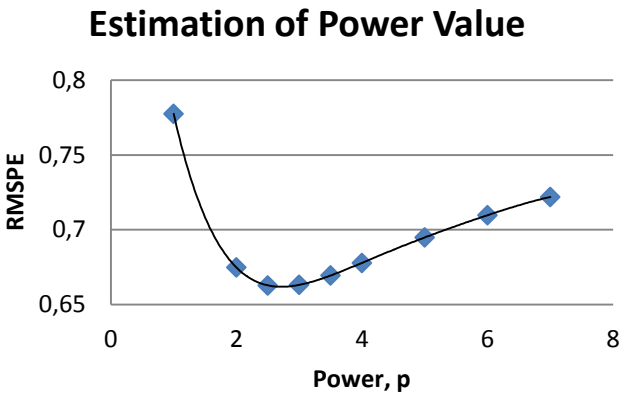

Figure 55: Estimation of the power value in the IDW minimizing the RMSPE with the power

After obtaining the RMSPE for different power values with the application Geostatical Analysis Wizard it could be seen that the RMSPE is minimized with a power value of 2,7.

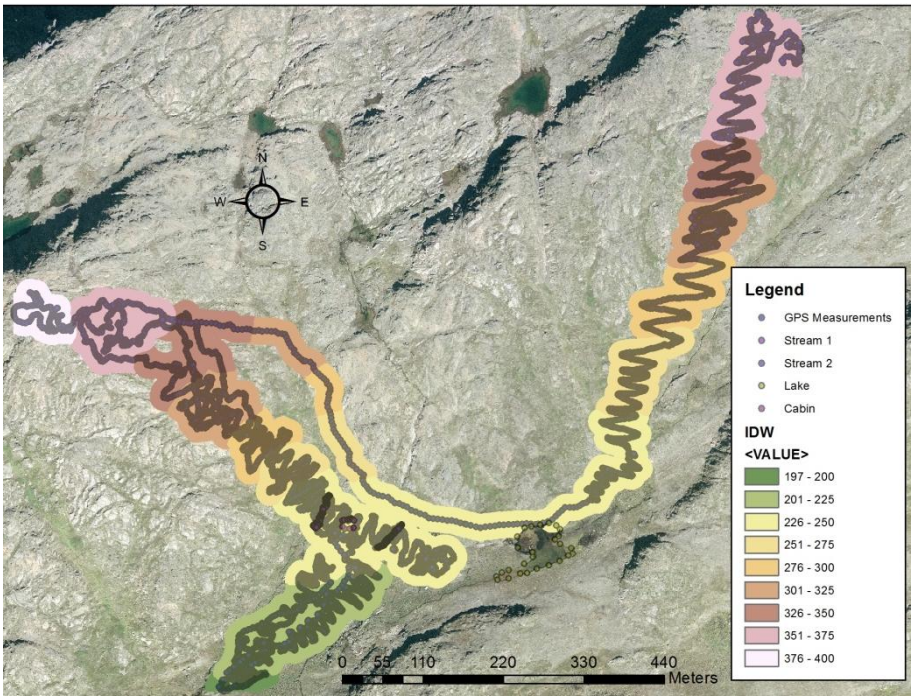

Figure 56: DEM (in meters) obtained with IDW interpolation (p=2,7; cell size 0,371 m and search radius distance 18,55 m)

Kriging

When applying Kriging as a interpolation method, the most important parameter to determinate is if Ordinary or Universal Kriging is going to be applied. Universal Kriging assumes that there is an overriding trend in the data (Drift) and it can be modeled by a deterministic function, a linear or polynomial function. As the elevation data has no drift, Universal Kriging should not be used as the obtained results have no significance. On the other hand, ordinary kriging allows to use 5 different semivariograms: circular, spherical, exponential, Gaussian or linear. Except of the linear model, which isn't a transitional model, as it even doesn't have a sill and it's usually used when a directional gradient is present in the analyzed surface, all the other methods have been analyzed with Geostatistical Analysis in ArcGIS and the most suitable has been found according to the Root Mean Square Error.

	Circular	Spherical	Exponential	Gaussian
RMS Error	0,6112157	0,6112119	0,611289	0,796624

Table 13: RMS Error with the different Semivariograms in the Kriging interpolation method

Except of the Gaussian model, which like the exponential semivariogram is an asymptotic model due to that both models don't have a real sill, none of the other models can be put before as their RMS errors are almost equal. Since the exponential model as mentioned doesn't have a zero autocorrelation, which would be logical for the rocky terrain that is going to be interpolated, this model has also been rejected. Finally, due to the more common use of

the spherical model and the similarity in the obtained results with both methods a spherical model was preferred.

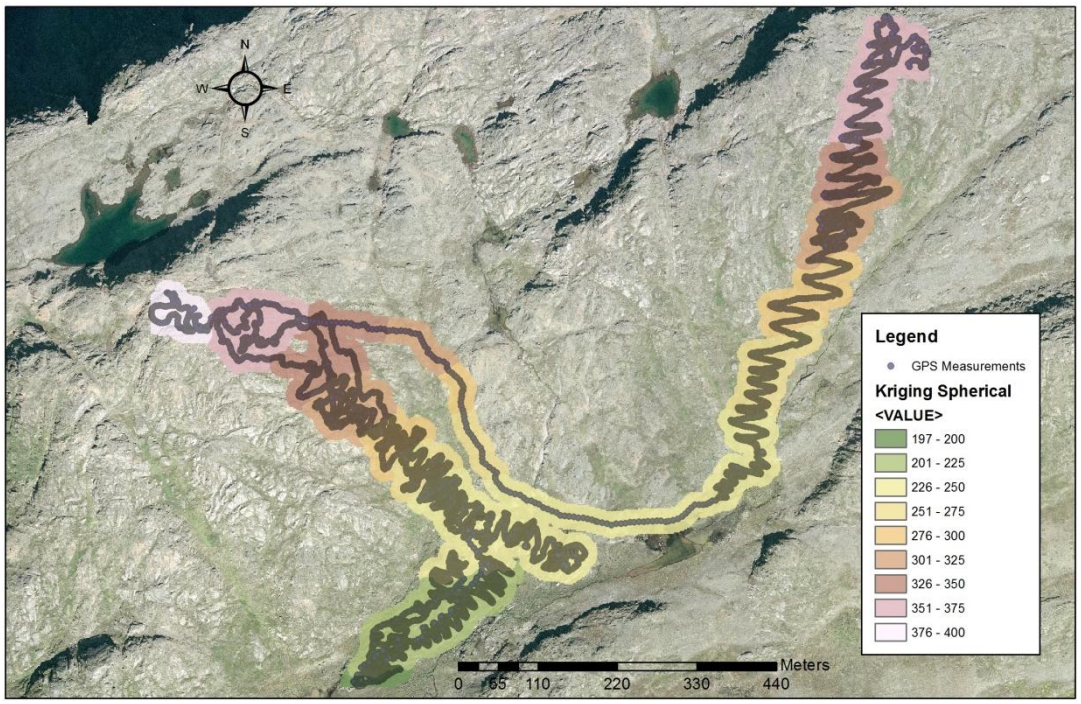

Figure 57: DEM (in meters) obtained with Kriging interpolation and a spherical semivariogram

Spline

Spline estimates the height values according to a mathematical function as mentioned before. Two types of spline interpolations can be used: regularized and tension. Although this interpolation method is best for generating gently varying surfaces, like elevation, it's not useful for this data, as it generates a rectangular surface not depending on the distance to the used values. It's probably a good estimation for the points in the surrounding of the measurements, but the created surface has an excessive extension and unnecessary values are estimated. These lets to altitude of unreasonable magnitude, as -2.400 m.

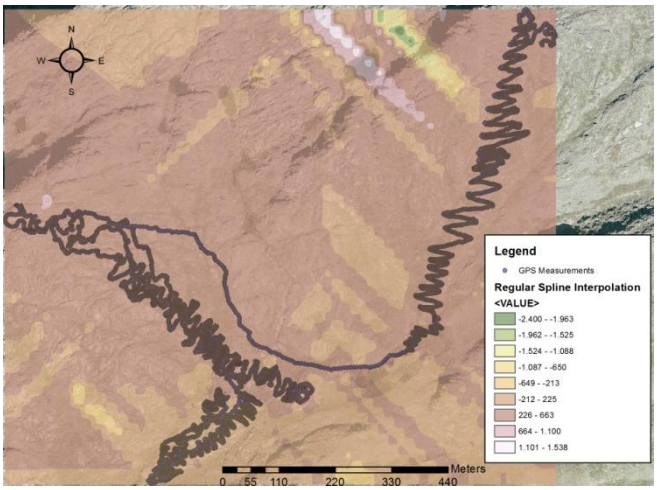

Figure 58: Regularized Spline Interpolation

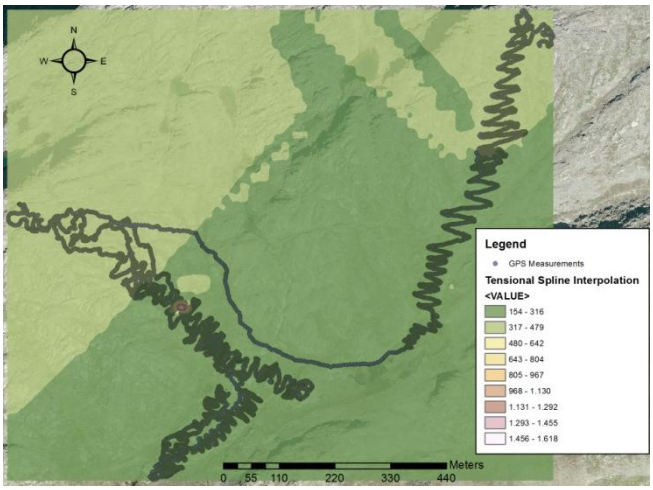

Figure 59: Tensional Spline Interpolation

Natural Neighbor

This type of interpolation has the problem that it interpolates points inside areas of the taken measurements. In this way a lot of points are being estimated in the inside the trace of the GPS measurements with values from very far away of placed points and no points are estimated in the borders of the GPS trace, so that the measurements in the contour aren't present in the raster surface.

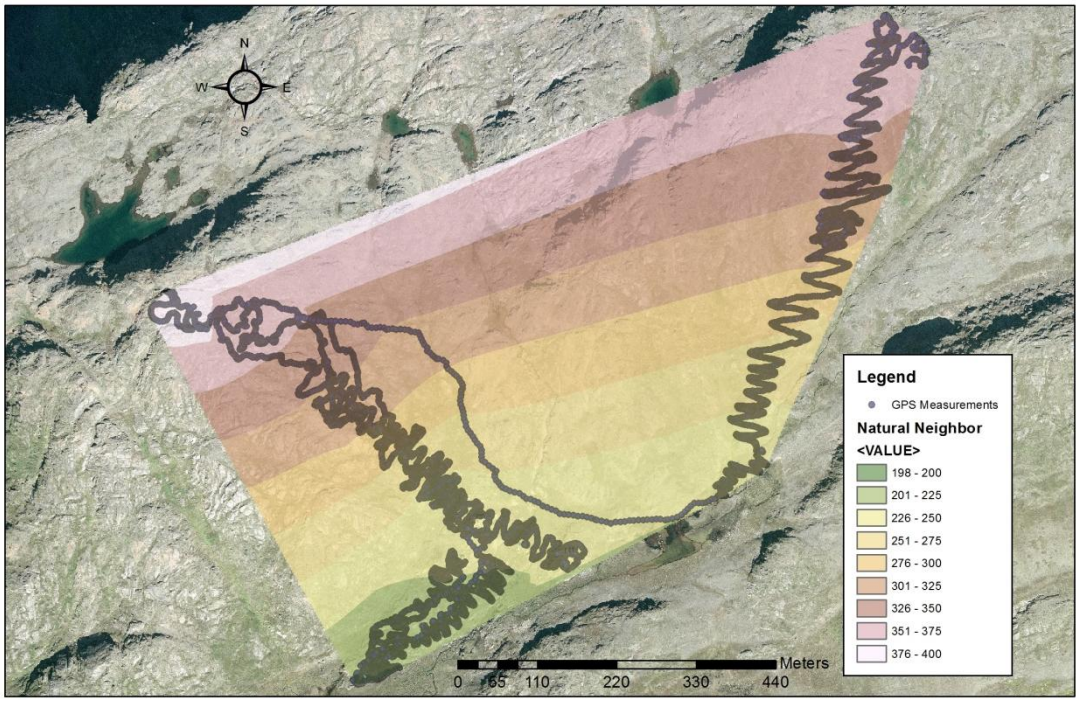

Figure 60: DEM (in meters) with Natural neighbor interpolation

7.1.4. Contour Lines

Once the raster surfaces were established the contour lines could be drawn on the map. As the contour lines obtained just considering the GPS measurements were not sufficiently precise, due to the lack of information in the areas surrounding the GPS points, the points obtained from other sources were also used to create them. A equidistance of 5 m was considered enough as less space would create a surface with a extreme high density of lines where nothing could be distinguished. The contour lines were created with the raster surface obtained from the TIN surface.

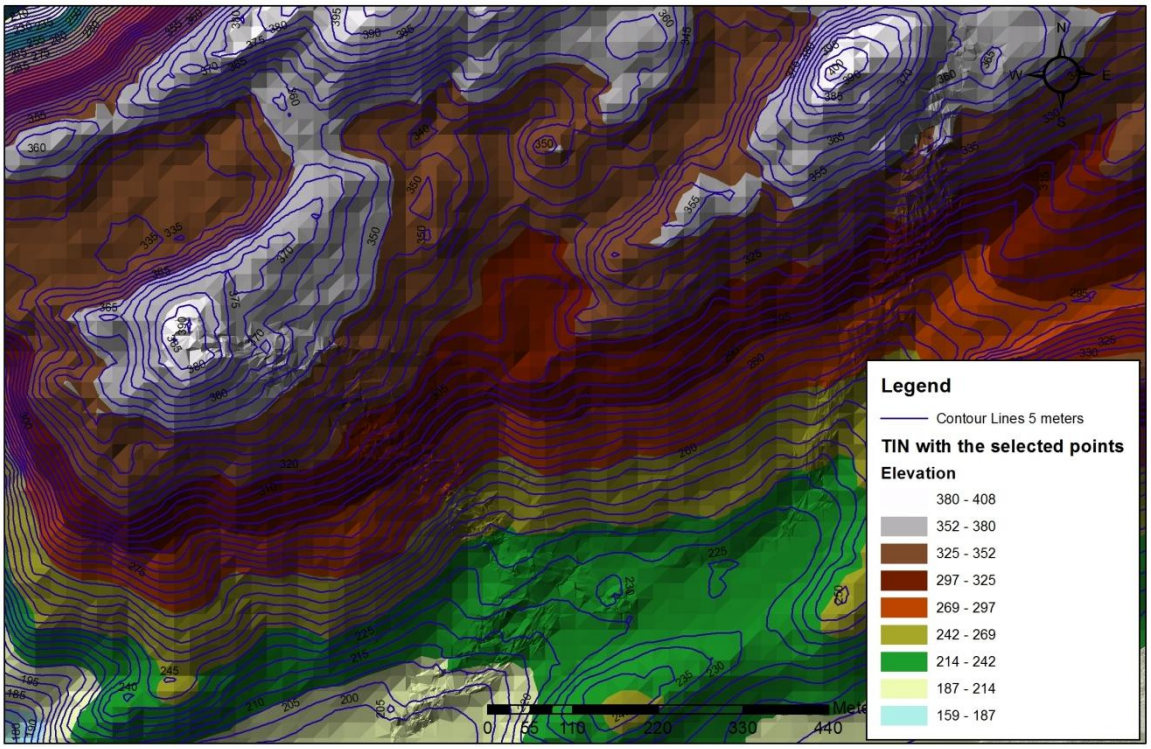

Figure 61: Contour lines and DEM (in meters) from the raster surface of triangulate irregular network

7.1.5. Aspect and Slope

Other important data that needed to be analyzed in a digital elevation model is the aspect and slope, also for the following kinematic analysis. These analysis was done with the same raster surfaces like the contour lines were drawn: the raster surface obtained after realizing TIN considering all breaklines and only the GPS points and raster surface of IDW interpolation.

Aspect:

The aspect identifies the down slope direction of the maximum rate of change in value from each cell to its neighbors and can be thought of as the slope direction (ESRI, 2010). The values of each cell in the output raster indicate the compass direction that the surface faces at that location.

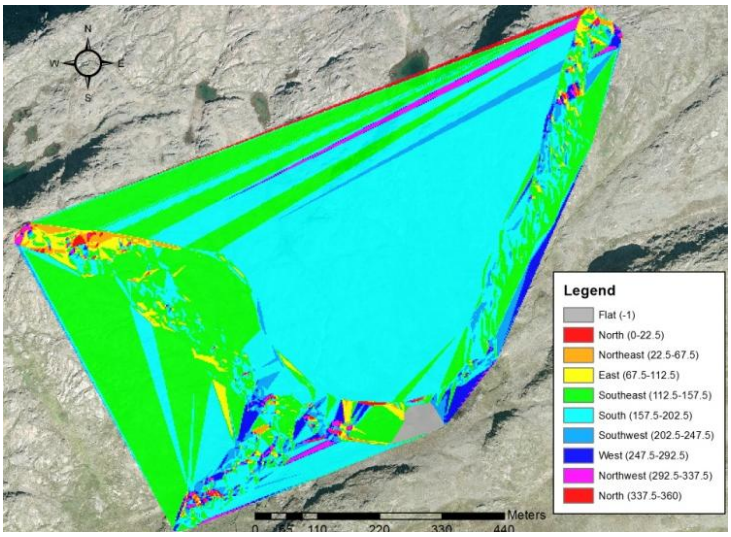

Figure 62: Aspect with the raster surface obtained after a TIN.

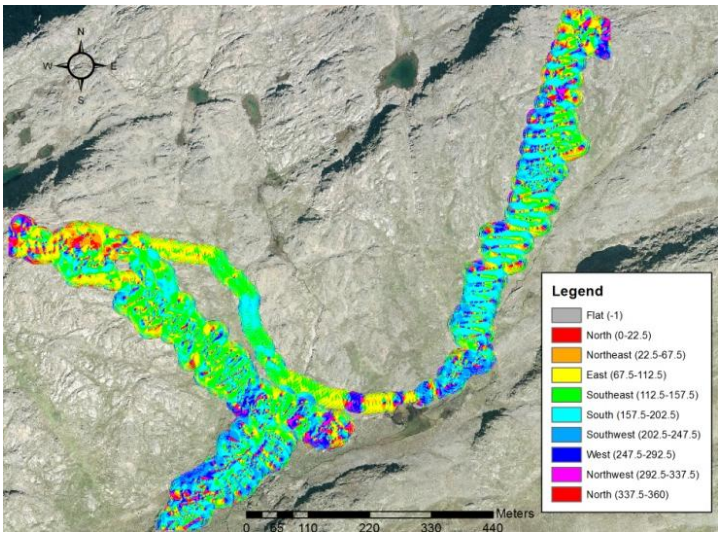

Figure 63: Aspect from the raster surface obtained with IDW interpolation

As it can be seen in the pictures, the results in the raster surface obtained with TIN are more homogenous due to the bigger extension of the triangles in comparison with the cells used in the raster surface. Nevertheless the same trends are seen in both analysis.

Slope:

The slope is calculated as the maximum rate of change in value from a specific cell to its neighbors (ESRI, 2010). The maximum change in elevation over the distance between the cell and its eight neighbors identifies the steepest downhill descent from the cell.

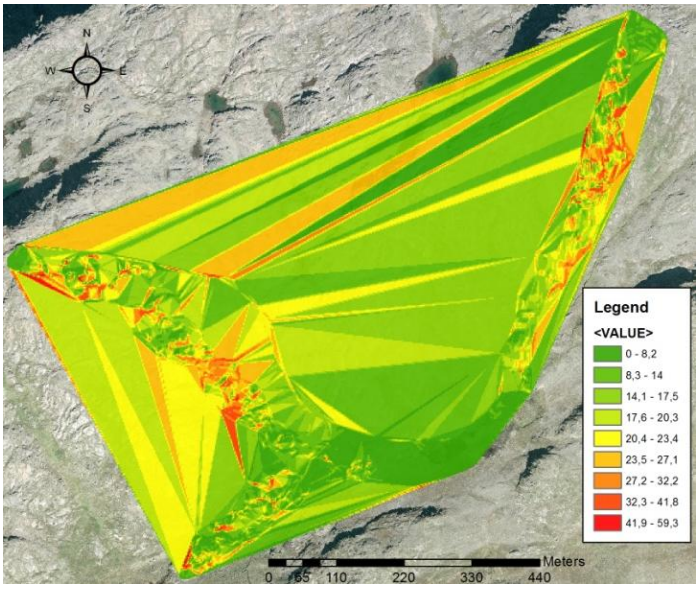

Figure 64: Slope analysis of the raster surface obtained after a TIN.

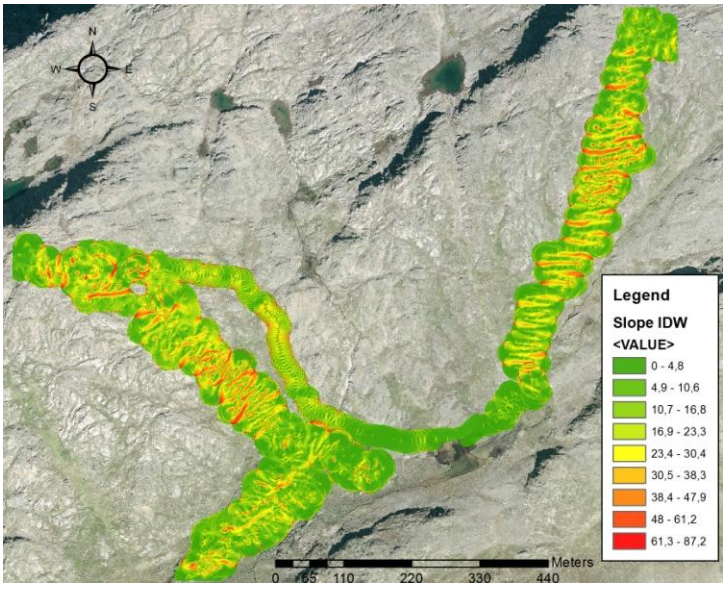

Figure 65: Slope analysis of the raster surface obtained with IDW interpolation

As it can be seen in the raster surface steeper slope faces have been found in this representation. When taking small cell size for the raster interpolation, close points can have higher altitude difference than with the TIN interpolation and therefore the slope faces of some points are steeper in the raster surface.

7.1.6. Profiles

Three profiles were taken from the planned location of the 2 ski lifts and one of the ski tow. A profile can be created interpolating a 3D line in the terrain and using after the Profile Graph Tool.

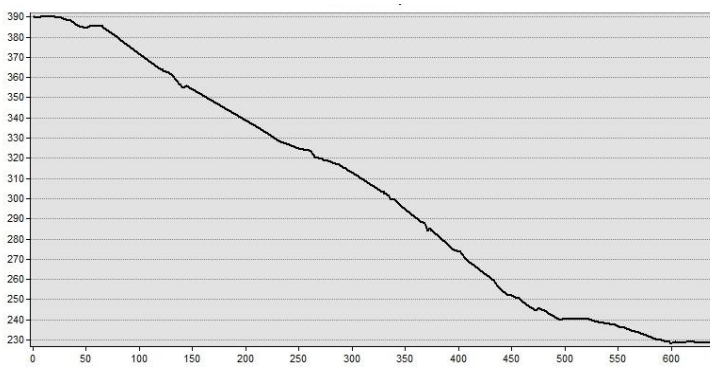

Figure 66: Profile of the location where the first ski lift is going to be constructed (distance and elevation in m)

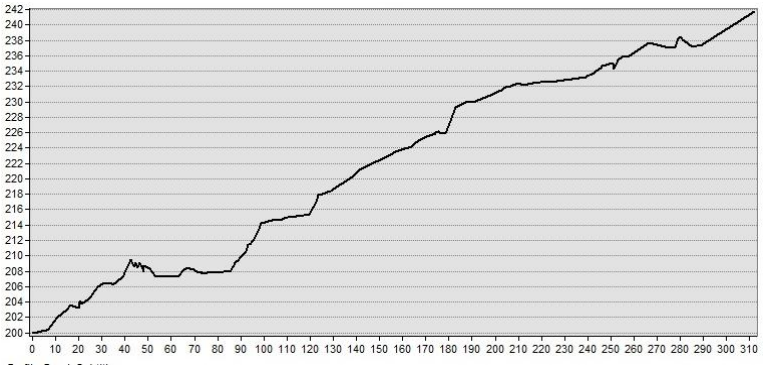

Figure 67: Profile of the location where the ski tow is going to be constructed (distance and elevation in m)

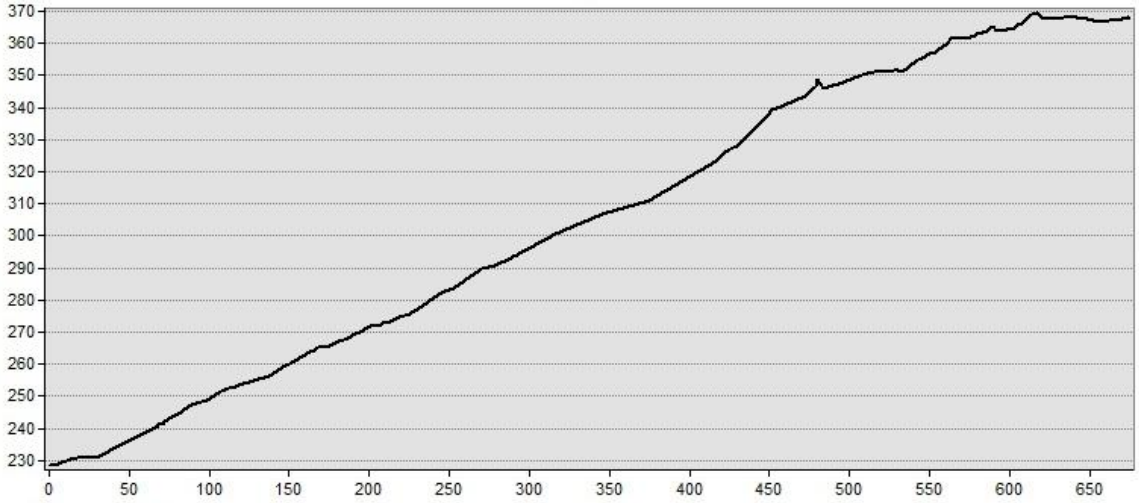

Figure 68: Profile of the location where the second ski lift is going to be constructed (distance and elevation in m)

7.2. Kinematic Analysis of Rock Slope Failure

Nowadays different slope stability analysis methods have been presented in order to design safe slope and determinate instability problems. These could be basically classified in deterministic methods, where the properties of the rock slope are known and the laws that

determine the failure can be established and probabilitstics, where the probability of slope failure is calculated considering specific rock slope failure conditions (Wyllie and Mah, 2005). Probably, the most common method is the deterministic where the ultimate state limit of the slope is calculated evaluating the stabilizing and the destabilizing forces, although other methods as the Hoek and Bray abacus or Taylors method are also used. Nevertheless, another well known analysis method is the kinematic, which is a purely geometric method as it examines the possible failures of the rock mass with respect to an existing or proposed rock slope (Kliche, 1999 and Yang and Lim, 2004).

In this geometric method, the analysis of failure is done after examining the orientation of the combination of discontinuities, the slope face, the upper or any other slope surface of interest and the friction of the rock mass, while the cohesion is ignored. Rejection of cohesion and the assumption that all the discontinuities are continuous and through going, when in reality they aren't, makes this type of analysis be a conservative method as it doesn't consider some stabilizing factors in the rock mass. The usual rock failure types that are analyzed in such a method are: planar, wedge, circular and toppling failure (Kliche, 1999).

7.2.1. Pole Density and Great Circles in The Different Analyzed Structural Domains

Due to the previous observations strike and dip observations were taken in 6 different locations, as rock quality decreased with altitude and some small faults observed between the location of ski lift 1 and 2 may let to strike and dip changes. The exact locations of these measurements can be observed in the figure 36 in the fieldwork description.

To realize a kinematic analysis with strike and dip measurements, first of all a brief stereographic analysis of the structural geology has to be done. Between 20 to 40 different strike and dip measurements have been taken in each rock mass so the most likely orientation of each set has to be determinate. By contouring the plot of the different poles of each plane of discontinuity, the most highly concentrated areas of poles can be more easily identified. In this way, the contouring package based on 1% area of the total area of Stereonet contained in the Stereonet program has realize a contour plot (figure 69). This density analysis can manually be done with the Kalsbeek contouring plot. Finally, a Bingham axial distribution which is a directional statistic whose theoretical background won't be discussed here, determines the predominant directions in each of the different analyzed rock masses (figure 70).

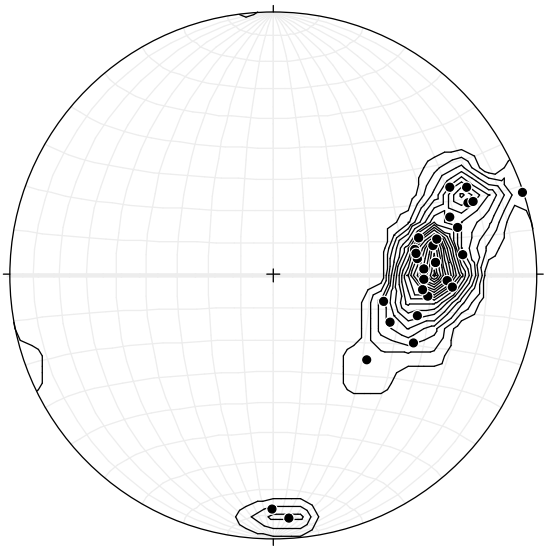

Figure 69: Schmidts equally-area contouring net, with the poles and density analysis of structural domain 1 (Stereonet).

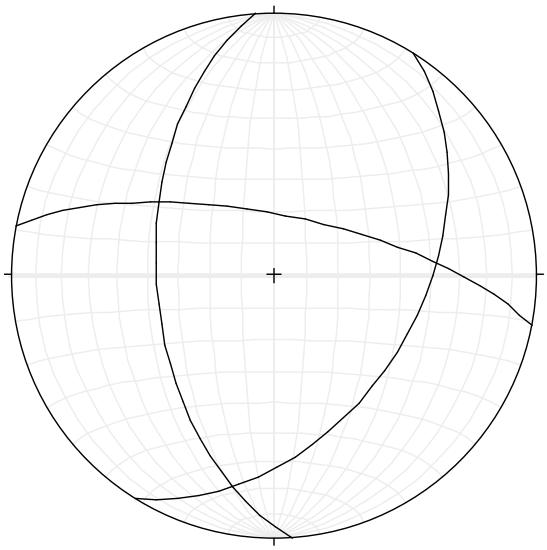

Figure 70: Schmidts equally-area countouring net, with the main planes obtained after the Bingham axial distribution (Stereonet).

The different contouring plots of each rock mass and the great circles of each of the more predominant discontinuity planes can be seen in Annex D.

7.2.2. Characterization of The Rock Slope

As it has been mentioned before, the other important thing that has to be determinate before realizing the kinematic analysis is the rock slope and the frictional angle of the rock mass. During the fieldwork, 3 different locations of rock mass have been analyzed and according to the obtained Rock Mass Rating evaluation, the Mohr-Coulomb parameters can be estimated with the following empirical relationships (Bieniawski, 1989), where c is the cohesion and φ the frictional angle.

$$c = 5 \cdot RMR\ (KPa) \qquad (7.1.)$$

$$\varphi = 5 + \frac{RMR}{2}\ (degrees) \quad (7.2.)$$

For the different rock masses that have been studied the values detailed in the next table were obtained:

	Rock mass 1	Rock mass 2	Rock mass 3
RMR	62	67	52
c (Kpa)	310	335	260
φ (deg)	36	38,5	31

Table 14: Cohesion and friction angle in the different rock masses

These values are a little bit higher than the ones expected for the materials recognized in the geological field survey, as according to Hoek and Bray (1981) gneisses and granites have a friction angle between 23-29 ° and 29-35°, respectively.

Once the only resisting parameter has been determinate the last important measurement needed for the kinematic analysis is the strike and dip direction of the slope. Those values have been estimated after realizing the DEM. After tracing the different profiles were the ski lifts should be placed, the slopes have been calculated manually, considering only abrupt changes in it and the strike direction has been measured with the azimuth of the line were the profile was taken.

		Altitude		
		Bottom	Medium	Top
Ski lift	1	29 / 3,64	51 / 19,46	15 / 10,37
	2	134 / 7,04	134 / 7,43	134 / 3,67
	3	110 / 13,52	110 / 15,24	110 / 3,86

Table 15: Strike and dip directions of the slope face in the different altitudes of the ski lift traces

While for the location of the two ski lifts a clear difference in slope has been found in the bottom and top of the lift compared with the normal trace of it (medium altitude) in the ski tow the slope has been almost constant. As the location of the lift has been considered almost like a line, no significant change in strike direction can be observed along the different altitudes.

The following table gives a clear overview of which type of the structural domain and material is going to be the predominant in the different slope faces that are going to be analyzed.

		Altitude		
		Bottom	Medium	Top
Ski lift	1	Structural domain 1	Structural domain 5	Structural domain 6
	2	Structural domain 4	Structural domain 4	Structural domain 4
	3	Structural domain 1	Structural domain 2	Structural domain 3

Table 16: Structural domains that can be found in each of the altitudes of the different ski traces

7.2.3. Failure Analysis

Once the discontinuity planes and the slope faces have been characterized, the kinematic failure analysis can be realized. Planar, wedge, circular and toppling failure are the four types of analysis that have been considered as no multi-faced rock types have been observed in the field (Yoon et al., 2002).

Planar Failure

Planar failure is a special case of the more general wedge type of failure, although the easiest to analyze and a comparatively rare sight in rock slope because it is only occasionally that all the geometric conditions occur (Wyllie and Mah, 2005). In this type of failure, the rock mass slides on a single surface.

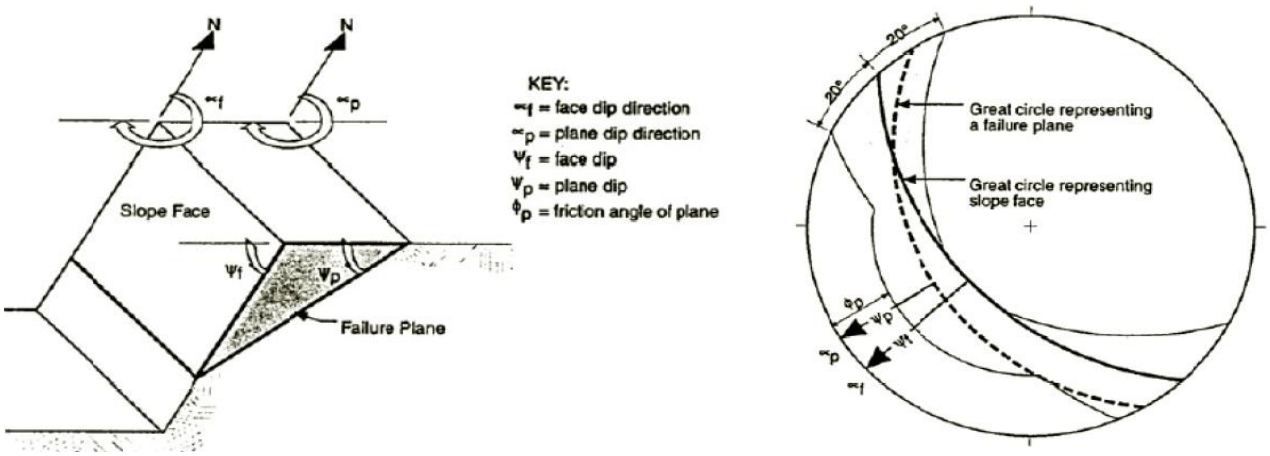

Figure 71: a) Planar Failure Model and b) Great Circle Representation (Hoek and Bray, 1981)

The four conditions for this type of failure are the following ones:

1. The sliding plane must "daylight" in the slope face, which means that the dip of the plane must be less than the dip of the slope face: $\psi_f > \psi_p$
2. The dip of the failure plane must be greater than the angle of friction of this plane: $\psi_p > \phi$
3. The sliding plane must strike parallel or nearly parallel (within approximately ±20°) to the slope face. $|\alpha_f - \alpha_p| < 20°$
4. Release surfaces (separation surfaces) that provide negligible resistance to sliding must be present in the rock mass to define the lateral boundaries of the failure block.

According to the first and second condition $\psi_f > \phi$, and as it can be seen from the tables 14 and 15, the slope face dip (highest value equal to 19,46°) isn't bigger than the friction angle (smallest value ϕ =31°) in any of the established comparison. Nevertheless, the worst case -which is considered the one with the steepest slope face-, will be analyzed:

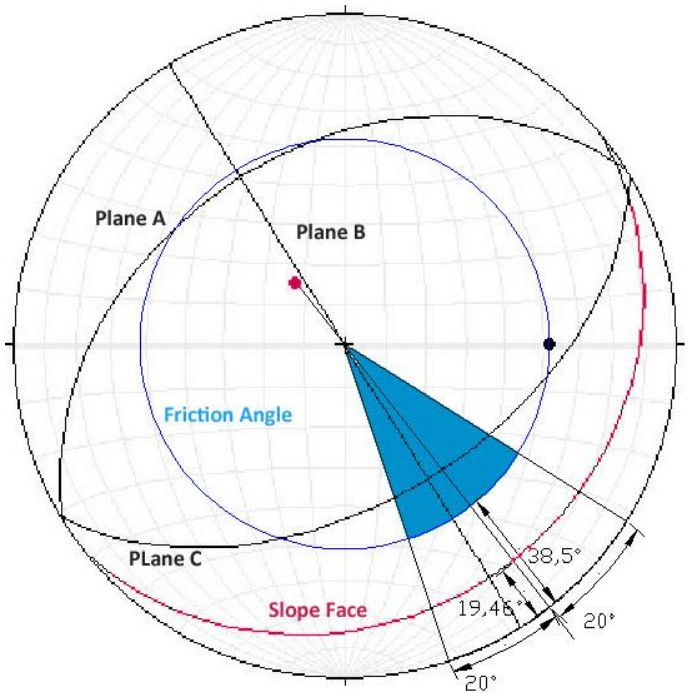

Figure 72: Planar failure analysis with the structural domain 5 and Slope face 51/19,47. As the slope face doesn't restrict the blue area on the upper part of the cone, no planar failure can occur.

As it can be seen from the tables 15 and 16, in the steepest slope face the discontinuity planes that have been observed are the ones of structural domain 5. The great circles of planes A, B and C show that only plane C is dipping in the same direction as the slope face, but this plane dips too steep to the slope face, so no planar failure can occur. At the same time, the friction angle is also too big for the flat slope face. If the slope face would be dipping at steeper angles than 51°, the plane C could present planar failure.

Wedge Failure

This type of failure happens when 2 discontinuity planes that are striking obliquely to the slope face intersect and a block of rock mass slides along the line of intersection of both planes.

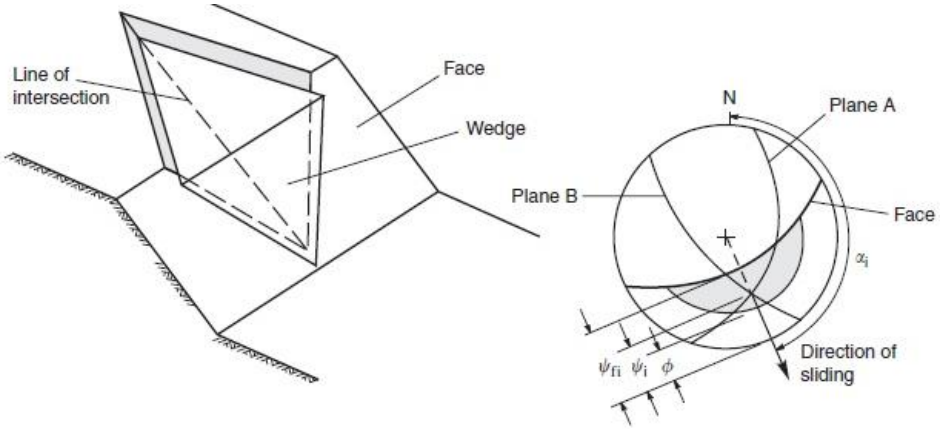

Figure 73: a) Wedge Failure Model and b) Great Circle Representation (Wyllie and Mah, 2005)

Wedge failure can occur over a much wider range of geologic and geometric conditions than plane failure. The geometric conditions for this type of failure are the following ones:

1. The plunge of the line of intersection must be flatter than the dip of the face: $\psi_{fi} > \psi_i$
2. The plunge of the line of intersection must be steeper than the average friction angle of the two slide planes: $\psi_i > \phi$
3. The line of intersection must dip in a direction out of the face for sliding to be feasible: $|\alpha_f - \alpha_i| < 20°$

For this type of analysis the trend and plunge direction of the intersection lines had to be found. This was done with Stereonet and although the most probably intersection are only the ones between planes A and B or C as plane A has the most density, the intersection between B and C was also considered.

	Intersection 1 (A & B)	Intersection 2 (A & C)	Intersection 3 (B & C)
Structural domain 1	57 / 47	191 / 19	086 / 38
Structural domain 2	04 / 29	249 / 27	123 / 49
Structural domain 3	19 / 42	225 / 27	113 / 37
Structural domain 4	02 / 29	266 / 14	153 / 58
Structural domain 5	32 / 40	239 / 00	148 / 51
Structural domain 6	86 / 33	030 / 35	153 / 39

Table 17: Trend/Plunge of the intersections between the 3 predominant planes

Looking at the fulfillment of the first condition, only the three red colored intersection lines have flatter dipping angle than the slope face, as the slope face dips at the steepest with 19°. The structural domain 1 is present in the bottom of the slope of the third ski lift an needs to be analyzed with the slope face 110 / 13,52, and the structural domain 5 is present in the middle altitude of the slope of the first ski lift and needs to be analyzed with 51 / 19,46 as in the planar failure. On the other hand the structural domain 4 present at the second ski lift doesn't fulfill the first requirement to produce wedge failure as it is present along the ski tow location, were the slope is less than the one of the red colored intersection. Although it's obvious that the wedge failure isn't going to be present as none of the mentioned intersections fulfill the second requirement -their dipping angle is flatter than the friction angle- the two first mentioned cases are going to be analyzed with stereographic projection.

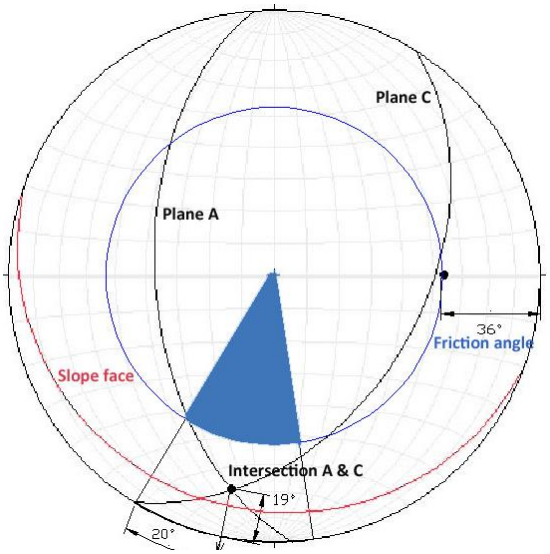

Figure 74: Structural domain 1 with Slope face 110 / 13,52

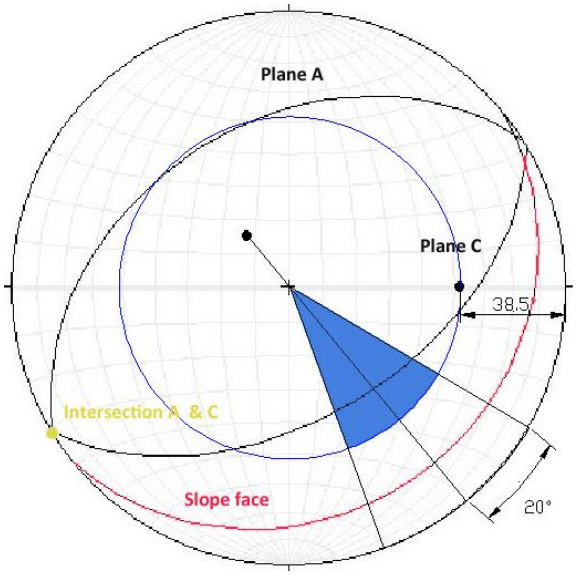

Figure 75: Structural domain 5 with Slope face 51 / 19,46

In order to occur wedge failure, the intersection of the planes should be inside the blue colored area, although this area had to be limited by the slope face, as the slope face had to be steeper than the plunge of the intersection and the friction angle. In the second case, even the intersection of both planes is not dipping in the direction of the slope face, so it's also impossible because it even doesn't fulfill the third condition.

Circular Failure

In weak materials such as highly weathered or closely fractured rock, failure occurs normally along a surface that approaches a circular shape. While in strong rock the failure of rock slopes is controlled by geological features such as bedding planes and joints that divide the rock into discontinuous mass, in the case of closely fractured or highly weathered rock the slide surface is free to find the line of least resistance through the slope (Wyllie and Mah, 2005). Therefore, this type of rock failure only occurs in closely fractured rock with randomly oriented discontinuities.

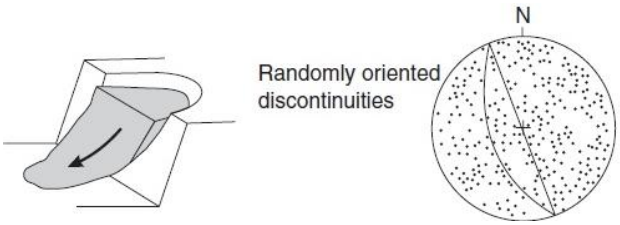

Figure 76: a) Circular Failure Model and b) Great Circle Representation (Wyllie and Mah, 2005)

When looking at the density of the discontinuities in the six different locations it can clearly be seen that almost all of them present two or three preferential discontinuity planes. In this way,

this type of failure is impossible to occur. Nevertheless, it's worth to mention that the observable weathering problem in the rock material can also be observed in the two measurements taken in the higher part of the mountain, namely number 3 and 6. In this two cases, more randomly oriented discontinuities have been found although not sufficiently enough to produce circular failure.

Toppling Failure

Toppling failure involves rotation of columns or blocks of rock about a fixed base and it usually occurs on rock masses where a high number of discontinuities are dipping towards the slope face with an elevate dipping angle. The following three test are useful for identifying potential toppling conditions:

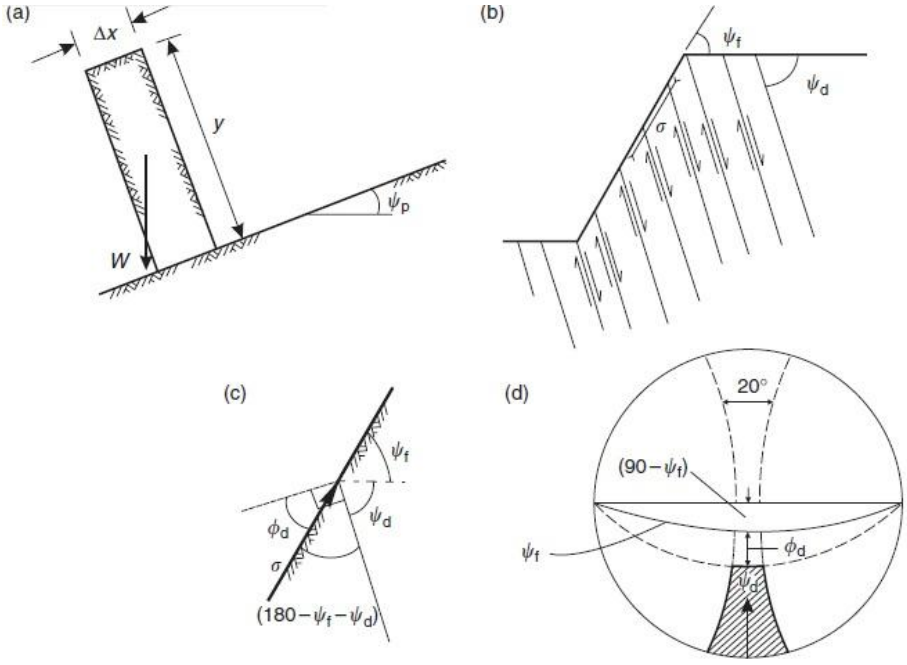

Figure 77: Toppling failure (Wyllie and Mah, 2005)

1. Block shape test

   A basic mechanical stability analysis of a block tells us that when the friction angle between the base of the block and the plane ϕ_p is bigger than the plane dipping angle ψ_p, the block will be stable ($\phi_p > \psi_p$) but when the center of gravity of the block lies outside the base it will topple ($\Delta x/y < \tan \psi_p$).(figure 77a)

2. Inter-layer slip test

   The requirement for toppling to occur is shear displacement on the face-to-face contacts on the top and bottom faces of the blocks. The condition of interlayer slip is given by: $\psi_d \geq (90- \psi_f) + \phi_d$.(figure 77c)

3. Block alignment test

Finally the last condition for toppling to occur is that the planes forming the blocks should strike approximately parallel to the slope face. In this way each layer is free to topple with little constraint from adjacent layers: $|\alpha_f - \alpha_d| < 10°$.

No toppling failure will occur in the hole field, as the inter-layer slip test is not fulfilled in the hole region. This can easily be seen as the smallest value in the right side of the inequality could be 100, considering a friction angle of 30 and a slope face dip of 19, which is impossible to exceed by other planes. Nevertheless, the following stereographic projection of the worst present case will clarify the impossibility of this type of failure:

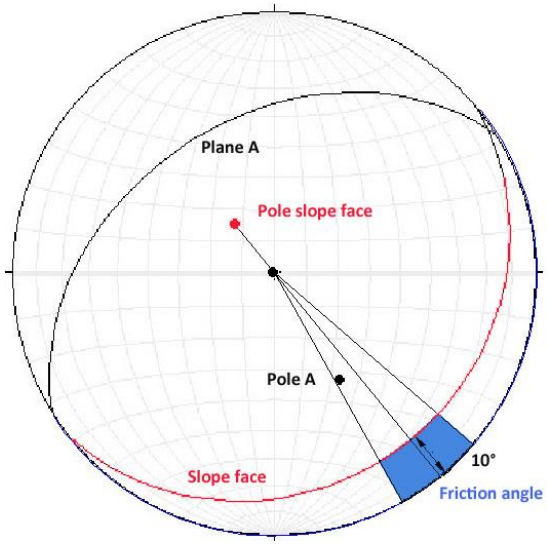

Figure 78: Toppling failure analysis with structural domain 5 and slope face 51/19,47

According to the Test of Goodman, toppling failure will occur if the pole of the discontinuity plane A would lie inside the blue area. In this case, the three mentioned criteria would be fulfilled. The criteria of inter-layer-slip test is not fulfilled as the dipping angle of the plane A is to flat to produce toppling failure.

The kinematic analysis has shown that none of the different failure types are going to be present along the different traces of the ski lift, basically because the friction angle of the material is good enough and also because the rock slope isn't steep enough to cause any of them. Nevertheless, it has to be said that the rock slope may be steeper in some places, but as an average measurement has been used for the analysis it could happen that in some cases were a local steep slope is present some of the mentioned failure types happen. In order to avoid this type of problem, a GIS-based kinematic has been developed.

7.3. GIS-Based Kinematic Slope Stability Analysis

7.3.1. Introduction

Recently different software for slope failure analysis has been developed, as LimiState:Geo who finds the critical slip surface with the Discontinuity Layout Optimization (DLO) method, Stable, which integrates Bishop Slip Circle Analysis among others or Slope/W, which uses limit equilibrium computations. On the other hand some software like Rockpack III and Slopemap (Günther, 2003) have been specialized in realizing kinematical analysis of rock failure.

The wide variability of slope face measurements and structural domains characterizations in the field, together with the characteristic of GIS to deal effectively with highly scattered and enormous amount of data leads to the idea of using this type of software for the kinematic analysis. Previous studies like Kim et al. (2004), Jaboyedoff et. al. (2004), Mote et al.(2004), Hadjigeorgiou and Grenon (2010), Yilmaz et al. (2011) and Singh et al. (2011) have successfully shown the effectiveness of GIS in this environment. Although, using the same theoretical background and the same system in these studies the same methodology has not been used. While Hadjigeorgiou and Grenon (2010) developed an analysis using a vector representation for kinematic analysis conditions in the MATLAB environment as well as the introduction of structural properties of fractures were defined in the same environment to be analyzed, Mote et al. (2004) used the tools Spatial Analyst and 3D Analyst Extension within the ESRI's ArcGIS platform to realize the analysis. The simplicity of this last method makes it a useful tool to be used in this type of analysis, although it just considers the deterministic method and not the probabilistic analysis, as Hadjigeorgiour and Grenon (2010) have also considered. In this study, a similar methodology to Mote et. al.(2004) has been applied.

7.3.2. Methodology

The slope and aspect of the terrain, which have been analyzed in figures 62 to 65 are equivalent to dip and dip direction used in rock engineering to define fracture and slope orientation. The structural domain which have been analyzed in Annex D have been added to the GIS system as feature classes considering that each of this structural domains was present in a determinant area. Another feature class with the values of the friction angle in each of the three altitudes has also been created.

In order to apply comparison commands with the obtained dip and dip direction, the created feature classes had to be converted to raster surfaces as well. This could be done with the application Feature to Raster in the Conversion Tools menu. In this way different surfaces were

created each of whom represented a different value of interested in the kinematic analysis: dip of discontinuities 1, 2 and 3, dip directions of discontinuities 1, 2 and 3 and trend and plunge of each intersection line. Totally 12 different raster surfaces were created. Once this was done the kinematic analysis could be realized with the Spatial Analyst Tool: Raster calculator. There, according to the conditions explained previously planar, wedge and toppling failure analysis was done and the outcome raster surface showed the results of a deterministic analysis: if failure could happen the outcome raster surface obtained a value of 1 and if not 0. This analysis was done for each of the discontinuities in planar and toppling analysis and for each of the intersection lines in wedge failure analysis. The analysis was carried out with the results from the raster surface obtained after TIN interpolation and from the Inverse Distance Weighting interpolation raster surface.

7.3.3. Results

The obtained results show more or less the same results that have been obtained with the previous kinematic analysis. Although some differences can be seen between the results from the analysis with the raster surface obtained with TIN and the raster surface created with IDW interpolation these aren't relevant, as more or less both results show similar behaviors specially in wedge and toppling were the more critical zone has been found to be the one with structural domain 5. This results is the same like the one obtained with the manual analysis, were emphasis was done in this zone, due to its more favorable failure conditions. While in the manual analysis no possible failure conditions have been found, the GIS-based analysis has shown that some critical conditions can occur in the structural domain 5. From the individual analysis of each different set of discontinuities and intersection lines, it has been found that the most critical is the second discontinuity for toppling failure and in the wedge failure, like in the manual analysis the only one presenting failure conditions is the intersection line between planes B and C.

On the opposite in the planar analysis it has been found that some failure conditions can occur, specially at the bottom of the first ski lift and the top of the ski tow (specially in the IDW interpolation, where the cell size is smaller than the ones from the raster surface converted from the TIN). In comparison to the manual analysis, were no possible failure conditions have been found, a lot of places where planar failure could occur, have been found when doing the GIS-based analysis. A reason for this difference is that while in the manual analysis a generalized slope face dip is considered in the GIS-based analysis all local slope face dips are

analyzed and it can clearly seen that in the region where the conditions for planar failure have been found a considerable change in slope dip has been found.

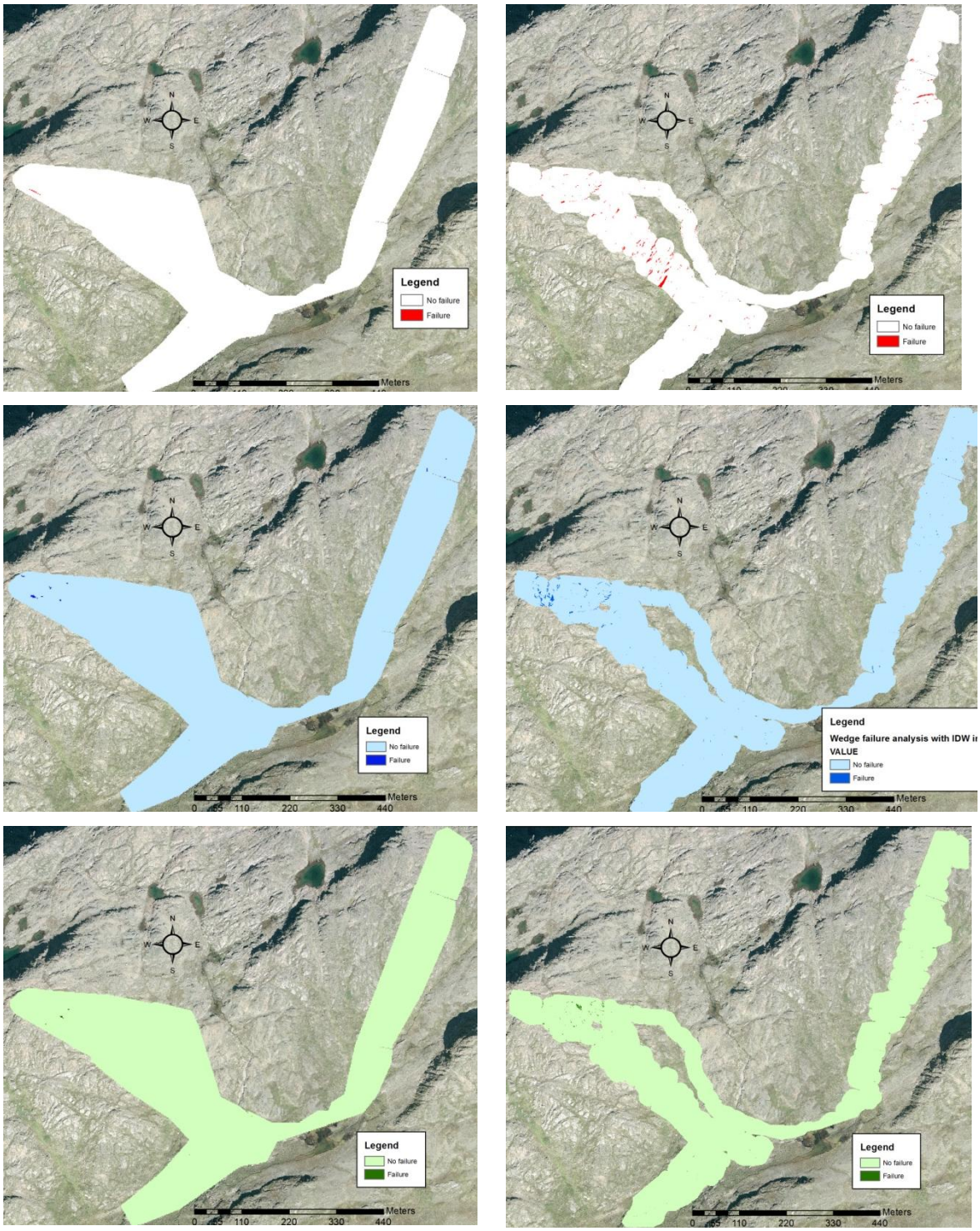

Figure 79: Planar, wedge and toppling (top to bottom) analysis with the raster surface obtained from TIN (left) and the raster surface with IDW interpolation (right).

To have a general view of the probable failure conditions also a complete map has been realized with the application Raster calculator where all 3 types of failure are represented.

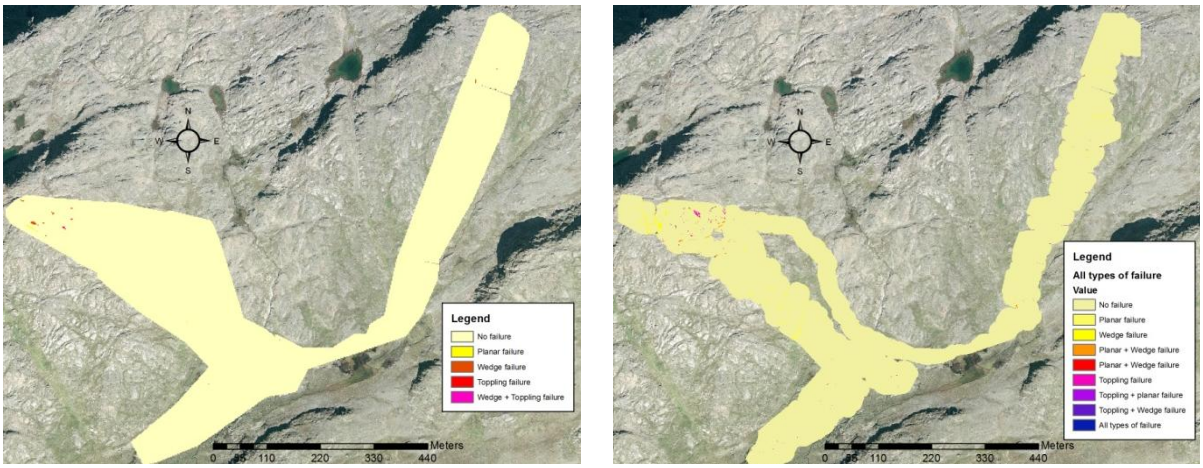

Table 18: Analysis of all types of failure with TIN surface (left) and raster surface (right)

Again, the results show that in the IDW interpolated raster surface more failure occasions have been found.

8. Discussion

After the realization of the digital terrain model and the kinematic analysis of the terrain a purpose for the trace of the ski lifts could be given. Furthermore, the expected placement of the ski lift piles should compliance with the recommendations of the DS/EN 12929-1, which have been summarized at the beginning of this study.

8.1. Ski Lifts

8.1.1. Ski Lift 1

As mentioned in point 3.1 the most important characterization of the ski lift is that it's running height above ground should not exceed 15 m. At the same time the line of the aerial ropeway has to be a straight line between the stations without any deviations except for special cases. For this reason, a straight line was interpolated between the locations of both stations and a profile was created with the 3D Analyst Tool. The data of the interpolation could be extracted as a Excel sheet, which afterwards could be processed with Matlab in order to find the most suitable placement of the piles for the construction. The Matlab file locates a pile in the extracted profile whenever the running height above ground exceeds the 15 m that are recommended and also whenever the running height above ground is less than 3 m. This second value represents the clearance envelope that is need in the carriers of the ski lift.

Two different lines between the base station and the top of the mountain where analyzed with the Matlab code and the proposed placement of the ski lifts can be seen in the following figures:

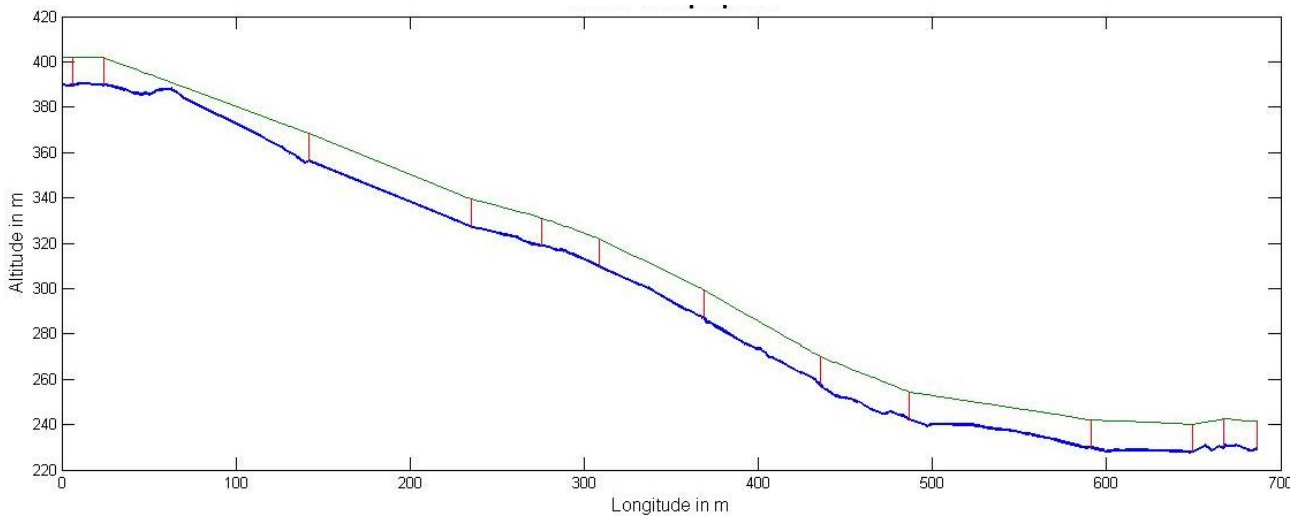

Figure 80: Ski lift 1 – First proposal

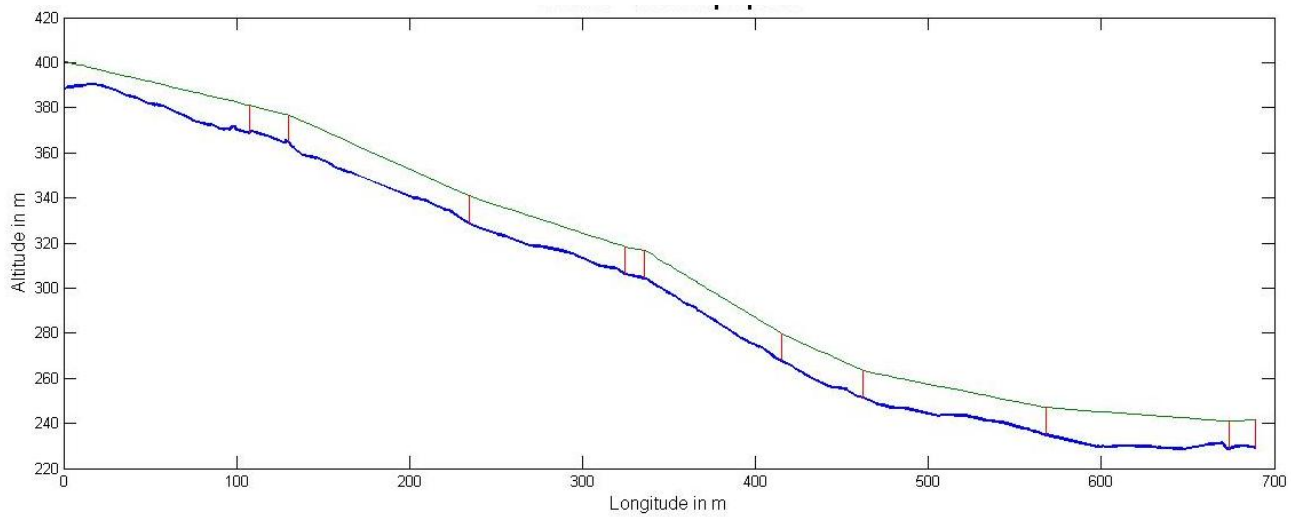

Figure 81: Ski lift 1 – Second proposal

As seen in the graphics, both proposed ski lifts use more or less the same amount of piles. Nevertheless, some extra piles should be used in both cases, as the Matlab code just considers that a pile is needed when the height above ground isn't between the expected values, and nothing else is considered as for example the need of a pile when the static forces are excessive. It is also important to mention, that the proposed trace for the chord doesn't take into account that the running height above ground has to be less in the surroundings of the loading and unloading areas as otherwise skiers couldn't get into the chairlift. Therefore, the chord span at the beginning and end of the shown profiles should not be considered.

When the found piles are drawn in the digital elevation model it can be seen that none of them would be constructed in a slope face with some probable failure conditions, except for some points on the top of both lines, specially close in the second proposal (figure 82). According to this, the first proposal would be considered from now on, to evaluate the loading and unloading areas for the ski lift. After drawing a more detailed profile in the lowest part of the ski lift and the top of it, the different zones that have to be taken into account in the loading and unloading areas where found without any problem. Both unloading and loading areas are already clearly defined as an almost regular flat area can be found at both ends of the lift.

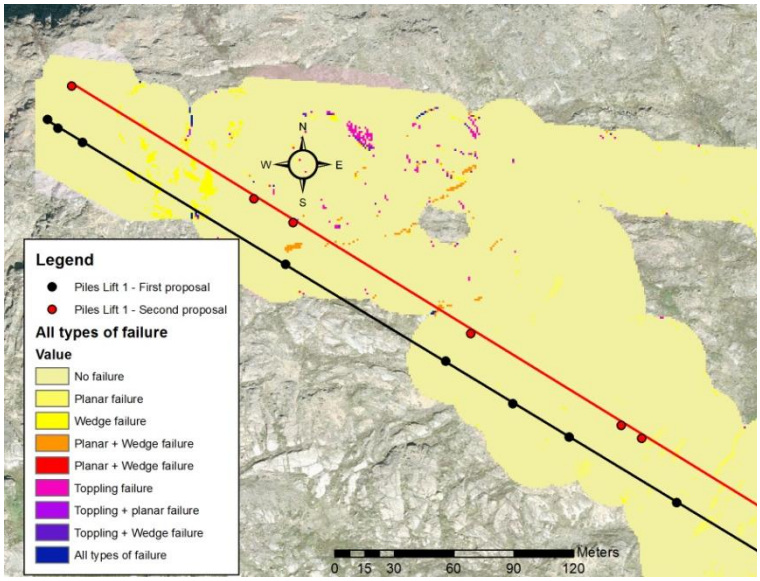

Figure 82: Ski lift lines and possible slope face failures

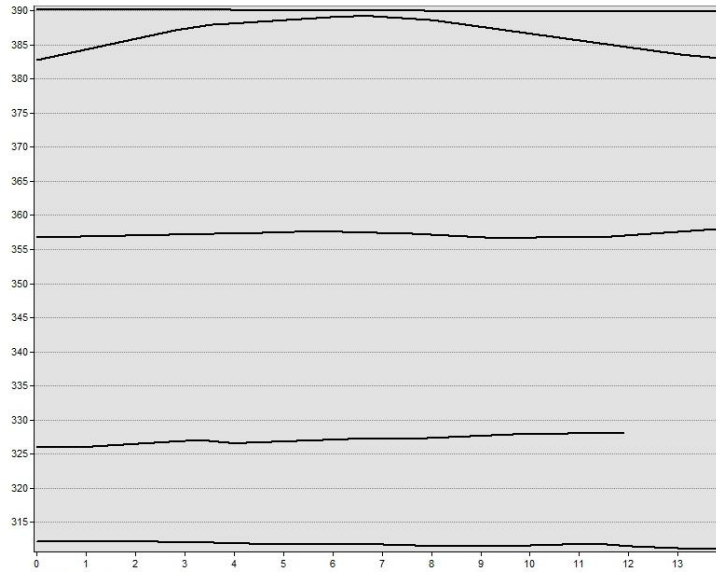

Figure 83: Transverse profiles in different altitudes

Regarding the clearance envelope and the foot and hand area, no problems will be found to fulfill the recommendations of the standard, as the ski lift would pass through an area without narrow passageways. To evaluate this assumption different profiles in the perpendicular direction of the ski lift trace have been taken and as it can be seen in figure 83, no extreme rough surface is passed as the height difference don't exceed 2 m for 10 m of longitude.

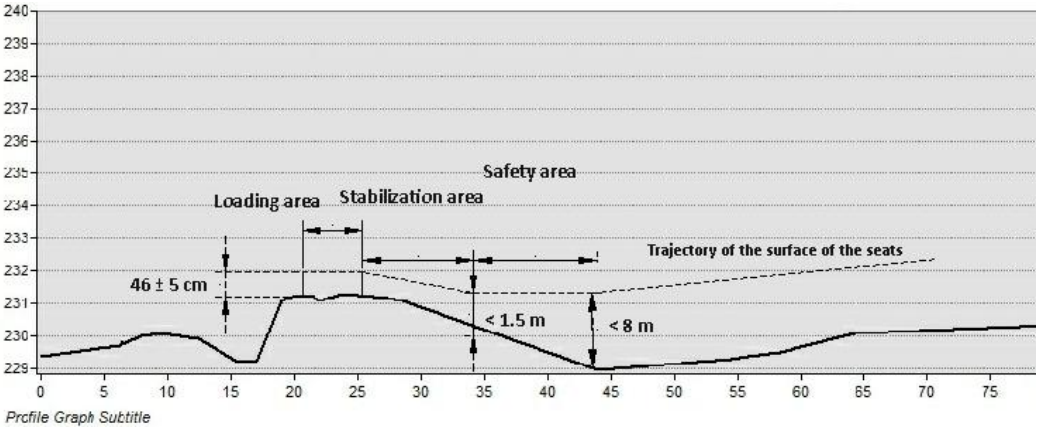

Figure 84: Loading, stabilization and safety area in the loading zone of the first ski lift (distance and elevation in meters)

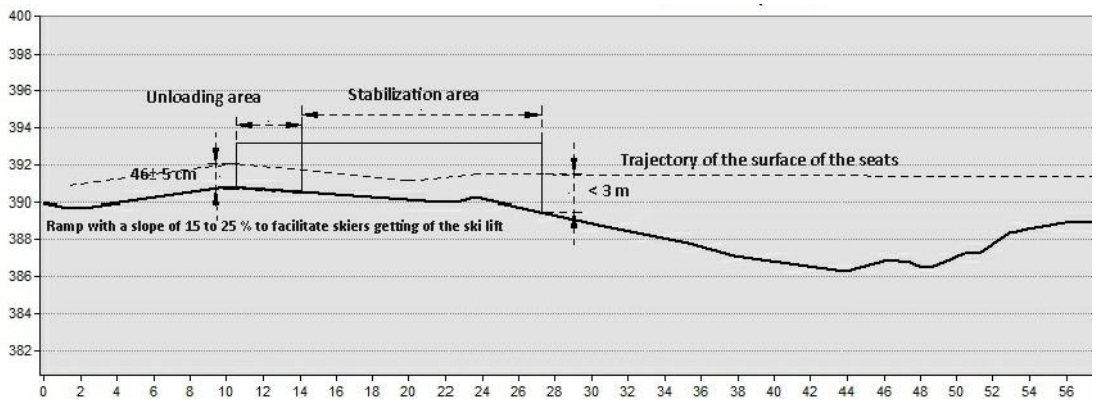

Figure 85: Unloading and stabilization area in the unloading area of the first ski lift (distance and elevation in meters)

The defined areas in the unloading and loading zones have been calculated considering a velocity of 2,5 m/s . The stabilization area and safety area have been defined with travelling distances and need therefore a consistent velocity as the one proposed in 9.2.6 of DS/EN 12929-1 to be established.

8.1.2. Ski Lift 2

The same procedure was undertaken with the location of the second ski lift. As seen from the digital elevation model, less GPS measurements were taken in this zone as the established trace of the ski lift was almost clear. Despite the terrain in this zone doesn't allow much varieties in the placement of the ski lift, the compiled profiles show that no kind of problems

will be expected in this zone, as the slope is almost constant along the trace. Therefore, the compliance of the height difference is fulfilled without any problems as the low number of piles demonstrate.

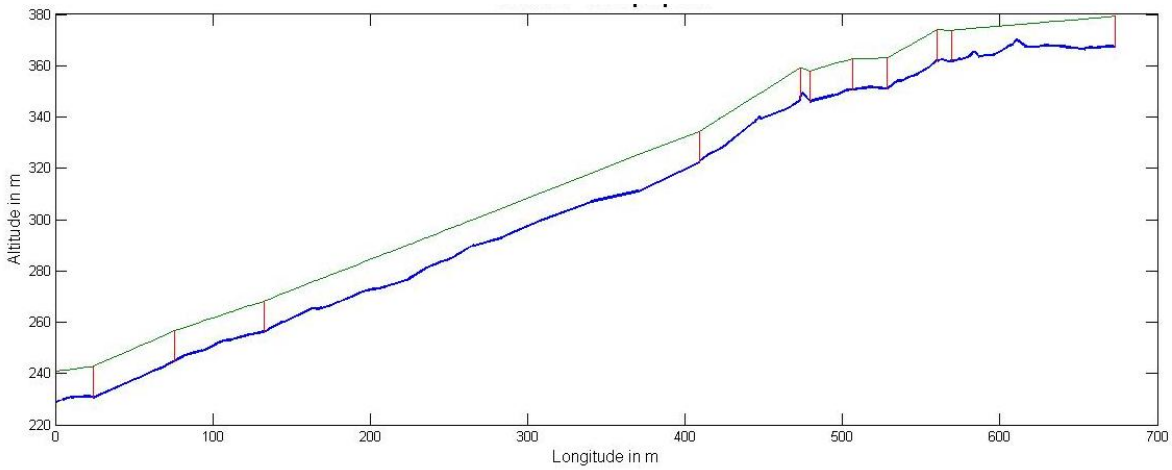

Figure 86: Ski lift 2 – First proposal

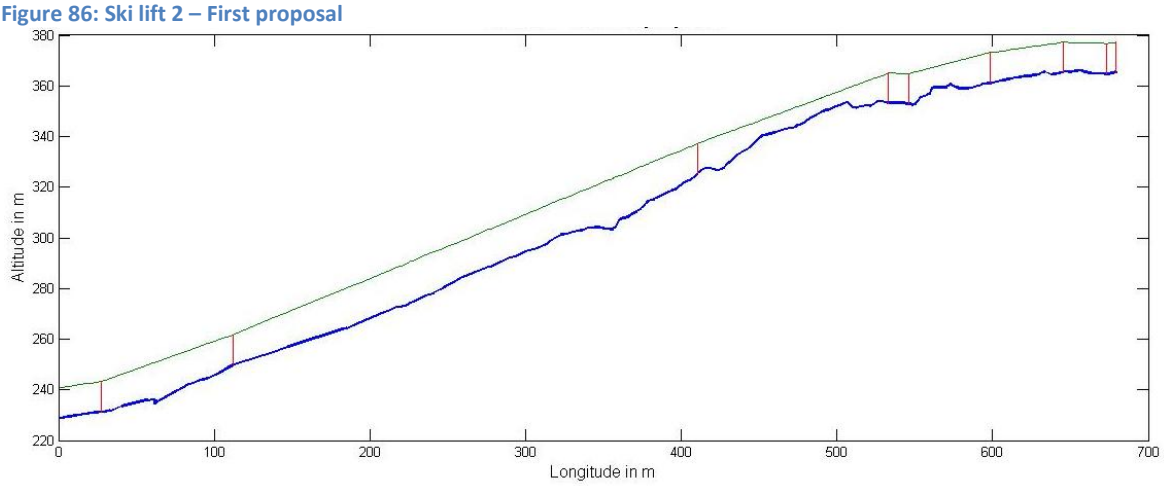

Figure 87: Ski lift 2 – Second proposal

After drawing the piles in the DEM it could be seen that none of them were placed in slope faces with any kind of failure mode and the transverse profiles taken in different altitudes demonstrate a smooth surface where no risks could be expected for the correct transportation of skiers.

8.2. Ski-Tow

The determinant recommendation for the line of a ski-tow is that the longitudinal gradient should not exceed at any point 40 % considering the use of tow-hangers and a low level ski-tow. The slope surface shows that some areas in the middle of the line have such a longitudinal gradient or even higher values and need therefore to be flatted to fulfill these recommendations. Different longitudinal profiles have shown that no downhill slopes will be

presented along the tow-track. On the other hand the realization of different transverse profiles cleared up that the ski-tow would have a flat area along the line without any excessive transverse gradient allowing skiers to abandon the ski tow at every point of the trace.

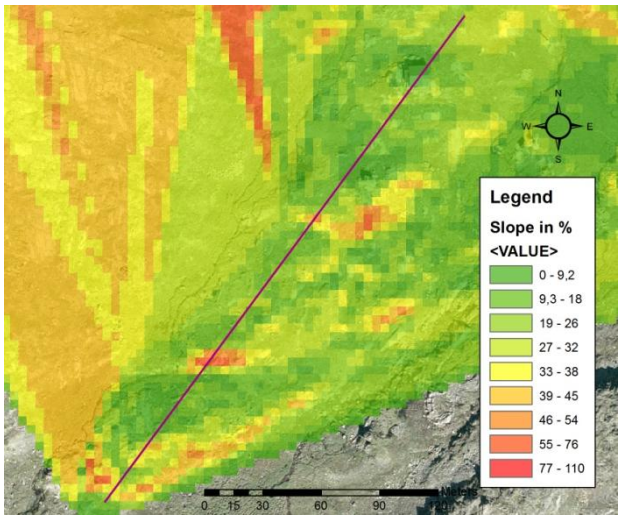

Figure 88: Slope analysis around the ski tow (in percentage)

8.3. 3D-Model

From the previous analysis its evident that no real hazard for the construction of the ski lifts and ski tows is present. With the modeling tools available at ArcGIS Desktop a 3D Model of each of the tracks where the ski lifts are being placed has been created. The raster surfaces created with the interpolation from the GPS measurements were well defined surfaces over which the proposed ski lift lines could be projected. Other elements, like the cabins and containers present in the area were also drawn to facilitate the identification and to make the model more realistic. Although it's a small area without a high diversity in the terrain, the drapping of the ortophoto over the raster surface makes it a little more realistic, although due to the small capacity of the used computer it is not projected with the same quality as the original picture.

The approximate ski runs that would be able for skiers after the construction of the new piles were also drawn and classified as previously depending on the difficulty of the slope. The lake is also colored as in the future an ice skating area will be available over it.

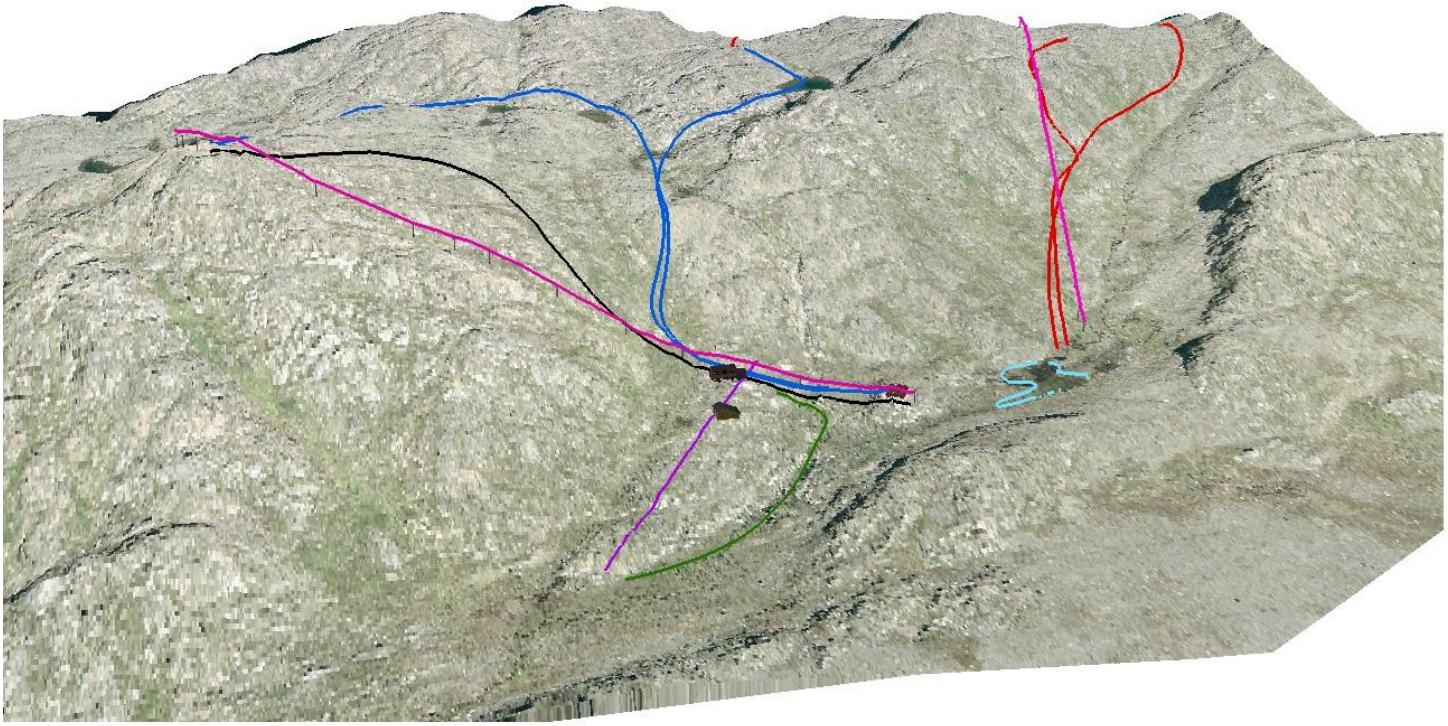

Figure 89: 3D-Model view (created with ArcScene)

9.Conclusion

9.1. Overall Conclusion

With this study some site investigations for the planning and construction of future ski lifts has been carried out. Although the main interest was to create the DEM for the evaluation of the compliance of the recommendations from DS/EN-12929-1, a kinematic analysis of the slopes was also realized to at least obtain some information about the stability of the slopes. Since no detailed geological survey had been previously realized in the surroundings of the area where the construction has been planned, rock mass rating classification and q-index values, as well as strike and dip measurements have been taken to evaluate the material. Due to the fact, that RMR classification considers the resistance to uniaxial stress as one of the main parameters for the correct evaluation, point load index tests have also been carried out with rock samples from the surroundings.

The realization of the DEM and the kinematic analysis leads to the conclusion that no particular hazard situation should be expected in the zone regarding the construction of the ski lifts. Profiles from the DEM show that the ski lifts won't cover zones with extreme steep slopes and the geological survey demonstrated the good quality of material coating the surroundings of Sisimiut. Although the kinematic analysis isn't a complete slope stability analysis as it just considers geometric characteristics of the structural domain, at least potentially unstable blocks were identified. Especially interesting and useful was found the application of GIS-based

kinematic analysis, as potentially unstable blocks could be identified easily after the creation of a DEM and an elaborated database with structural domain measurements.

Due to the lack of previous information especially in strike and dip measurements, an extreme refinement in the results could not be expected. With additional GPS measurements in the area, a smoother DEM could have been created and more strike and dip measurements in the area could have provided a more realistic GIS-based kinematic analysis, as only 6 different geological structures were identified.

Regarding the GPS survey, the obtained GPS points had a high error (in the order of cm) which should have been improved with the use of a base station situated closer to the survey area, or with real time kinematic survey.

On the other hand, RMR and Q-Index values have classified, except in one zone, the material in the same category. Although the point load index tests results show a high variability in the obtained values, expressed by the standard deviation, these have characterized the material in the same way as the geological hammer. Due to the difficulty in carrying a high number of rock samples to the laboratory a better accuracy of these results could not be guaranteed.

9.2. Future Perspective

Further studies can be developed in both investigated areas: spatial analysis and geology. First of all a ski slope analysis could be developed according to slope measurements from the DEM and in this way manage in a proper way the tracks of ski runs, avoiding crossings of ski runs with different demanding skiing levels for example. The addition of methereological data in the DEM and the creation of hillshade surfaces, which identifies shadow and lighted areas depending on the illumination of the sun, could produce the simulation of average duration of the snow layer in the terrain or if it would be the case, also analyze the risk of snow avalanches. On the other hand, a detailed DEM of the whole mountain with the analysis of the probable ski runs could also examine the best placement of a cafeteria for skiers as this should be laying so that most skiers reach it without any problems. Finally, a complete Geographic Information System could be helpful for both the daily operations and long term decision-making at a ski resort and therefore considered as necessary when creating one of them.

Regarding the geological part, other slope failure analysis should be considered and used for the evaluation. The kinematic analysis as already mentioned is a potential tool for the identification of unstable blocks in rock slopes and a conservative method as it ignores the effects of cohesion and it assumes that all the discontinuities are continuous and thoroughgoing. Nevertheless, another analysis method should also be used to confirm the

results and obtain a security factor, which could suggest the employment of a stabilization method in case the slope faces are not that reliable.

10. References

101, C. (2011). "Ciencia 101." Retrieved 20. September, 2011, from http://www.ciencia101.com.

Analysis, I. t. S. (2011). "The Essentials of a TIN model." Retrieved 20. September, 2011, from http://planet.botany.uwc.ac.za/nisl/GIS/spatial/chap_1_50.htm.

Bieniaski, Z. T. (1989). Engineering Rock Mass Classification: A Complete Manual for Engineers and Geologists in Mining, Civil and Petroleum Engineering, Wiley-Interscience Publication.

Childs, C. (2004) Interpolating Surfaces in ArcGIS Spatial Analysis. 32-35

Collinse, F. and J.-C. Loubier (2003). "Managing a Hill of Data." Point of Beginning(How ski slopes are managed with the use of a multi-tiered geomatics tool.).

Council, G. T. B. (2011, 13.10.2011). "The Official Turism Site of Greenland." Retrieved 30. May, 2011, from http://www.greenland.com.

Dahl, M. (2009). Tekniske undersøgelser for anlægsarbejde i fjeld i Grønland, Danmarks Tekniske Universitet.

de Berg, M., O. Cheong, et al. (2008). Computational Geometry: Algorithms and Applications, Springer-Verlag.

Department of Housing, I. a. T., Planning and Projects (2011). "NunaGIS - Greenland on maps." Retrieved 20. September, 2011, from http://www.nunagis.gl/.

Dude, C. (2011). "Compass - How To Use One." Retrieved 25. September, 2011, from http://www.compassdude.com.

Environment, D. M. o. t. (2011). "National Survey and Cadastre." Retrieved 15. May, 2011, from http://www.kms.dk.

Eppstein, D., M. T. Goodrich, et al. (2005). "The Skip Quadtree: A Simple Dynamic Data Structure for Multidimensional Data."

Escher, A. and W. S. Watt (1976). Geology of Greenland. Copenhagen 1976, Grønlands Geologiske undersøgelse (København).

ESRI (2010). ArcGIS Desktop 10.0, ESRI.

Evans, V. (2011). Own taken pictures.

Felicísimo, A. M. (1995). Modelos Digitales del Terreno: Introducción y aplicaciones en las ciencias ambientales.

Foote, K. E. and M. Lynch (1995). "Geographic Information Systems as an Integrating Technology: Context, Concepts, and Definitions." Retrieved 1. September, 2011, from http://www.colorado.edu/geography/gcraft/notes/intro/intro_f.html.

Günther, A. (2003). "SLOPEMAP: programs for automated mapping of geometrical and kinematical properties of hard rock hill slopes." Elsevier - Computer & Geosciences **29**: 865-875.

Hadjigeorgiou, M. and J. Grenon (2010). "Integrated structural stability analysis for preliminary open pit design." Elsevier - International Journal of Rock Mechanics & Mining Sciences **47**: 450-460.

Hegarty, C. and E. D. Kaplan (2005). Understanding GPS: Principles and Applications, Artech House.

Henriksen, N., A. K. Higgins, et al. (2009). "Greenland from Archaean to Quaternary." Geological Survey of Denmark and Greenland Bulletin.

Hippolyte, P. L. (2011). "Análisis urbano a través de herramientas SIG." Retrieved 2. May, 2011, from http://sig-seu.blogspot.com.

Hoek, E. (2006). Practical Rock Engineering.

Hoek, J. W. and E. Bray (1981). Rock Slope Engineering.

Hollis, J. A., M. Keiding, et al. (2006). "Evolution of Neoarchaean supracrustal belts at the northern margin of the North Atlantic Craton, West Greenland." Geological Survey of Denmark and Greenland Bulletin.

Holm, A. (2011). Geofysisk forundersøgelse for anlæggelse af mine i Grønland, Danmarks Tekniske Universitet.

Huisman, M. and R. Hack, Eds. (2002). Estimating the Intact Rock Strength of a Rock Mass by Simple Means. Engineering Geology for Developing Countries. Proceedings of 9th Congress of the International Association for Engineering Geology and the Environment.

Imaging, T. (2011). "3D Terrain and Elevation Data." Retrieved 20. September, 2011, from http://terraimaging.com/photogrammetry/.

ISRM, I. S. f. R. M. (1984). "Suggested Method for Determining Point Load Strength." 53-60.

Jaboyedoff, M., R. Couture, et al. (2004). Structural Analysis of Turtle Mountain (Alberta) Using Digital Elevation Model. Conférence Canadienne de Geotéchnique. Québec, Canada.

Jensen, S. M., H. Hansen, et al. (2001). "Kimberlites and other ultramafic alkaline rocks in the Sisimiut–Kangerlussuaq region, southern West Greenland." Geological Survey of Denmark and Greenland Bulletin: 57-66.

Jensen, S. M. and K. Secher (2004). "Diamond Exploration in Greenland." Geological Survey of Denmark and Greenland Bulletin.

Kim, K. S., H. J. Park, et al. (2004). "Geographic Information System (GIS) based stability analysis of rock cut slopes." Geosciences Journal **8**: 391-400.

Kliche, C. A. (1999). Rock Slope Stability, Society for Mining, Metallurgy and Exploration.

Landsurveyors.com (2011). "Land Surveyor Directory." Retrieved 20. September, 2011, from http://www.landsurveyors.com.

Larsen, H. S. (2008). Forundersøgelser for anlæggelse af svømmehal i fjeld, Danmarks Tekniske Universitet.

Ltd, G. U. (2011). "Land Surveys, Mechanical Surveys, Building Surveys." Retrieved 20. September, 2011, from http://www.geomatics-uk.com/index.php.

Ltd., L. R. C. S. P. (2011). "Langford & Rowe Consulting Surveyors Pty. Ltd.". Retrieved 20. September, 2011, from http://www.lrsurveyors.com.au/?page=gps.

Lumholt, M. (2010). "Stuck in Greenland." Retrieved 13. October, 2011, from http://stuckingreenland.wordpress.com/category/background/.

Maps, G. (2011). "Google Maps." Retrieved 1. September, 2011, from http://maps.google.es.

Mote, T., D. Morley, et al. (2004). "GIS-based Kinematic Slope Stability Analysis."

Mountain, I. (2011). "Solbakken Skiliften." Retrieved 20. May, 2011, from http://www.ski.gl/Solbakken/tabid/63/Default.aspx.

NASA (2004). "ASTER - Advanced Spaceborne Thermal Emission and Reflection Radiometer." Retrieved 10. September, 2011, from http://asterweb.jpl.nasa.gov/.

Nielsen, A. A. (2009) Geostatistics and Analysis of Spatial Data. 7

O.I.T.A.F (2011). "Official Website of the Organizzazione Internazionale Transporti a Fune." Retrieved 5. May, 2011, from http://www.oitaf.org/.

Pantelidis, L. (2009). "Rock slope stability assessment through rock mass classification systems." Elsevier - International Journal of Rock Mechanics & Mining Sciences **46**: 315-325.

Research, R. O. o. B. G. (2011). "http://www.gps.oma.be." Retrieved 10. September, 2011, from http://www.gps.oma.be/systems_tutorial.php.

Roberts, D. H., A. J. Long, et al. (2009). "Ice sheet extent and early deglacial history of the southwestern sector of the Greenland Ice Sheet." Quaternary Science Reviews **28**(25-26): 2760-2773.

Rodríguez, F. J. A. (2007). Ingeniería Geológica: Caracterización de macizos rocosos.

Romana, M. R. (1993). A Geomechanical Classification for Slopes: Slope Mass Rating, Pergamon Press.

Satellites, C. L. (2011). "Radar Altimetry Tutorial." Retrieved 20. September, 2011, from http://www.altimetry.info/html/alti/principle/basic_en.html.

SIG, L. (2011). Retrieved 20. September, 2011, from http://www.uca.edu.sv/investigacion/nejapa/laboratorio2.html.

Singh, T. N., S. P. Pradhan, et al. (2011). "Stability of slopes in a fire-prone mine in Jharia Coalfield, India."

Sisorarfiit (2011, 13. October 2011). "Sisorarfiit Skiliften." Retrieved 1. September, 2011, from http://www.skilift.gl.

Standardization, E. C. f. (2004). Safety requirements for cableway installations designed to carry persons - General requirements - Part 1: Requirements for all installations, CEN. **EN 12929-1:** 52.

Survey, U. S. G. (2011). "U.S. Geological Survey." Retrieved 20. September, 2011, from http://rmmcweb.cr.usgs.gov/frontrange/aggregate/hammer/hammer.htm.

Trussty-Jasmine.blogspot.com (2011). "Detecting Earthquakes with Satellites." Retrieved 20. September, 2011, from http://trussty-jasmine.blogspot.com/2011/07/detecting-earthquakes-with-satellite.html#axzz1aff3A83X.

USGS (1998). "GTOPO30 - Global Topographic Data." Retrieved 1. September, 2011, from http://www1.gsi.go.jp/geowww/globalmap-gsi/gtopo30/gtopo30.html.

Vallejo, L. I. G. d. (2002). Ingeniería Geológica, Pearson Educacion.

Wolf, P. R. and C. D. Ghilani (2008). Elementary Surveying - An Introduction to Geomatics.

Wyllie, D. C. and C. W. Mah (2005). Rock Slope Engineering, Spoon Press.

Yang, S. S. and H. S. Lim (2004). "An Analysis of Plane Failure of Rock Slopes by Quantified Stereographic Projection." Elsevier - International Journal of Rock Mechanics & Mining Sciences **41**.

Yilmaz, I., M. Marschalko, et al. (2011). "GIS-based kinematic slope instability and slope mass rating (SMR) maps: application to a railway route in Sivas (Turkey)." Bulleting of Engineering Geology and the Environment.

Yoon, W. S., U. J. Jeong, et al. (2002). "Kinematic analysis for sliding failure of multi-faced rock slopes." Elsevier - International Journal of Rock Mechanics & Mining Sciences **67**: 51-61.

Annex

Annex A: Rock Mass Rating Evaluation

A. CLASSIFICATION –PARAMETERS AND THEIR RATINGS									
Parameter			Range of values						
1	Strength of intact rock material	Point-load strength index	>10 MPa	4 - 10 MPa	2 - 4 MPa	1 - 2 MPa	For this low range - uniaxial compressive test is preferred		
		Uniaxial comp. strength	>250 MPa	100 - 250 MPa	50 - 100 MPa	25 - 50 MPa	5 - 25 MPa	1 - 5 MPa	< 1 MPa
	Rating		15	12	7	4	2	1	0
2	Drill core Quality *RQD*		90% - –100%	75% - –90%	50% - 75%	25% - 50%	< 25%		
	Rating		20	17	13	8	3		
3	Spacing of discontinuities		> 2 m	0.6 - 2 . m	200 - 600 mm	60 - 200 mm	< 60 mm		
	Rating		20	15	10	8	5		
4	Condition of –discontinuities (See E)		Very rough –surfaces Not continuous No separation Unweathered wall rock	Slightly rough surfaces Separation < 1 mm Slightly weathered walls	Slightly rough surfaces Separation < 1 mm Highly weathered walls	Slickensided surfaces or Gouge < 5 mm thick or Separation 1-5 mm Continuous	Soft gouge >5 mm thick or Separation –> 5 mm Continuous		
	Rating		30	25	20	10	0		
–5	Ground water	Inflow per 10 m tunnel length (l/m)	None	< 10	10 - 25	25 - 125	> 125		
		(Joint water press)/ (Major principal σ)	0	< 0.1	0.1, - 0.2	0.2 - 0.5	> 0.5		
		General conditions	Completely dry	Damp	Wet	Dripping	Flowing		
	Rating		15	10	7	4	0		

B. RATING ADJUSTMENT FOR DISCONTINUITY ORIENTATIONS (See F)						
Strike –and dip orientations		Very favourable	Favourable	Fair	Unfavourable	Very Unfavourable
Ratings	Tunnels & mines	0	-2	-5	-10	-12
	Foundations	0	-2	-7	-15	-25
	Slopes	0	-5	-25	-50	

C. ROCK MASS CLASSES DETERMINED FROM TOTAL RATINGS					
Rating	100 ← 81	80 ← 61	60 ← 41	40 ← 21	< 21
Class number	I	II	III	IV	V
Description	Very good rock	Good rock	Fair rock	Poor rock	Very poor rock

D. MEANING OF ROCK CLASSES					
Class number	I	II	III	IV	V
Average stand-up time	20 yrs for 15 m span	1 year for 10 m span	1 week for 5 m span	10 hrs for 2.5 m span	30 min for 1 m span
Cohesion of rock mass (kPa)	> 400	300 - 400	200 - 300	100 - 200	< 100
Friction angle of rock mass (deg)	> 45	35 - 45	25 - 35	15 - 25	< 15

E. GUIDELINES FOR CLASSIFICATION OF DISCONTINUITY conditions					
Discontinuity length (persistence) Rating	< 1 m 6	1 - 3 m 4	3 - 10 m 2	10 - 20 m 1	> 20 m 0
Separation (aperture) Rating	None 6	< 0.1 mm 5	0.1 - 1.0 mm 4	1 - 5 mm 1	> 5 mm 0
Roughness Rating	Very rough 6	Rough 5	Slightly rough 3	Smooth 1	Slickensided 0
Infilling (gouge) Rating	None 6	Hard filling < 5 mm 4	Hard filling > 5 mm 2	Soft filling < 5 mm 2	Soft filling > 5 mm 0
Weathering Ratings	Unweathered 6	Slightly weathered 5	Moderately weathered 3	Highly weathered 1	Decomposed 0

F. EFFECT OF DISCONTINUITY STRIKE AND DIP ORIENTATION IN TUNNELLING**			
Strike perpendicular to tunnel axis		Strike parallel to tunnel axis	
Drive with dip - Dip 45 - 90°	Drive with dip - Dip 20 - 45°	Dip 45 - 90°	Dip 20 - 45°
Very favourable	Favourable	Very favourable	Fair
Drive against –dip - Dip 45-90°	Drive against –dip - –Dip 20-45°	–Dip 0-20 - Irrespective of strike°	
Fair	Unfavourable	Fair	

* Some conditions are mutually exclusive . –For example, if infilling is present, the roughness of the surface will be overshadowed by the influence of the gouge. –In such cases use A.4 directly.
** Modified after Wickham et al (1972).

Annex B: Rock Quality Designation Index, Q

DESCRIPTION	VALUE	NOTES
1. ROCK QUALITY DESIGNATION	*RQD*	
A. Very poor	0 - 25	1. Where *RQD* is reported or measured as ≤ 10 (including 0), a nominal value of 10 is used to evaluate *Q*.
B. Poor	25 - 50	
C. Fair	50 - 75	
D. Good	75 - 90	2. *RQD* intervals of 5, i.e. 100, 95, 90 etc. are sufficiently accurate.
E. Excellent	90 - 100	
2. JOINT SET NUMBER	J_n	
A. Massive, no or few joints	0.5 - 1.0	
B. One joint set	2	
C. One joint set plus random	3	
D. Two joint sets	4	
E. Two joint sets plus random	6	
F. Three joint sets	9	1. For intersections use ($3.0 \times J_n$)
G. Three joint sets plus random	12	
H. Four or more joint sets, random, heavily jointed, 'sugar cube', etc.	15	2. For portals use ($2.0 \times J_n$)
J. Crushed rock, earthlike	20	
3. JOINT ROUGHNESS NUMBER	J_r	
a. Rock wall contact		
b. Rock wall contact before 10 cm shear		
A. Discontinuous joints	4	
B. Rough and irregular, undulating	3	
C. Smooth undulating	2	
D. Slickensided undulating	1.5	1. Add 1.0 if the mean spacing of the relevant joint set is greater than 3 m.
E. Rough or irregular, planar	1.5	
F. Smooth, planar	1.0	
G. Slickensided, planar	0.5	2. J_r = 0.5 can be used for planar, slickensided joints having lineations, provided that the lineations are oriented for minimum strength.
c. No rock wall contact when sheared		
H. Zones containing clay minerals thick enough to prevent rock wall contact	1.0 (nominal)	
J. Sandy, gravely or crushed zone thick enough to prevent rock wall contact	1.0 (nominal)	
4. JOINT ALTERATION NUMBER	J_a	ϕr degrees (approx.)
a. Rock wall contact		
A. Tightly healed, hard, non-softening, impermeable filling	0.75	1. Values of ϕr, the residual friction angle, are intended as an approximate guide to the mineralogical properties of the alteration products, if present.
B. Unaltered joint walls, surface staining only	1.0	25 - 35
C. Slightly altered joint walls, non-softening mineral coatings, sandy particles, clay-free disintegrated rock, etc.	2.0	25 - 30
D. Silty-, or sandy-clay coatings, small clay-fraction (non-softening)	3.0	20 - 25
E. Softening or low-friction clay mineral coatings, i.e. kaolinite, mica. Also chlorite, talc, gypsum and graphite etc., and small quantities of swelling clays. (Discontinuous coatings, 1 - 2 mm or less)	4.0	8 - 16

4, JOINT ALTERATION NUMBER	J_a	ϕr degrees (approx.)	
b. Rock wall contact before 10 cm shear			
F. Sandy particles, clay-free, disintegrating rock etc.	4.0	25 - 30	
G. Strongly over-consolidated, non-softening clay mineral fillings (continuous < 5 mm thick)	6.0	16 - 24	
H. Medium or low over-consolidation, softening clay mineral fillings (continuous < 5 mm thick)	8.0	12 - 16	
J. Swelling clay fillings, i.e. montmorillonite, (continuous < 5 mm thick). Values of J_a depend on percent of swelling clay-size particles, and access to water.	8.0 - 12.0	6 - 12	
c. No rock wall contact when sheared			
K. Zones or bands of disintegrated or crushed	6.0		
L. rock and clay (see G, H and J for clay	8.0		
M. conditions)	8.0 - 12.0	6 - 24	
N. Zones or bands of silty- or sandy-clay, small clay fraction, non-softening	5.0		
O. Thick continuous zones or bands of clay	10.0 - 13.0		
P. & R. (see G,H and J for clay conditions)	6.0 - 24.0		
5. JOINT WATER REDUCTION	J_w	approx. water pressure (kgf/cm^2)	
A. Dry excavation or minor inflow i.e. < 5 l/m locally	1.0	< 1.0	
B. Medium inflow or pressure, occasional outwash of joint fillings	0.66	1.0 - 2.5	
C. Large inflow or high pressure in competent rock with unfilled joints	0.5	2.5 - 10.0	1. Factors C to F are crude estimates; increase J_w if drainage installed.
D. Large inflow or high pressure	0.33	2.5 - 10.0	
E. Exceptionally high inflow or pressure at blasting, decaying with time	0.2 - 0.1	> 10	2. Special problems caused by ice formation are not considered.
F. Exceptionally high inflow or pressure	0.1 - 0.05	> 10	
6. STRESS REDUCTION FACTOR		***SRF***	
a. Weakness zones intersecting excavation, which may cause loosening of rock mass when tunnel is excavated			
A. Multiple occurrences of weakness zones containing clay or chemically disintegrated rock, very loose surrounding rock any depth)		10.0	1. Reduce these values of *SRF* by 25 - 50% but only if the relevant shear zones influence do not intersect the excavation
B. Single weakness zones containing clay, or chemically disintegrated rock (excavation depth < 50 m)		5.0	
C. Single weakness zones containing clay, or chemically disintegrated rock (excavation depth > 50 m)		2.5	
D. Multiple shear zones in competent rock (clay free), loose surrounding rock (any depth)		7.5	
E. Single shear zone in competent rock (clay free). (depth of excavation < 50 m)		5.0	
F. Single shear zone in competent rock (clay free). (depth of excavation > 50 m)		2.5	
G. Loose open joints, heavily jointed or 'sugar cube', (any depth)		5.0	

Annex C: Point Load Index Measurements

Bottom Altitude

	D (mm)	L (mm)	W (mm)	Weight (gr)	P (kN)	Area (mm^2)	V (cm^3)	ρ (cm^3/gr)	De (mm)	F	$I_{s(50)}$ (Mpa)	σ (Mpa)
1	48,6	72,1	26,8	234,6	5,8	1302	94	2,50	40,7	0,91	3,19	76,5
2	36,3	73,0	64,2	332,3	7,4	2329	170	1,95	54,5	1,04	2,59	62,2
3	53,5	74,5	47,3	403,5	15,5	2531	189	2,14	56,8	1,06	5,09	122,2
4	65,0	70,4	37,6	415,7	NVF	2444	172	2,42	55,8	1,05	--	--
5	43,6	77,5	32,5	232,4	8,5	1417	110	2,12	42,5	0,93	4,38	105,1
6	47,3	88,2	47,4	349,0	4,1	2240	198	1,77	53,4	1,03	1,48	35,5
7	51,6	65,4	34,4	244,5	NVF	1775	116	2,11	47,5	0,98	--	--
8	39,3	88,4	39,9	336,7	4,2	1568	139	2,43	44,7	0,95	2,00	48,0
9	52,5	63,4	28,1	189,0	4,7	1475	94	2,02	43,3	0,94	2,35	56,3
10	37,5	68,7	29,3	200,2	7,1	1099	75	2,65	37,4	0,88	4,45	106,9
11	59,5	76,1	72,5	512,9	12,5	4314	328	1,56	74,1	1,19	2,72	65,2
12	25,3	75,8	57,4	295,6	8,0	1452	110	2,69	43,0	0,93	4,04	97,0
13	43,4	87,6	51,1	362,3	8,5	2216	194	1,87	53,1	1,03	3,10	74,3
14	55,2	76,0	52,9	452,2	13,5	2920	222	2,04	61,0	1,09	3,97	95,3
15	42,2	114,2	71,2	632,4	6,9	3003	343	1,84	61,8	1,10	1,99	47,7
16	63,9	107,6	82,3	857,4	30,6	5259	566	1,52	81,8	1,25	5,70	136,9
17	35,6	83,7	58,7	327,3	5,0	2090	175	1,87	51,6	1,01	1,91	45,7
18	38,2	94,6	47,6	307,5	5,4	1816	172	1,79	48,1	0,98	2,29	55,1
19	57,2	84,0	43,7	452,9	10,0	2497	210	2,16	56,4	1,06	3,32	79,7
20	55,2	97,0	29,7	444,5	5,0	1637	159	2,80	45,6	0,96	2,30	55,3
21	75,6	136,0	43,9	702,6	1,0	3315	451	1,56	65,0	1,13	0,27	6,4
22	48,5	82,4	41,3	498,5	1,0	2001	165	3,02	50,5	1,00	0,39	9,5
Mean values								**2,13**			**2,88**	**69,1**

Middle Altitude

	D (mm)	L (mm)	W (mm)	Weight (gr)	P (kN)	Area (mm^2)	V (cm^3)	ρ (cm^3/gr)	De (mm)	F	$I_{s(50)}$ (Mpa)	σ (Mpa)
1	25,6	71,1	41,7	197,1	7,2	1066	76	2,60	36,8	0,87	4,62	110,9
2	58,0	67,6	44,4	468,3	4,6	2572	174	2,69	57,2	1,06	1,49	35,8
3	55,7	73,6	50,2	538,0	19,8	2796	206	2,61	59,7	1,08	6,02	144,5
4	29,0	46,1	51,7	161,8	13,5	1499	69	2,34	43,7	0,94	6,66	159,7
5	36,9	78,5	50,8	335,5	17,3	1875	147	2,28	48,9	0,99	7,17	172,2
6	61,3	60,0	47,8	552,7	17,5	2927	176	3,15	61,0	1,09	5,14	123,3
7	49,0	85,0	65,2	709,4	17,1	3192	271	2,61	63,8	1,12	4,69	112,6
8	42,7	88,1	47,6	430,0	24,0	2033	179	2,40	50,9	1,01	9,35	224,3
9	32,0	78,4	39,0	260,1	4,0	1246	98	2,66	39,8	0,90	2,28	54,6
10	36,6	66,0	53,2	311,6	10,0	1945	128	2,43	49,8	1,00	4,03	96,7
11	33,8	86,7	45,8	336,0	18,8	1548	134	2,50	44,4	0,95	9,04	217,0
Mean values								**2,57**			**5,48**	**131,4**

Top Altitude

	D (mm)	L (mm)	W (mm)	Weight (gr)	P (kN)	Area (mm2)	V (cm3)	ρ (cm3/gr)	De (mm)	F	Is(50) (Mpa)	σ (Mpa)
1	44,1	96,2	51,0	541,8	2,8	2249	216	2,50	53,5	1,03	1,01	24,2
2	44,0	90,2	79,8	503,5	0,5	3511	317	1,59	66,9	1,14	0,13	3,1
3	24,9	88,0	79,4	315,4	6,0	1977	174	1,81	50,2	1,00	2,39	57,3
4	27,0	73,0	53,9	229,5	1,0	1454	106	2,16	43,0	0,93	0,50	12,1
5	49,8	81,9	72,0	615,6	11,0	3586	294	2,10	67,6	1,15	2,76	66,2
6	37,5	124,2	72,4	640,5	4,0	2715	337	1,90	58,8	1,08	1,24	29,9
7	27,6	87,6	78,3	331,5	0,3	2160	189	1,75	52,4	1,02	0,11	2,7
8	48,0	109,5	67,1	696,9	5,5	3221	353	1,98	64,0	1,12	1,50	36,0
9	51,0	89,3	33,0	356,9	6,8	1680	150	2,38	46,3	0,97	3,07	73,7
10	33,3	91,5	92,1	530,1	4,3	3065	280	1,89	62,5	1,11	1,22	29,2
11	23,6	93,1	70,2	453,1	4,0	1656	154	2,94	45,9	0,96	1,83	43,8
12	48,5	140,6	69,4	954,9	4,2	3366	473	2,02	65,5	1,13	1,11	26,6
Mean value								**2,08**			**1,35**	**32,4**

The red colored measurements have been rejected according to ISRM standard, as they are the two lowest and highest values in each test.

Annex D: Pole Density Analysis and Great Circles

Structural domain 1

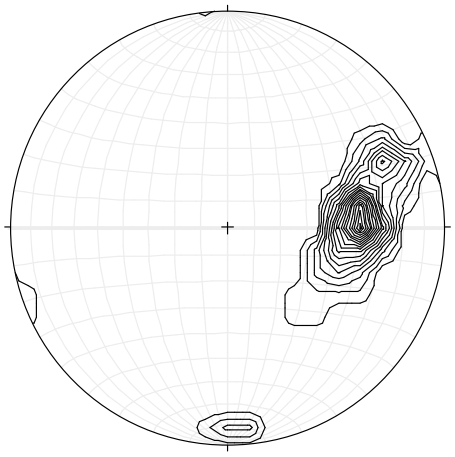

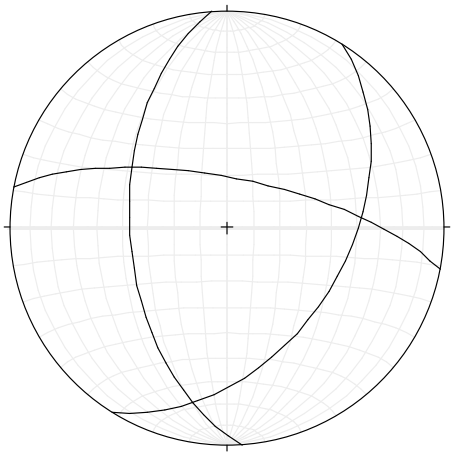

Strike and dip of the predominant planes:

1. 176 / 53 W (0.8618)
2. 281 / 71 N (0.1189)
3. 32 / 44 W (0.0193)

Structural domain 2

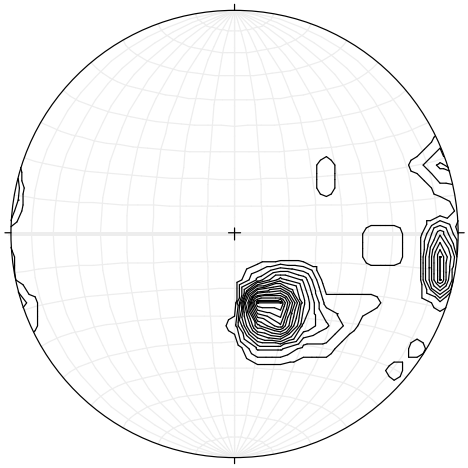

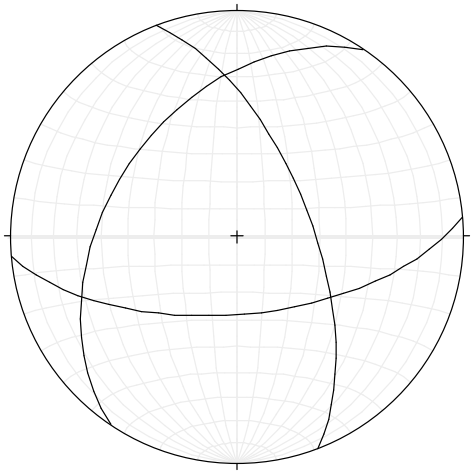

Strike and dip of the predominant planes:

1. 214 / 42 W (0.7213)
2. 339 / 63 E (0.2405)
3. 85 / 62 S (0.0382)

Structural domain 3

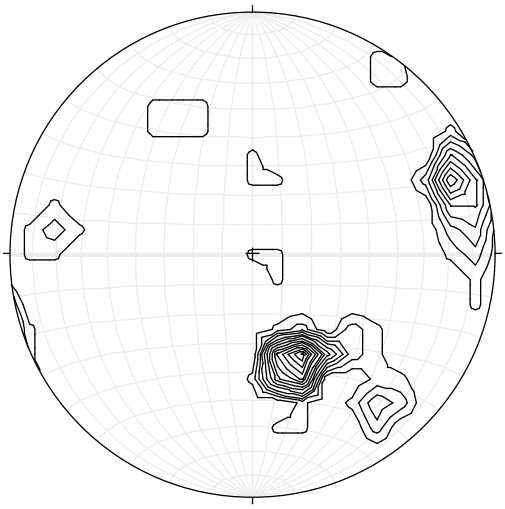

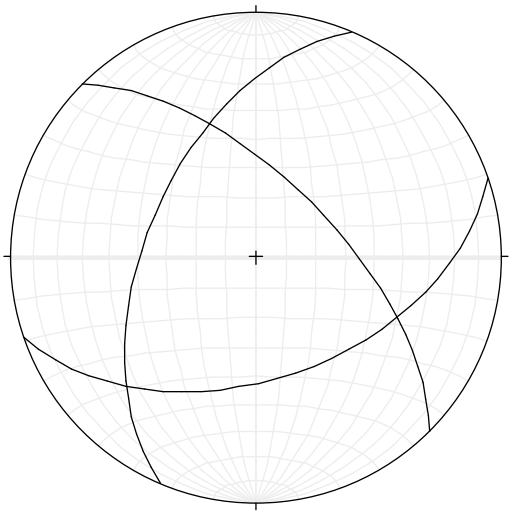

Strike and dip of the predominant planes:

1. 203 / 53 W (0.5493)
2. 315 / 64 N (0.3171)
3. 71 / 49 S (0.0382)

Structural domain 4

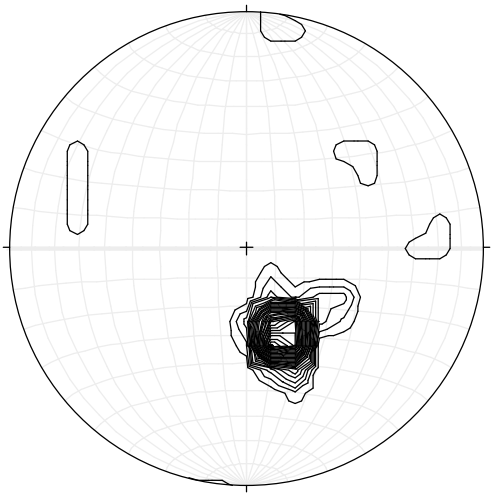

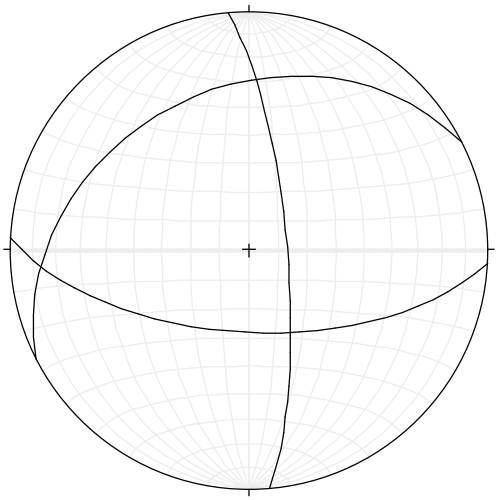

Strike and dip of the predominant planes:

1. 243 / 32 N (0.3387)
2. 355 / 77 E (0.3349)
3. 93 / 62 S (0.3263)

Structural domain 5

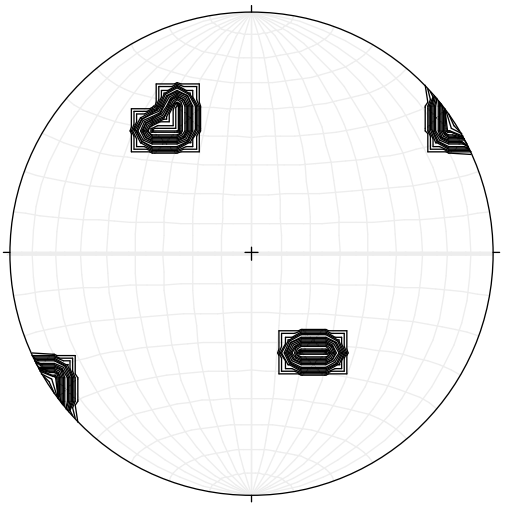

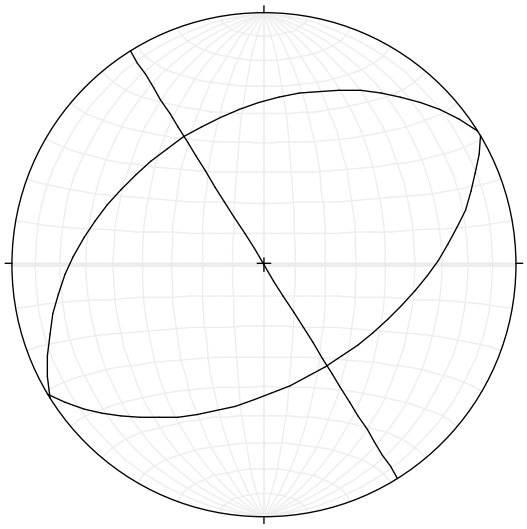

Strike and dip of the predominant planes:

1. 238 / 40 N (0.6719)
2. 328 / 90 E (0.2801)
3. 59 / 51 S (0.0480)

Structural domain 6

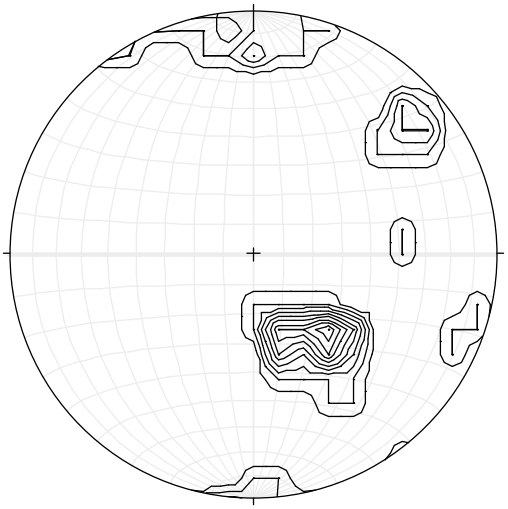

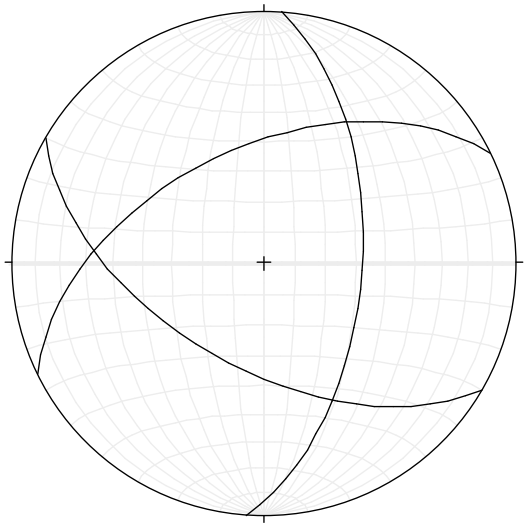

Strike and dip of the predominant planes:

1. 244 / 52 N (0.5894)
2. 120 / 56 S (0.3198)
3. 4 / 58 E (0.0909)

Annex E: Contour Lines Map

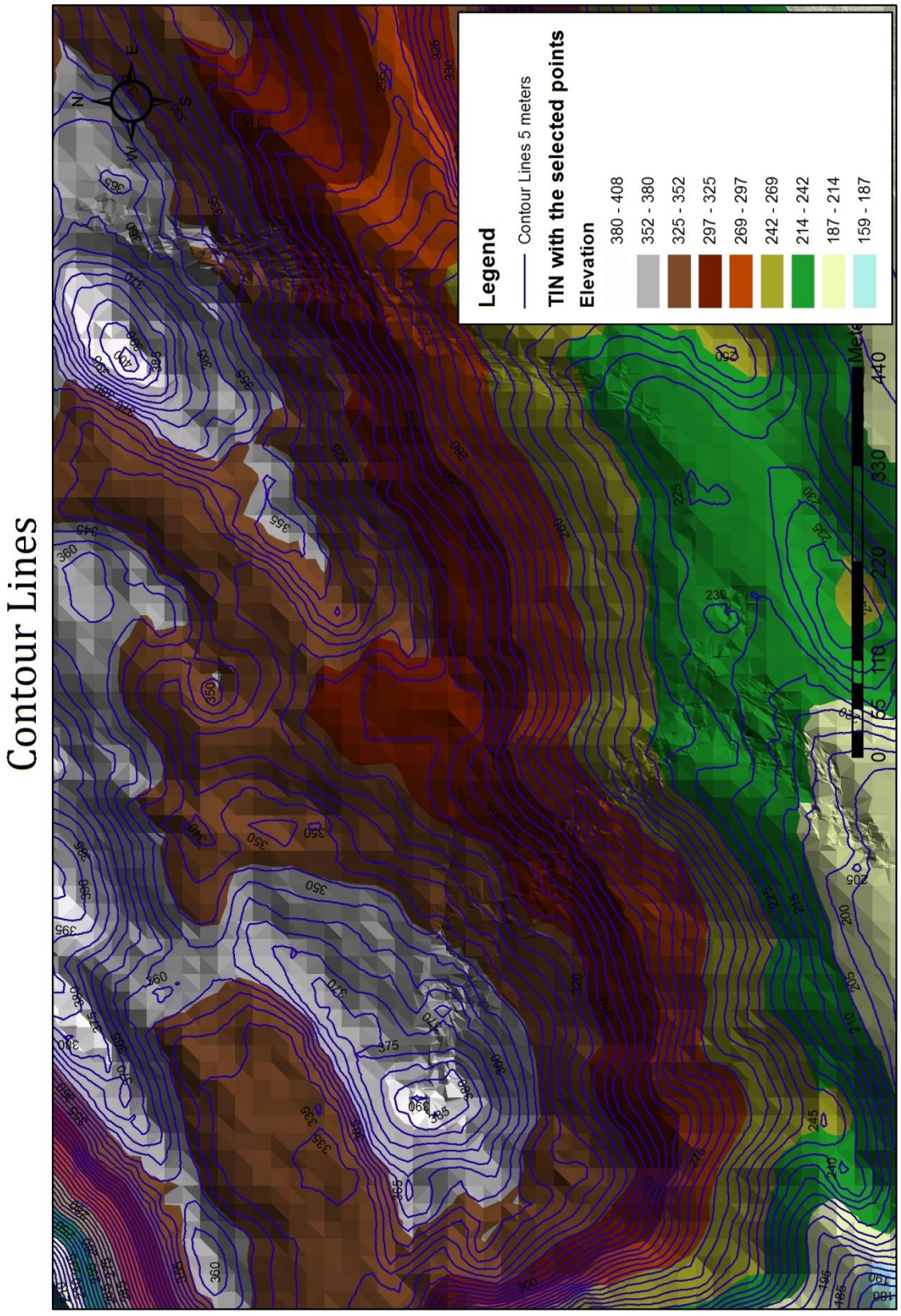

Annex F: All Types of Failure Analysis